UNCLASSIFIED

AD NUMBER

AD-B099 063

NEW LIMITATION CHANGE

TO

DISTRIBUTION STATEMENT: A

Approved for public release; Distribution is unlimited.

LIMITATION CODE: 1

- -

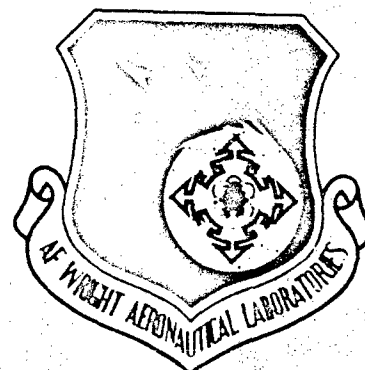**FROM**   DISTRIBUTION STATEMENT: B

LIMITATION CODE: 3

AUTHORITY

D/A ltr; Nov 1990

THIS PAGE IS UNCLASSIFIED

AFWAL-TR-85-3064

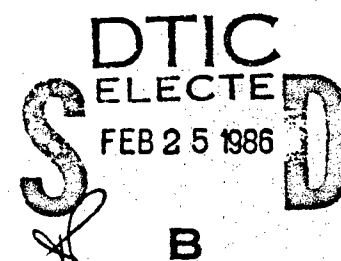# STRENGTH ANALYSIS OF COMPOSITE AND METALLIC PLATES BOLTED TOGETHER BY A SINGLE FASTENER

R.L. Ramkumar, et al.

Northrop Corporation, Aircraft Division
One Northrop Avenue
Hawthorne, California 90250

August 1985

Interim Report for Period January 1983 – December 1984

AD-B099 063

DTIC FILE COPY

DTIC
ELECTE
FEB 2 5 1986
B

FLIGHT DYNAMICS LABORATORY

AIR FORCE WRIGHT AERONAUTICAL LABORATORIES

AIR FORCE SYSTEMS COMMAND

WRIGHT-PATTERSON AIR FORCE BASE, OHIO 45433

19990407186

36   2   24   030

NOTICE

When Government drawings, specifications, or other data are used for any purpose other than in connection with a definitely related Government procurement operation, the United States Government thereby incurs no responsibility nor any obligation whatsoever; and the fact that the government may have formulated, furnished, or in any way supplied the said drawings, specifications, or other data, is not to be regarded by implication or otherwise as in any manner licensing the holder or any other person or corporation, or conveying any rights or permission to manufacture use, or sell any patented invention that may in any way be related thereto.

This technical report has been reviewed and is approved for publication.

VIPPERLA B. VENKAYYA
Project Engineer
Design & Analysis Methods Group

FREDERICK A. PICCHIONI, Lt Col, USAF
Chief, Analysis & Optimization Branch

FOR THE COMMANDER

ROGER J. HEGSTROM, Col, USAF
Chief, Structures & Dynamics Div.

AD·B099063L

REPORT DOCUMENTATION PAGE

1a. REPORT SECURITY CLASSIFICATION Unclassified	1b RESTRICTIVE MARKINGS
2a SECURITY CLASSIFICATION AUTHORITY	3 DISTRIBUTION/AVAILABILITY OF REPORT Distribution limited to U.S. Government Agencies only; test and evaluation; August 1985; Other requests must be referred to AFWAL/FIBRA, WPAFB,OH45433
2b DECLASSIFICATION·DOWNGRADING SCHEDULE	
4 PERFORMING ORGANIZATION REPORT NUMBER(S) NOR 85-278	5. MONITORING ORGANIZATION REPORT NUMBER(S) AFWAL-TR-85-3064

6a. NAME OF PERFORMING ORGANIZATION Northrop Corporation Aircraft Division	6b. OFFICE SYMBOL (If applicable)	7a NAME OF MONITORING ORGANIZATION Flight Dynamics Laboratory Air Force Wright Aeronautical Laboratories
6c. ADDRESS (City State and ZIP Code) One Northrop Avenue Hawthorne, CA 90250		7b ADDRESS (City, State and ZIP Code) Air Force Systems Command Wright-Patterson Air Force Base Dayton, Ohio 45433
8a NAME OF FUNDING/SPONSORING ORGANIZATION See Item 7	8b. OFFICE SYMBOL (If applicable) AFWAL/FIBRA	9 PROCUREMENT INSTRUMENT IDENTIFICATION NUMBER Contract F33615-82-C-3217

8c ADDRESS (City, State and ZIP Code)	10 SOURCE OF FUNDING NOS			
	PROGRAM ELEMENT NO	PROJECT NO	TASK NO	WORK UNIT NO
	62201F	2401	01	55

11. TITLE (Include Security Classification) See Reverse

12. PERSONAL AUTHOR(S) R. L. Ramkumar. et al.

13a. TYPE OF REPORT Interim	13b. TIME COVERED FROM 1/1/83 TO 12/1/84	14 DATE OF REPORT (Yr, Mo, Day) August 1985	15 PAGE COUNT 130

16. SUPPLEMENTARY NOTATION

17	COSATI CODES		18. SUBJECT TERMS (Continue on reverse if necessary and identify by block number) Bolted Joints in Composites, Analysis of Finite Plates; Fastener Analysis, Bilinear Ply Behavior, Progressive Failure Analysis, Strength Predictions for General Bearing/By-Pass Situations.
FIELD	GROUP	SUB GR	
0103	1305	1313	

19. ABSTRACT (Continue on reverse if necessary and identify by block number)

This report presents a strength analysis for laminated and/or metallic plates bolted together by a single fastener. The analysis has been programmed to be the SASCJ (Strength Analysis of Single Fastener Composite Joints) computer code. SASCJ includes:a two dimensional analysis of doubly-connected anisotropic plates accounting for finite plate dimensions (FIGEOM); a fastener analysis that approximately accounts for the local three dimensional effects (FDFA); and a progressive failure procedure that predicts a sequence of two-stage ply failures (assuming a bilinear ply behavior) using average stress failure criteria at the ply level. Predictions made by FIGEOM and FDFA are independently validated using available analytical and numerical solutions. Strength predictions made by SASCJ are compared with experimental results generated in the program, including the general bearing/by-pass situations. Analytical predictions demonstrate a good correlation with observed failure modes and measured joint strengths. The use of the SASCJ computer code will be explained, with examples, in the design guide that will be issued at the conclusion of the program.

20. DISTRIBUTION/AVAILABILITY OF ABSTRACT UNCLASSIFIED/UNLIMITED ☐ SAME AS RPT. ☒ DTIC USERS ☐	21. ABSTRACT SECURITY CLASSIFICATION Unclassified
22a. NAME OF RESPONSIBLE INDIVIDUAL V. B. Venkayya	22b TELEPHONE NUMBER (Include Area Code) (513) 255-6992	22c. OFFICE SYMBOL AFWAL/FIBRA

DD FORM 1473, 83 APR   EDITION OF 1 JAN 73 IS OBSOLETE.

11. Title

Strength Analysis of Composite and Metallic Plates Bolted Together By a Single Fastener

PREFACE

DTIC
S ELECTE D
FEB 2 5 1986
B

Accession For

NTIS GRA&I	☐
DTIC TAB	✔
Unannounced	☐
Justification	

PER CALL JC

By
Distribution/
Availability Codes
Avail and/or
Dist   Special

A-3 5

TABLE OF CONTENTS

TABLE OF CONTENTS (Concluded)

LIST OF ILLUSTRATIONS

LIST OF ILLUSTRATIONS (CONTINUED)

LIST OF TABLES

SECTION 1

INTRODUCTION

The ultimate objective of the Northrop/AFWAL program in Reference 1-1 is to develop an analytical methodology to predict the strength and lifetime of bolted composite and metallic structural components. The development of a strength analysis for plates bolted by many fasteners involves: (1) an analysis that computes the distribution of an applied load among the various fasteners in a bolted plate; and (2) a strength analysis that can be applied at every fastener location. The second analysis addresses a segment of a bolted laminate that includes a single fastener, and is the subject of this report. Figure 1-1 presents a schematic representation of all the analytical steps involved in the strength prediction of bolted structural components.

At the initiation of the Northrop/AFWAL program (Reference 1-1), BJSFM was the only available computer code that performed a strength analysis of a bolted laminate that transferred loads via a single fastener. Reference 1-2 presents the details of the analysis that is performed by the BJSFM code. The BJSFM analysis can be used to approximately predict the strength of bolted joints when (1) the fastener loads have already been computed using other analyses, (2) the fasteners are not too close to one another or to a neighboring cut-out, (3) the fasteners are rigid and their displacement with respect to the plate is uniform in the plate thickness direciton, and (4) the first ply failure at a fastener location essentially precipitates joint failure.

The conditions mentioned above severely restrict the application of the BJSFM code as an analytical tool in the design of bolted structures. An improved strength analysis was developed in the referenced Northrop/AFWAL program to overcome most of the limitations in the BJSFM analysis. Details of this improved strength analysis, programmed to be the SASCJ (Strength Analysis of Single Fastener Composite Joints) computer code, are presented in the following sections.

Figure 1-1. Schematic Breakdown of the Strength Analysis of Bolted Joints.
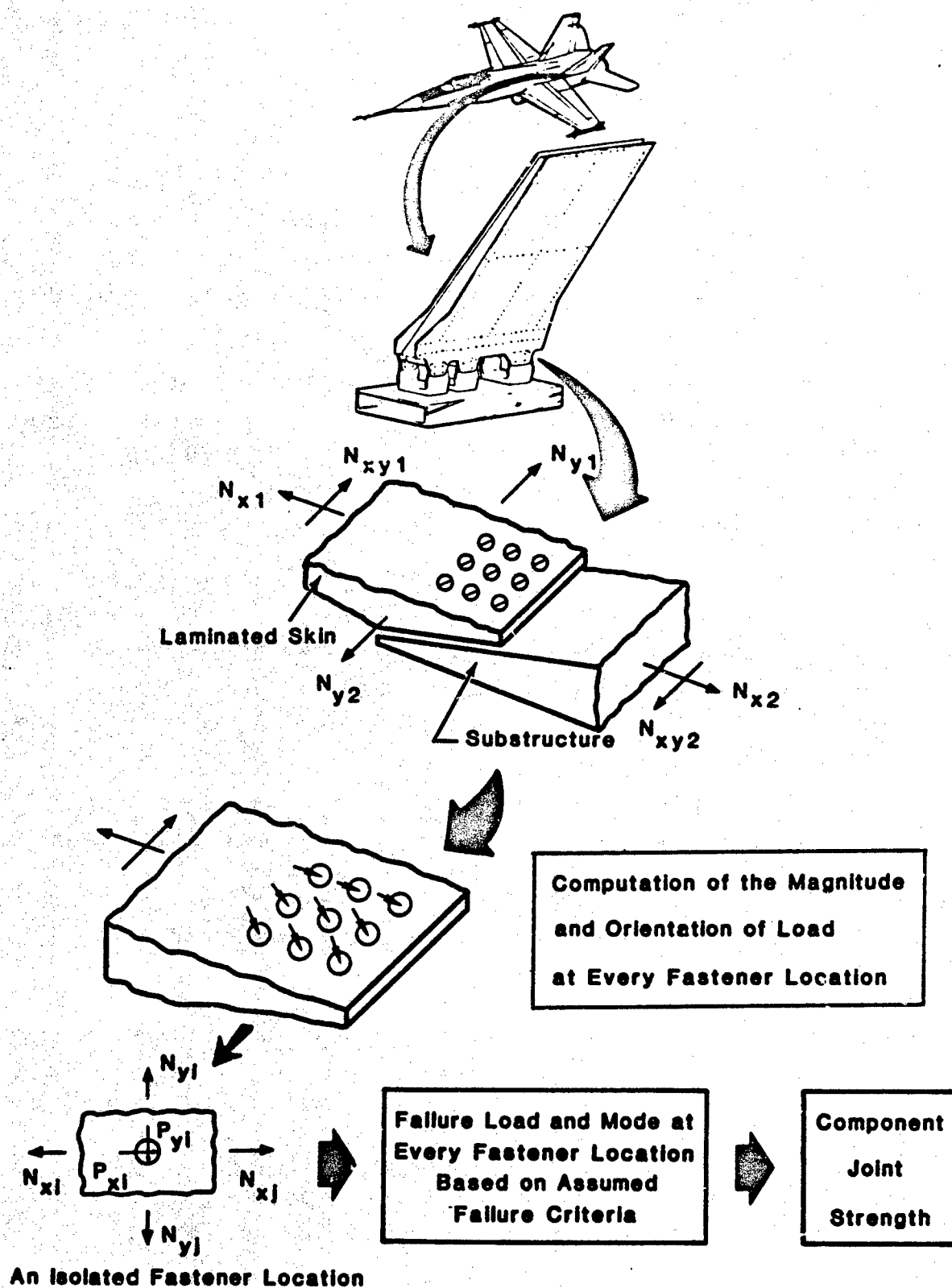
From an analytical standpoint, the major limitations of the BJSFM analysis are:

(1) It assumes the planform dimensions of the bolted laminate to be infinite (L and W $\rightarrow\infty$ in Figure 1-2).

(2) It circumvents the bolt/laminate contact problem by assuming a coŝinusoidal bearing load distribution over half the hole boundary. It also ignores the effect of friction between the fastener and the laminate (see Figure 2-1).

(3) It does not account for the effect of many joint parameters that render the two dimensional analysis inaccurate. Load transfer in a single shear situation, for example, is assumed to be equivalent to a double shear situation. The fastener is also assumed to be rigid in shear and bending, and the effects of fastener torque are ignored.

(4) Joint failure is assumed to be precipitated by the first ply failure, each ply is assumed to be linear elastic to failure, and ply failure modes are not predicted. Consequently, a comparison between predicted joint strengths and measured values exhibits a poor correlation in many situations.

The SASCJ code discussed in this report overcomes all the above BJSFM limitations with the exception of item (2). In overcoming these limitations, an improved two-dimensional plate analysis, a fastener analysis and a progressive failure analysis were developed.

A brief summary of the program contributions to the strength analysis of bolted composite and metallic plates, via the SASCJ code, is presented in Table 1-1. These accomplishments represent a significant improvement over the state of the art at the program initiation stage (the BJSFM computer code), and aided the development of a validated strength analysis computer code (SASCJ).

Section 2 describes the two-dimensional analysis that accounts for the influence of finite planform dimensions on the solutions for a plate bolted by a single fastener. Section 3 presents the fastener analysis that

3
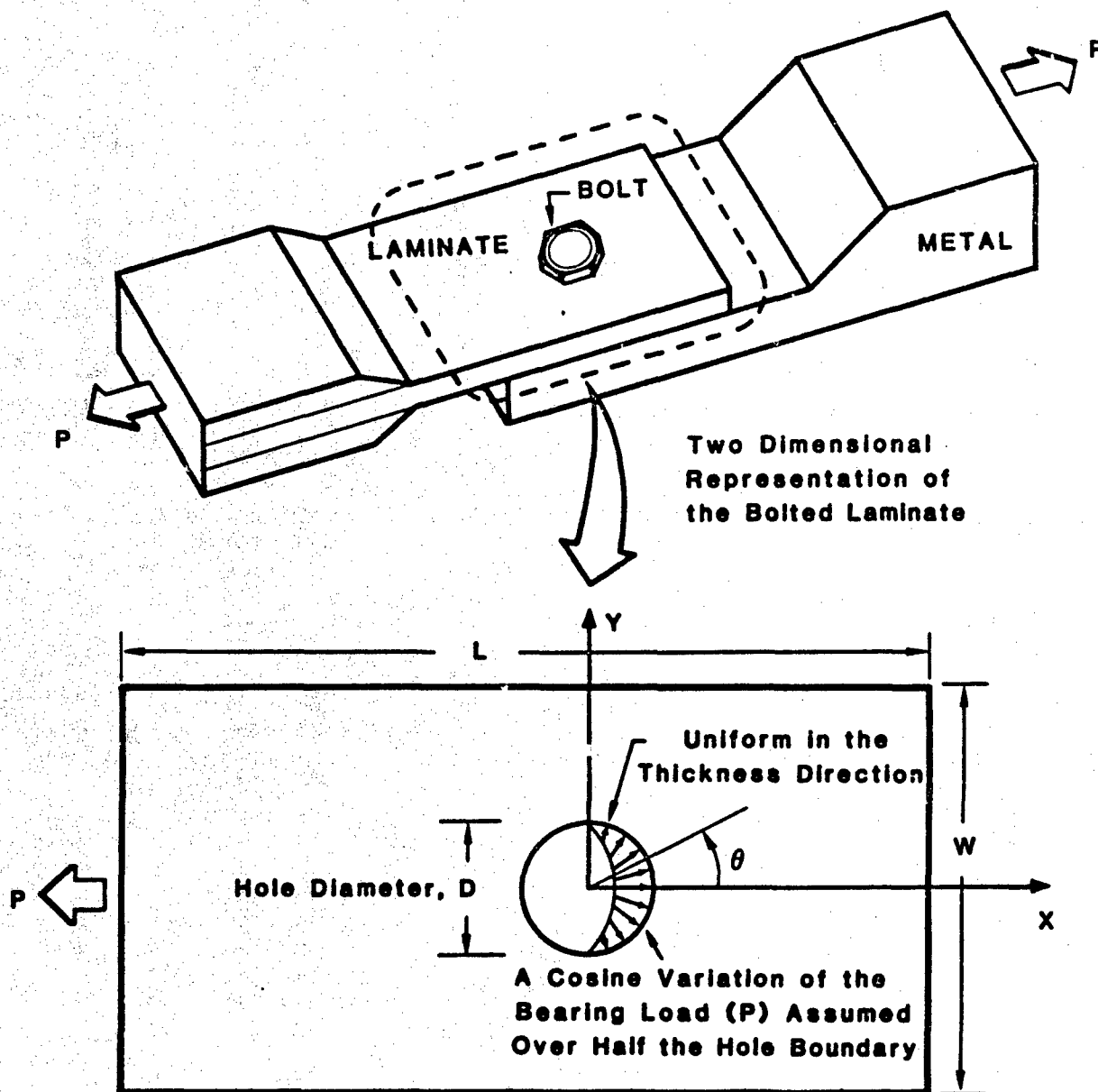
Figure 1-2. Schematic Representation of a Bolted Laminate with Finite Dimensions.

4

Table 1-1. SUMMARY OF PROGRAM CONTRIBUTIONS TO THE STRENGTH
ANALYSIS OF PLATES BOLTED BY A SINGLE FASTENER

	Prior to Program Initiation	Program Accomplishments
Available Strength Analysis Computer Code	BJSFM	SASCJ
Bolted Plate Geometry	Planform dimensions are assumed to be infinite.	Actual (finite) planform dimensions are accounted for.
Bolted Laminate Layup	Analysis is independent of (ignores) laminate stacking sequence.	Analysis accounts for the actual laminate stacking sequence.
Fastener Properties	Fastener is assumed to be a rigid, frictionless pin. Its bending and shear effects are ignored.	Fastener flexibility (bending and shear) effects are accounted for.
Fastener Torque	The effect of fastener torque is unaccounted for.	Fastener torque effects are included in the fastener analysis.
Load Eccentricity	Analysis only represents a double shear load transfer situation	Analysis differentiates between single and double shear situations.
Strength Prediction	Prediction is based on first ply failure, and demonstrates a poor correlation with measured strengths.	Prediction is based on a progressive failure procedure, assuming two-stage ply failures, and agrees well with measured strengths.

5

accounts for fastener flexibility, load eccentricity and fastener torque. Section 4 describes the developed failure procedure that assumes nonlinear (bilinear) ply behavior and predicts the progression of local (ply) failures until the joint cannot carry any additional load (joint failure). Section 5 demonstrates an excellent agreement between SASCJ predictions and test results from Reference 1-1, validating the improved strength analysis.

SECTION 2

TWO-DIMENSIONAL ANALYSIS OF A FINITE LAMINATED
PLATE BOLTED BY A SINGLE FASTENER

As discussed in Section 1, a two-dimensional analysis of a finite bolted laminate is a primary requirement in the development of an analysis that predicts the strength of bolted laminates. In the following sub-sections, a brief description of the two-dimensional analysis developed in Reference 2-1 is presented along with sample predictions.

2.1   Governing Equation

The two-dimensional stress field in a finite bolted plate is expressed in terms of the Airy stress function $F(x,y)$ that automatically satisfies equilibrium equations everywhere in the plate domain. The corresponding displacement solution satisfies compatibility requirements when the following equation is satisfied by the stress function:

$$a_{22}F_{,xxxx} - 2a_{26}F_{,xxxy} + (2a_{12} + a_{66})F_{,xxyy} - 2a_{16}F_{,xyyy} +$$

$$a_{11}F_{,yyyy} = 0 \qquad\qquad (2-1)$$

where a_{ij} are laminate compliances as defined in Reference 2-2. Equation 2-1 is the governing equation for the problem of interest.

2.2   Complex Variables Approach

A complex variables approach, described in Reference 2-3, is undertaken to obtain the solution to Equation 2-1. This approach has been pursued by other investigators to solve similar problems (see References 2-4 to 2-7). Equation 2-1 can be written as follows, in terms of four linear differential operators of the first order:

$$D_1 D_2 D_3 D_4 F = 0 \qquad\qquad (2-2)$$

where D_i ($i=1,2,3,4$) denotes the linear differential operator

$$D_i = \frac{\partial}{\partial y} - \mu_i \frac{\partial}{\partial x} \qquad\qquad (2-3)$$

7

and μ_i are the roots of the following characteristic equation:

$$a_{11}\mu^4 - 2a_{16}\mu^3 + (2a_{12} + a_{66})\mu^2 - 2a_{26} + a_{22} = 0 \qquad (2\text{-}4)$$

For physically meaningful values of the constants a_{ij}, two solution types are possible:

(1) The roots of Equation 2-4 are two pairs of complex conjugates:

$$\mu_1 = \alpha + i\beta, \quad \mu_2 = \gamma + i\delta, \quad \mu_3 = \overline{\mu}_1, \text{ and } \mu_4 = \overline{\mu}_2 \qquad (2\text{-}5)$$

where a bar denotes a complex conjugate, and $\beta, \delta > 0$.

(2) The roots are pairwise equal:

$$\mu_1 = \mu_2 = \alpha + \beta i, \quad \overline{\mu}_1 = \overline{\mu}_2 = \alpha - \beta i \quad (\beta > 0) \qquad (2\text{-}6)$$

For an isotropic plate, $\mu_1 = \mu_2 = i$.

Rewrite Equation 2-2 as follows:

$$D_4 F = g_3; \quad D_3 D_4 F = g_2; \quad D_2 D_3 D_4 F = g_1; \quad D_1 g_1 = \frac{\partial g_1}{\partial y} - \mu_1 \frac{\partial g_1}{\partial x} = 0 \qquad (2\text{-}7)$$

The solution to the last equation may be written as:

$$g_1 = F_1(x + \mu_1 y) \qquad (2\text{-}8)$$

The general solution for F may then be written as:

(1) In the case of different complex roots,

$$F = F_1(x + \mu_1 y) + F_2(x + \mu_2 y) + F_3(x + \overline{\mu}_1 y) + F_4(x + \overline{\mu}_2 y) \qquad (2\text{-}9)$$

(2) In the case of pairwise equal complex roots,

$$F = F_1(x + \mu_1 y) + (x + \mu_1 y) F_2(x + \mu_1 y) + \text{ } (x + \overline{\mu}_1 y) + (x + \overline{\mu}_1 y)$$

$$F_4(x + \overline{\mu}_1 y) \qquad (2\text{-}10)$$

F_1, F_2, F_3 and F_4 are arbitrary functions of the corresponding variables. Redefining these variables as:

$$z_1 = x + \mu_1 y, \quad z_2 = x + \mu_2 y, \quad \overline{z}_1 = x + \overline{\mu}_1 y, \quad \overline{z}_2 = x + \overline{\mu}_2 y, \qquad (2\text{-}11)$$

and, recognizing that the stress function is a real function of x and y, Equations 2-9 and 2-10 may be written as:

(1) $F = 2\mathrm{Re}\ [F_1(z_1) + F_2(z_2)]$ when the roots are different, and $\qquad$ (2-12)

(2) $F = 2\mathrm{Re}\ [F_1(z_1) + z_1 F_2(z_1)]$ when the roots are equal. $\qquad$ (2-13)

In the computer code developed to do this analysis (FICEOM), the properties of an isotropic plate are perturbed very slighty so that only the solution case with unequal roots have to be considered. For this case, the following new complex functions ϕ_1 and ϕ_2 are introduced for convenience:

$$\phi_1(z_1) = \frac{dF_1}{dz_1}, \quad \phi_2(z_2) = \frac{dF_2}{dz_2} \qquad (2\text{-}14)$$

Derivatives of these functions are denoted as follows:

$$\phi_1'(z_1) = \frac{d\phi_1}{dz_1} \text{ and } \phi_2'(z_2) = \frac{d\phi_2}{dz_2}. \qquad (2\text{-}15)$$

Equations 2-12 and 2-14 provide the following expressions for stresses and displacements in the plate:

$$\sigma_x = 2\mathrm{Re}\ [\mu_1^2 \phi_1'(z_1) + \mu_2^2 \phi_2'(z_2)]$$

$$\sigma_y = 2\mathrm{Re}\ [\phi_1'(z_1) + \phi_2'(z_2)]$$

$$\tau_{xy} = -2\mathrm{Re}\ [\mu_1 \phi_1'(z_1) + \mu_2 \phi_2'(z_2)] \qquad (2\text{-}16)$$

$$u = 2\mathrm{Re}\ [p_1 \phi_1(z_1) + p_2 \phi_2(z_2)]$$

$$v = 2\mathrm{Re}\ [q_1 \phi_1(z_1) + q_2 \phi_2(z_2)]$$

where p_1, p_2, q_1 and q_2 are the complex constants defined below:

$$p_1 = a_{11}\mu_1^2 + a_{12} - a_{16}\mu_1, \quad p_2 = a_{11}\mu_2^2 + a_{12} - a_{16}\mu_2$$

$$\qquad (2\text{-}17)$$

$$q_1 = a_{12}\mu_1 + a_{22}/\mu_1 - a_{26}, \quad q_2 = a_{12}\mu_2 + a_{22}/\mu_2 - a_{26}$$

9

Any expression for F in terms of arbitrarily assumed ϕ_1 (z_1) and ϕ_2 (z_2) functions is a solution to the two-dimensional problem, provided these expressions satisfy the appropriate boundary conditions. Recall that ϕ_1 (z_1) and ϕ_2 (z_2) automatically satisfy the governing equation. The problem of interest involves a finite anisotropic plate with a loaded or unloaded circular or elliptical hole (see Figure 2-1). In general, for arbitrary geometry and boundary conditions, one cannot determine closed form solutions for ϕ_1 and ϕ_2. One method of obtaining approximate solutions is to consider series expansions of the functions with unknown coefficients. These unknown coefficients are then determined by satisfying the boundary conditions approximately. In contrast to series expansions in z_1 and z_2, faster convergence is obtained if series expansions are assumed in coordinates ξ_1 and ξ_2, obtained by using the following mapping functions:

$$\xi_1 = (z_1 \pm \sqrt{z_1^2 - a^2 - \mu_1^2 b^2})/(a - i\mu_1 b) \geq 1$$

$$\xi_2 = (z_2 \pm \sqrt{z_2^2 - a^2 - \mu_2^2 b^2})/(a - i\mu_2 b) \geq 1 \qquad (2\text{-}18)$$

In a laminate with a circular or an elliptical hole, the internal boundary gets transformed to an ellipse in the $z_1 - z_2$ plane (see Equation 2-11). The functions in Equation 2-18 map the internal boundary to a unit circle in the $\xi_1 - \xi_2$ plane, and the physical region of the laminate to the exterior of the unit circle (see Figure 2-1). The signs of the square root terms in Equation 2-18 are chosen such that the internal boundary is mapped on to the unit circle. Note that these mapping functions are analytic functions, and hence the mapping is conformal.

In the $\xi_1 - \xi_2$ plane, ϕ_1 and ϕ_2 are assumed to be the following modified Laurent series expansions:

$$\phi_1(\xi_1) = \alpha_0 \ln\xi_1 + \sum_{n=1}^{\infty} (\alpha_{-n}\xi_1^{-n} + \alpha_n\xi_1^n)$$

$$\phi_2(\xi_2) = \beta_0 \ln\xi_2 + \sum_{n=1}^{\infty} (\beta_{-n}\xi_2^{-n} + \beta_n\xi_2^n) \qquad (2\text{-}19)$$

10
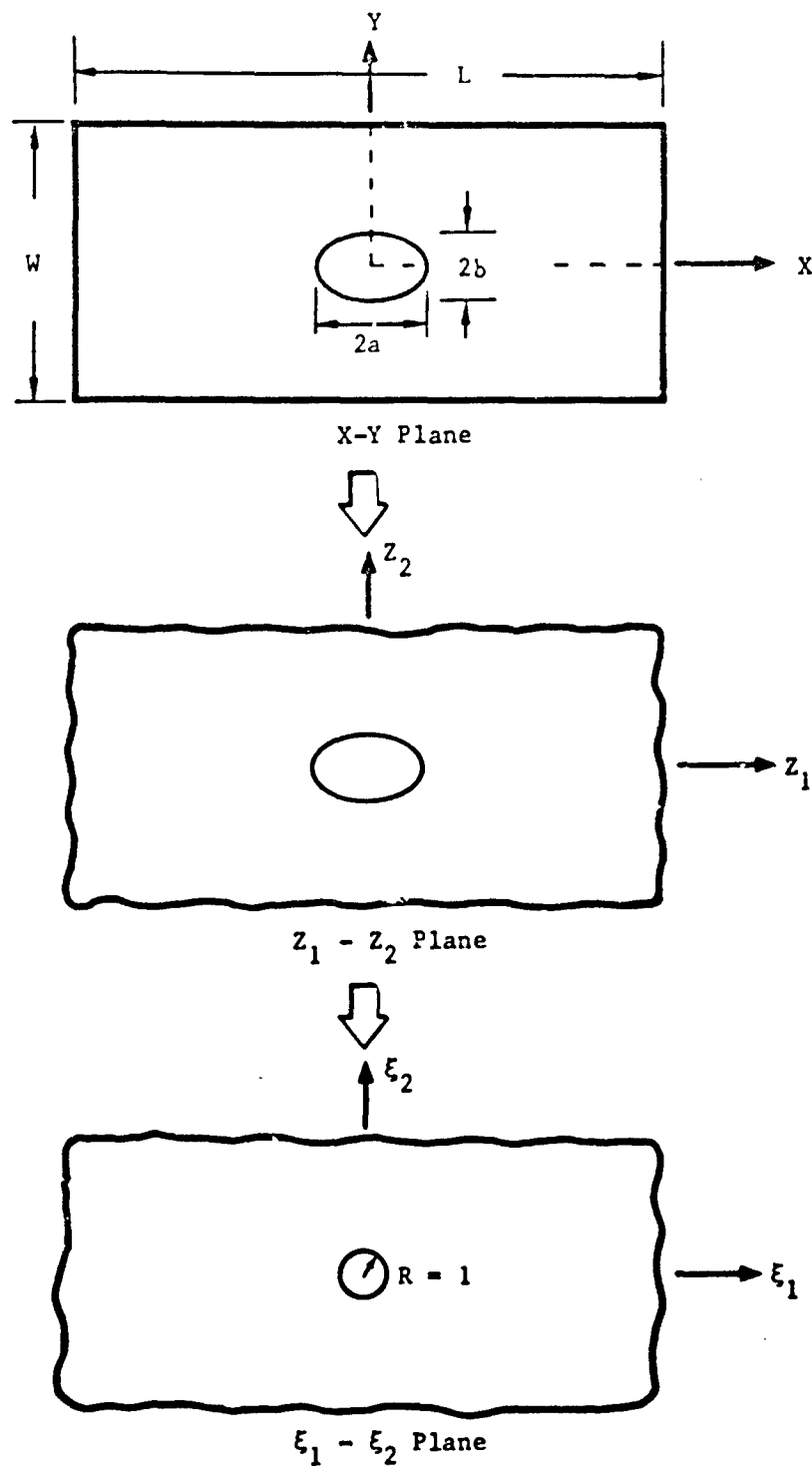
Figure 2-1. Conformal Mapping of the Finite Anisotropic Plate to the Z_1-Z_2 and ξ_1 - ξ_2 Planes.

11

In the above expressions, α_i and β_i are complex coefficients which are determined so as to satisfy the boundary conditions. The logarithmic terms drop out if the force resultants on the internal boundary are zero (see Reference 2-7).

The stresses   ons of ϕ_1' and ϕ_2', and these derivatives are expressed as:

$$\phi_1' = (\alpha_0 + \sum_{n=1}^{\infty} (n\alpha_n \xi_1^n - n\alpha_{-n}\xi_1^{-n})) / \sqrt{z_1^2 - a^2 - \mu_1^2 b^2}$$

$$\phi_2' = (\beta_0 + \sum_{n=1}^{\infty} (n\beta_n \xi_2^{-n} - n\beta_{-n}\xi_2^{-n})) / \sqrt{z_2^2 - a^2 - \mu_2^2 b^2} \tag{2-20}$$

In specific cases, the above expressions simplify. For example, in the solutions for infinite plates, the positive exponent terms drop out as the stresses have to be bounded at infinity. For most infinite plate problems, the solutions reduce to a one term solution (see Reference 2-3).

In the general case of a finite anisotropic plate with a loaded or unloaded hole, the coefficients can be numerically calculated to satisfy the boundary conditions. Generally, a convergent solution is obtained by truncating the series in Equation 2-19 as follows:

$$\phi_1 = \alpha_0 \ln\xi_1 + \sum_{n=1}^{N} (\alpha_{-n}\xi_1^{-n} + \alpha_n \xi_1^n)$$

$$\phi_2 = \beta_0 \ln\xi_2 + \sum_{n=1}^{N} (\beta_{-n}\xi_2^{-n} + \beta_n \xi_2^n) \tag{2-21}$$

In order to determine the finite number of unknown coefficients, we can select the same total number of points on the inner and outer boundaries, and compute the unknown coefficients by satisfying the boundary conditions exactly at these points. However, in this case, the calculated solutions at other boundary points are significantly different from the imposed boundary conditions (see Reference 2-4). As shown in Reference 2-4, a more desirable approach is to choose a larger number of boundary points than the number of unknown coefficients, and to satisfy the boundary conditions at these points

12

in a least squares sense. This solution procedure has been adopted in the analysis in Reference 2-1. Prior to applying the least squares boundary collation procedure, the single-valuedness of the displacements and the rigid body rotational constraint have to be imposed.

2.3 Single-Valuedness of Displacements

In the series expansions for ϕ_1 and ϕ_2 (Equation 2-21), the logarithmic terms are multi-valued and give rise to multi-valued displacements. To be physically meaningful, the displacement functions have to be single-valued, and these conditions have to be explicitly imposed on the coefficients of the logarithmic terms.

From Equations 2-16 and 2-21, the contributions of the logarithmic terms to the displacements u and v are seen to be $2Re(p_1\alpha_o\ln\xi_1 + p_2\beta_o\ln\xi_2)$ and $2Re(q_1\alpha_o\ln\xi_1 + q_2\beta_o\ln\xi_2)$, respectively. For the displacements to be single-valued, the increment acquired by the above functions in describing the internal boundary should be zero (see Reference 2-8). On the internal boundary, $|\xi_1| = |\xi_2| = 1$, and $\xi_1 = \xi_2 = e^{i\theta}$. Therefore, $Re\left\{p_1\alpha_o(i\theta) + p_2\beta_o(i\theta)\right\}\Big|_o^{2\pi} = 0$ and $Re\left\{q_1\alpha_o(i\theta) + q_2\beta_o(i\theta)\right\}\Big|_o^{2\pi} = 0$. Or,

$$Im(p_1\alpha_o + p_2\beta_o) = p_1\alpha_o + p_2\beta_o - \bar{p}_1\bar{\alpha}_o - \bar{p}_2\bar{\beta}_o = 0$$

$$Im(q_1\alpha_o + q_2\beta_o) = q_1\alpha_o + q_2\beta_o - \bar{q}_1\bar{\alpha}_o - \bar{q}_2\bar{\beta}_o = 0 \qquad (2-22)$$

Imposition of the above two conditions will ensure that the computed displacements are single-valued. Equations 2-22 eliminate two of the unknown constants:

$$\alpha_o = \left[(p_2\bar{q}_1 - q_2\bar{p}_1)\bar{\alpha}_o + (p_2\bar{q}_2 - q_2\bar{p}_2)\bar{\beta}_o\right]/(q_1p_2 - q_2p_1) \qquad (2-23)$$

$$\beta_o = \left[(q_1\bar{p}_1 - \bar{q}_1p_1)\bar{\alpha}_o + (q_1\bar{p}_2 - \bar{q}_2p_1)\bar{\beta}_o\right]/(q_1p_2 - q_2p_1) \qquad (2-24)$$

2.4 Zero Rigid Body Rotation

The rotation ω of an infinitesimal element at any point (x, y) in the laminate is given by:

$$\omega(x, y) = \frac{\partial u}{\partial x} - \frac{\partial v}{\partial y} \tag{2-25}$$

Using Equation 2-16,

$$\omega(x,y) = \text{Re}\left\{(\mu_1 p_1 - q_1)\phi_1' + (\mu_2 p_2 - q_2)\phi_2'\right\}$$

$$= \text{Re}\left\{(\mu_1 p_1 - q_1)\alpha_1\left[z_1/\sqrt{z_1^2 - a^2 - \mu_1^2 b^2}^2 + 1/(a - i\mu_1 b)\right]\right.$$

$$\left. + (\mu_2 p_2 - q_2)\beta_1\left[z_2/\sqrt{z_2^2 - a^2 - \mu_2^2 b}^2 + 1/(a - i\mu_2 b)\right]\right\}$$

+ terms involving ξ_1 and ξ_2 with negative and positive exponents ≥ 2

$$= \text{Re}\left[(\mu_1 p_1 - q_1)\alpha_1/(a - i\mu_1 b) + (\mu_2 p_2 - q_2)\beta_1/(a - i\mu_2 b)\right] \tag{2-26}$$

+ terms which are functions of x and y (i.e., are not constant)

For the rigid body rotation of the laminate to be zero, the constant term above should be zero. Hence,

$$\text{Re}\left[(\mu_1 p_1 - q_1)\alpha_1/(a - i\mu_1 b) + (\mu_2 p_2 - q_2)\beta_1/(a - i\mu_2 b)\right] = 0$$

Or,

$$(\mu_1 p_1 - q_1)\alpha_1/(a - i\mu_1 b) + (\mu_2 p_2 - q_2)\beta_1/(a - i\mu_2 b)$$

$$+ (\bar{\mu}_1\bar{p}_1 - \bar{q}_1)\bar{\alpha}_1/(a + i\bar{\mu}_1 b) + (\bar{\mu}_2\bar{p}_2 - \bar{q}_2)\bar{\beta}_1/(a + i\bar{\mu}_2 b) = 0 \tag{2-27}$$

This eliminates one more unknown constant:

$$\alpha_1 = -\frac{a - i\mu_1 b}{\mu_1 p_1 - q_1}\left[\frac{\mu_2 p_2 - q_2}{a - i\mu_2 b}\beta_1 + \frac{\bar{\mu}_1\bar{p}_1 - \bar{q}_1}{a + i\bar{\mu}_1 b}\bar{\alpha}_1 + \frac{\mu_2 p_2 - q_2}{a + i\bar{\mu}_2 b}\bar{\beta}_1\right] \tag{2-28}$$

14

2.5 Least Squares Solution to an Over-Determined System of Linear Equations

Consider the following over-determined system of linear algebraic equations:

$$[A] \ \{x\} = \{b\} \tag{2-29}$$

where $[A]$ is $M \times N$, $\{x\}$ is $N \times 1$, and $\{b\}$ is $M \times 1$ in size, and $M > N$.

The least squares solution, i.e., the solution that minimizes the sum of the squares of the error in each equation, is given by:

$$\frac{\partial}{\partial x_k} \left(\sum_{i=1}^{M} \left(\left(\sum_{j=1}^{N} A_{ij} x_j \right) - b_i \right)^2 \right) = 0 \text{ for } k=1,2,\ldots N \tag{2-30}$$

Or,

$$\sum_{i=1}^{M} \left(\sum_{j=1}^{N} A_{ij} x_j - b_i \right) A_{ik} = 0 \quad \text{for } k = 1,2,\ldots.N \tag{2-31}$$

The above N equations can be combined to produce the following matrix equation:

$$[A]^T \ [A] \ \{x\} - [A]^T \{b\} = \{0\} \tag{2-32}$$

The least squares solution is then expressed as:

$$\{x\} = \left([A]^T \ [A] \right)^{-1} [A]^T \{b\} \tag{2-33}$$

2.6 Least Squares Boundary Collocation Solution Procedure

Consider the finite anisotropic plate in Figure 2-1. If it has an unloaded hole, every point on the hole boundary is stress-free. That is, the normal and tangential stress components (σ_r and $\tau_{r\theta}$) are zero along the boundary. In this case, the applied loads on the external boundaries are self-equilibrating. Let a total of M collocation points be selected on the hole boundary and the external boundaries. At each point, the normal and shear stress components are known. Using Equation 2-16, all the 2M boundary conditions are written in terms of the unknown constants in Equation 2-21. Stress boundary conditions on the hole boundary are transformed from the r-θ

15

coordinates in which they are easily specified, to the x - y coordinates in which Equation 2-16 is expressed, using appropriate transformation equations (see Reference 2-2). The 2M boundary conditions are expressed in matrix form as:

$$2Re\left([B] \{\delta\}\right) = \{R\} \tag{2-34}$$

$$\text{Or,} \quad [B \quad \bar{B}] \begin{Bmatrix} \delta \\ \bar{\delta} \end{Bmatrix} = \{R\} \tag{2-35}$$

where $[B]$ is a 2M x (4N+2) complex matrix, $\{\delta\}$ is a (4N+2) x 1 vector of the unknown complex coefficients $(\alpha_{-N}) \ldots, \alpha_{-1}, \alpha_o, \ldots \alpha_N, \beta_{-N}, \ldots, \beta_o, \beta_1, \ldots \beta_N)$, and $\{R\}$ is a 2M x 1 real vector that contains the specified boundary values.

Imposition of the displacement single-valuedness and zero rigid body rotation conditions (Equations 2-23, 2-24 and 2-28) eliminates three unknowns. Using the form in Equation 2-35, the vector of unknown complex coefficients reduces in size from (8N+4) x 1 to (8N+1) x 1. The reduced system of equations is written as:

$$[C] \{\gamma\} = \{R\} \tag{2-36}$$

where $[C]$ is a 2M x (8N+1) complex matrix and $\{\gamma\}$ is the vector of 8N+1 unknown complex coefficients $(\alpha_{-N}, \bar{\alpha}_{-N}, \ldots, \bar{\alpha}_N, \beta_{-N}, \bar{\beta}_{-N}, \ldots, \bar{\beta}_N,$ except $\alpha_o,$ α_1 and $\beta_o)$. Pre-multiplying equation 2-36 by $[\bar{C}]^T$, its least squares solution is:

$$\{\gamma\} = \left([\bar{C}]^T [C]\right)^{-1} [\bar{C}]^T \{R\} \tag{2-37}$$

Once the complex coefficients in Equation 2-21 are determined, the stresses and the displacements are calculated using Equation 2-16. The accuracy of the solution is determined by recalculating the stresses at the boundaries and comparing them to the imposed boundary conditions. As discussed later, an N value of 7 and approximately 100 points on the boundary are sufficient to recover the imposed boundary conditions with 5%.

If the anisotropic plate in Figure 2-1 has a loaded hole, the assumptions made in Reference 2-9 are retained. The fastener is assumed to be frictionless and is assumed to bear over half the hole boundary. The fastener/laminate contact problem is by-passed, and the contact solution is assumed to be a cosinusoidal distribution of the radial stress (σ_r) around the hole (see

16

Figure 1-2). The tangential stress ($\tau_{r\theta}$) is zero around the frictionless hole boundary. Results from recent investigations (References 2-5 and 2-6) indicate that the contact problem could affect the local stresses significantly. Nevertheless, once the contact stress conditions around the hole boundary are computed and incorporated into the least squares boundary collocation solution procedure, the two-dimensional solution is computed as explained earlier.

The discussed boundary collocation solution procedure has been programmed to be the FIGEOM (Finite Geometry) computer code (see Reference 2-1).

2.7   Effect of Number of Terms in the Assumed Series

The FIGEOM computer code was initially used to determine the effect of the number of terms in the assumed series expressions (N in Equation 2-21) on the computed solution. For this purpose, a 50/40/10 laminate (from Reference 2-10) with a 1/4 inch diameter unloaded hole was considered. The laminate was subjected to a tensile loading as shown in Figure 2-2, and σ_x (0,D/2)/σ_o was computed for various values of N. The width of the laminate was assumed to be small (W/D=2) to influence the computed σ_x (0,D/2) value. A plot of σ_x (0,D/2)/σ_o versus N indicates that the solution coverages when N exceeds 6 in value (see Figure 2-2).

Similar studies were also conducted on other laminate layups and on metallic plates. For large W/D and E/D values (outer boundaries located with respect to the center of the hole by distances in excess of 4D), a smaller N value (N < 6) yields a converged solution. Based on these studies, N was set equal to 7 for subsequent analyses, to ensure converged solutions under all situations.

2.8   Effect of Number of Collocation Points

Let N_H be the number of collocation points along the hole boundary, and let N_R be the number of collocation points on the remote boundaries. The total number of collocation points, M, is then equal to $N_H + N_R$. Referring to Section 2.6, M has to be greater than 4N + 2, where N is the number of terms in the assumed stress functions (see Equation 2-21). When N = 7, M has to be greater than 30.
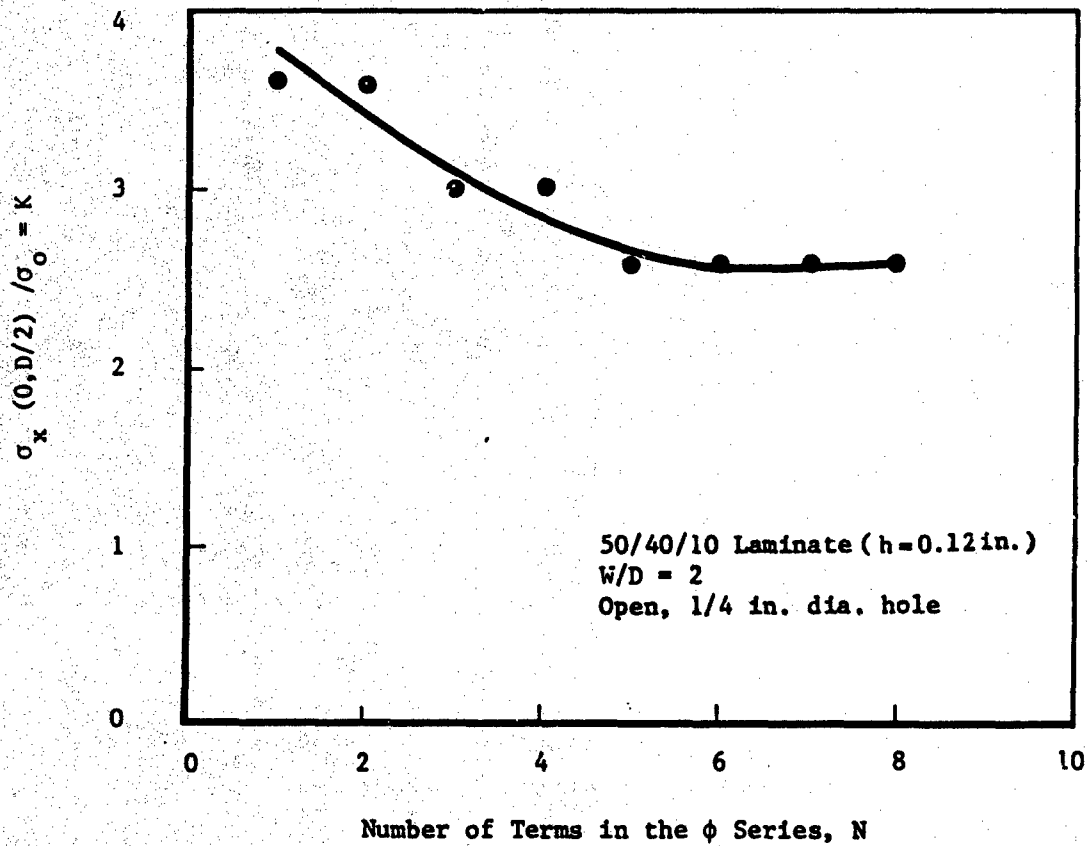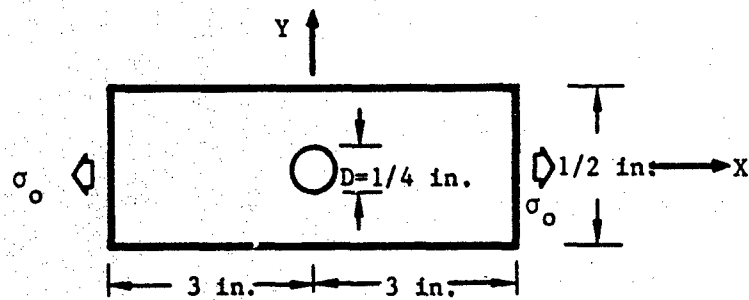
Figure 2-2. Effect of N on Solution Convergence.

Cons.der a 50/40/10 laminate subjected to a static tensile load in
double sheai (see Figure 2-3). The applied load is fully resisted by the
fastener. Three situations are analyzed to evaluate the effect of the number
of collocation points on the convergence of the solution. The first situation
involves a 5/16 inch diameter hole and a laminate geometry defined by E/D = 1.2
and W/D 1.6. The second situation involves D = 1/4 inch, E/D = 1.5 and W/D = 2.0.
The last example considers a laminate with D = 1/4 inch, E/D = 3 and W/D = 4.
In every case, the computed σ_x value at (0, D/2) is normalized with respect to
the applied remote stress value (1 ksi) to obtain a stress concentration value
of K. The results for the three laminate geometries are presented in Figure 2-3.
Every remote boundary contains $N_R/4$ collocation points. It is seen that, when
E/D and W/D are very small (1.2 and 1.6, respectively), K converges slowly with
N_R. But, when E/D and W/D are not very small (E/D $\gtrsim$ 1.5, W/D$\gtrsim$2), K converges
more rapidly when N_R is increased. N_H = 30 and N_H = 50 provide approximately
the same results (first example). If E $\geq$ 1.5 D and W $\geq$ 2D, K changes by less
than 5% when $N_R/4$ is increased beyond a value of 10.

Tased on the results in Figure 2-3, subsequent analyses using the
FIGEOM computer code were carried out with N_H = 50 and $N_R/4$ = 10, using a
total of 90 collocation points, unless specified otherwise.

2.9   Sample FIGEOM Predictions

Having established N, N_H and N_R values (7, 50 and 40, respectively)
for solution convergence, FIGEOM is now applied to a few sample test cases
to demonstrate its predictive capability. The first example considers a
50/40/10 laminate with an unloaded hole (Reference 2-10), subjected to a
uniform tensile loading. The hole diameter is 1/4 inch and E/D and W/D are
small (2). Figure 2-4 compares the normalized σ_x (0, y) variation across
the hole, predicted by FIGEOM, with the predictions using two other analyses
(References 2-7 and 2-9). FIGEOM predictions agree well with those based on
a similar analysis (Reference 2-7), but a considerable difference is observed
in comparison to the infinite plate solution (Reference 2-9). The infinite
plate solution will be approximately equal to the finite plate solution
(FIGEOM) when E/D and W/D values are much larger than four.
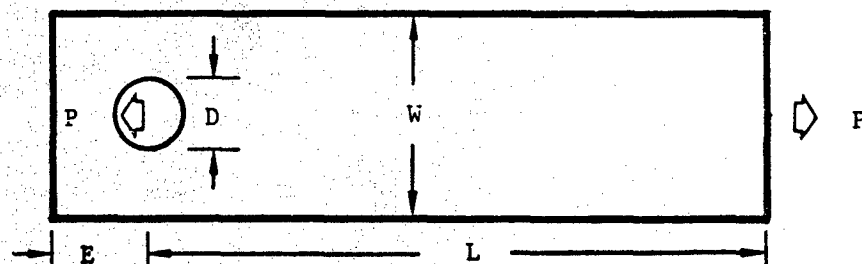
50/40/10 Laminate (Ref. 2-10); h = 0.119 in.
L = 3in.; Full bearing in double shear (0.15 in. Al)
N_R = number of collocation points on the remote boundaries
N_H = number of collocation points on the hole boundary
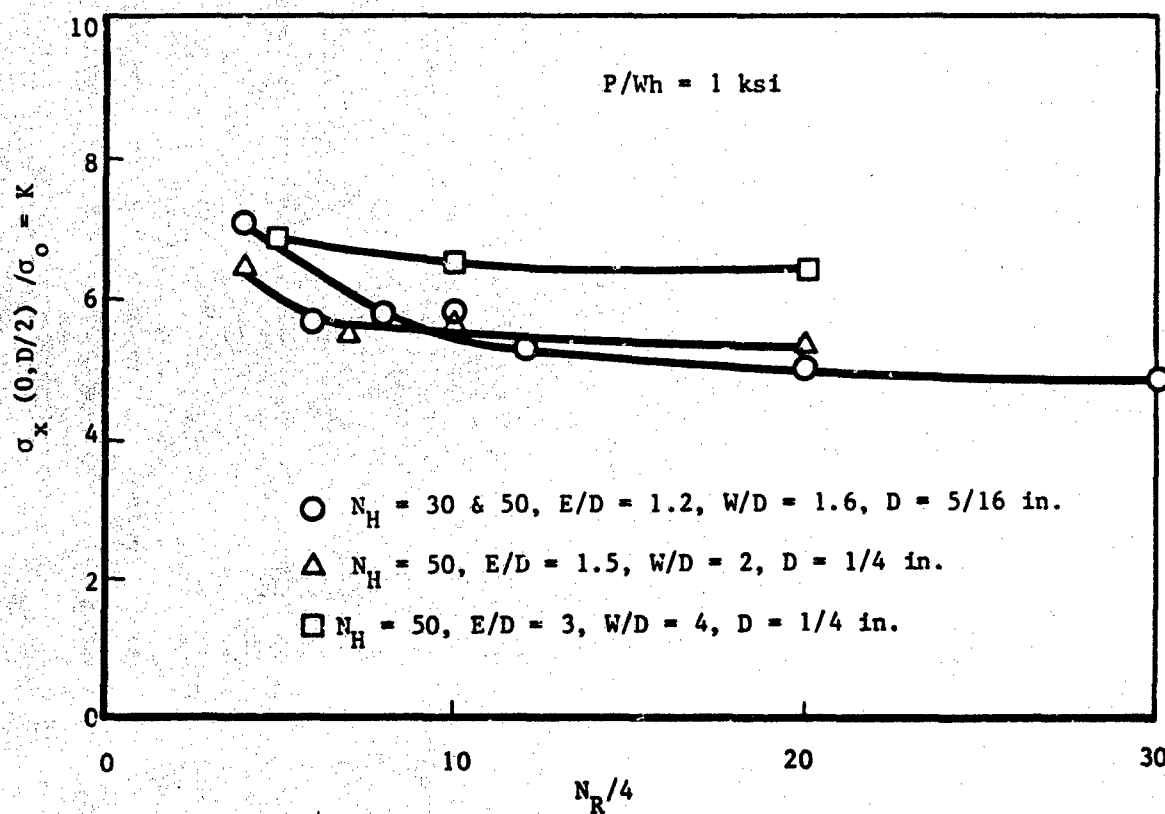
Figure 2-3. Effect of Number of Collocation Points on
Solution Convergence.

20
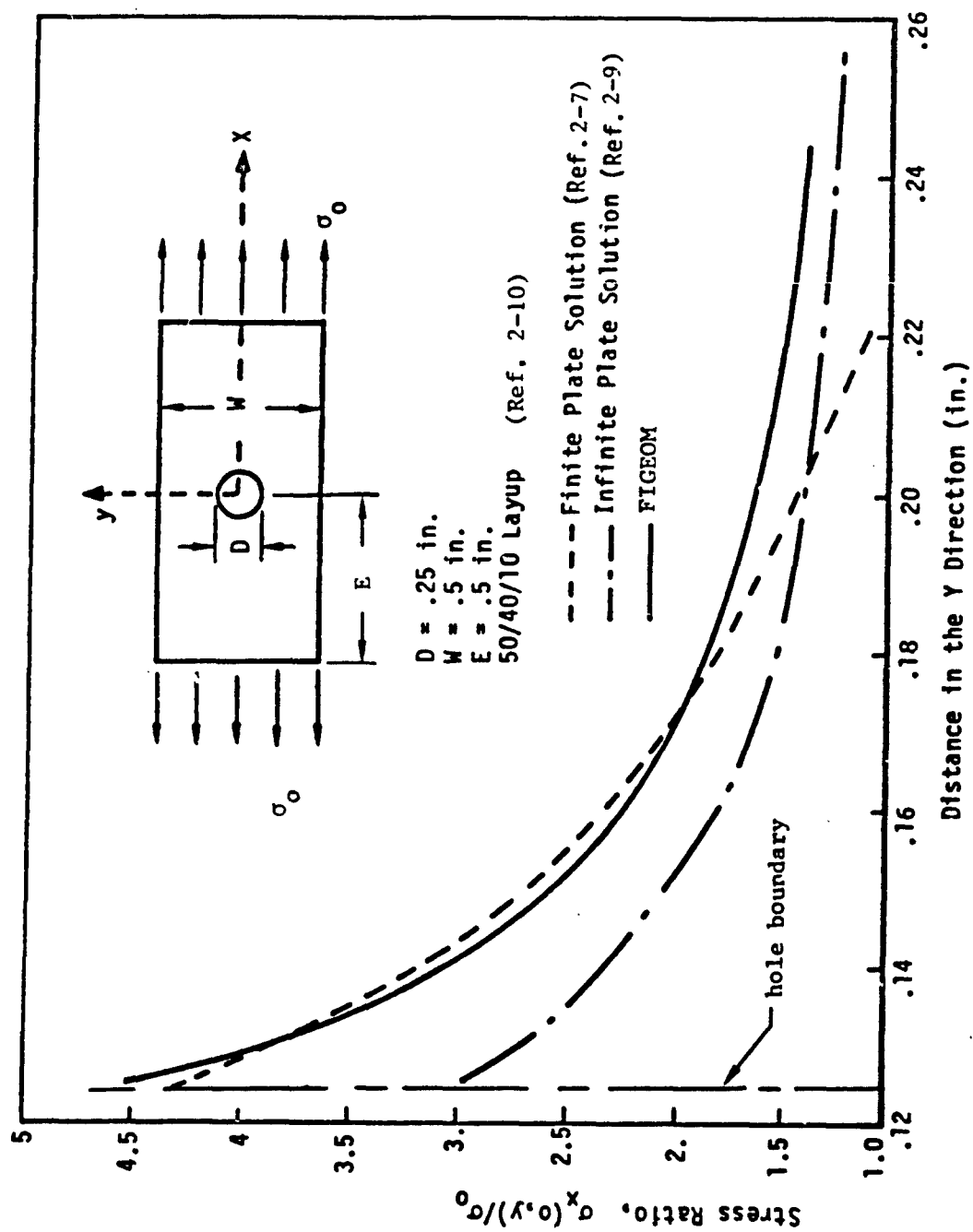
Figure 2-4. Stress Distribution in a Laminate with an Unloaded Hole.

The effect of plate width, or the W/D ratio, on the stress concentration
at (0, D/2) is shown in Figure 2-5. The unloaded hole is 1/4 inch in diameter
and E/D is equal to 3. Three laminates from Reference 2-10 are considered.
It is seen that the stress concentration is relatively unchanged beyond W/D=4,
but increases significantly when W/D is decreased below four.

The effect of the edge distance on the stress concentration at (0, D/2)
is shown in Figure 2-6. In this case, E/D has relatively no effect on the
stress concentration in all three laminates. If the hole had been a loaded
hole, E/D would have had a more significant effect on K.

The effects of E/D and W/D on the tangential stress distribution
around the boundary of a loaded hole are shown in Figures 2-7 and 2-8. The
solutions from Reference 2-9, in both the figures, correspond to a location
0.02 inch from the hole boundary, and therefore yield lower stress concentra-
tions. The finite plate solution (FIGEOM) yields a larger stress concentra-
tion at $\theta = 90^{\circ}$ in comparison to the infinite plate solution, the approximate
finite width solution and the finite element solution presented in Reference
2-9. FIGEOM predictions, corresponding to a location 0.02 inch away from the
hole boundary, are expected to agree well with the finite element solutions.
At $\theta = 90^{\circ}$, $\sigma_{\theta} = \sigma_{x}$ (0, D/2). If E/D is reduced below three and W/D is re-
duced below six, the effect of the closer boundaries will result in much
larger stress concentrations at $\theta = 90^{\circ}$.

A non-rectangular plate geometry is shown in Figure 2-9. This sample
considers a laminated lug that transfers the applied load to aluminum plates
in a double shear configuration. The lug has a 50/40/10 layup, and the effect
of R/r on its stress concentration at x = 0 and y = r is shown in Figure 2-9.
In this case, $N_{R}/4$ was selected to be 20 instead of the value (10) used in other
sample analyses. The results in Figure 2-9 indicate that $\sigma_{x}(o,r)$, normalized
with respect to the average bearing stress, decreases when the outer boundary
is moved away from the loaded hole (R/r increases). A rectangular geometry
at R/r = 2 yields a lower normalized stress than the non-rectangular geometry.

The final example considers a situation where a fraction of the total
applied tensile load is transferred directly to the fastener hole location.

22
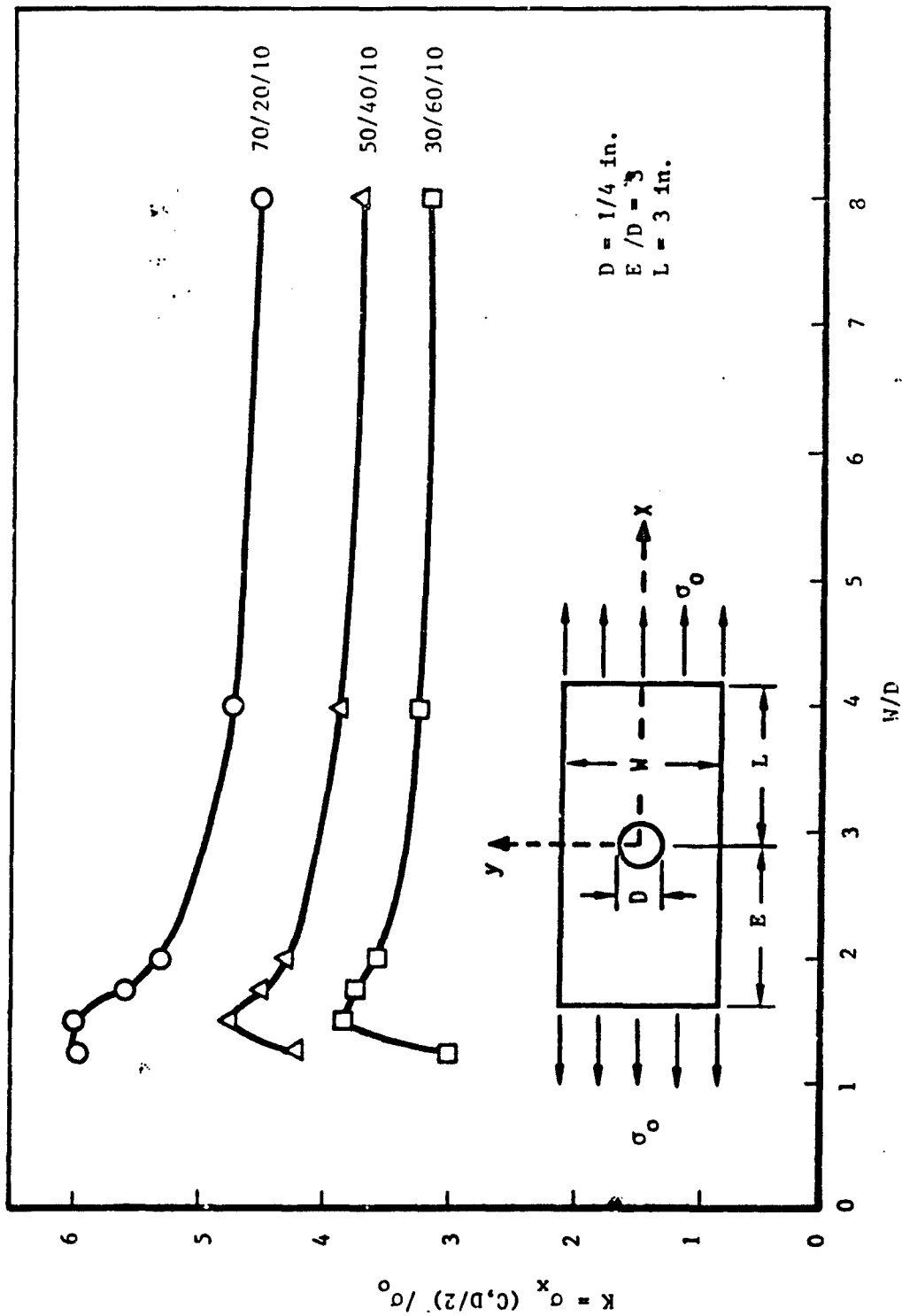
Figure 2-5. Effect of Plate Width (W/D Ratio) on Stress Concentration.

23
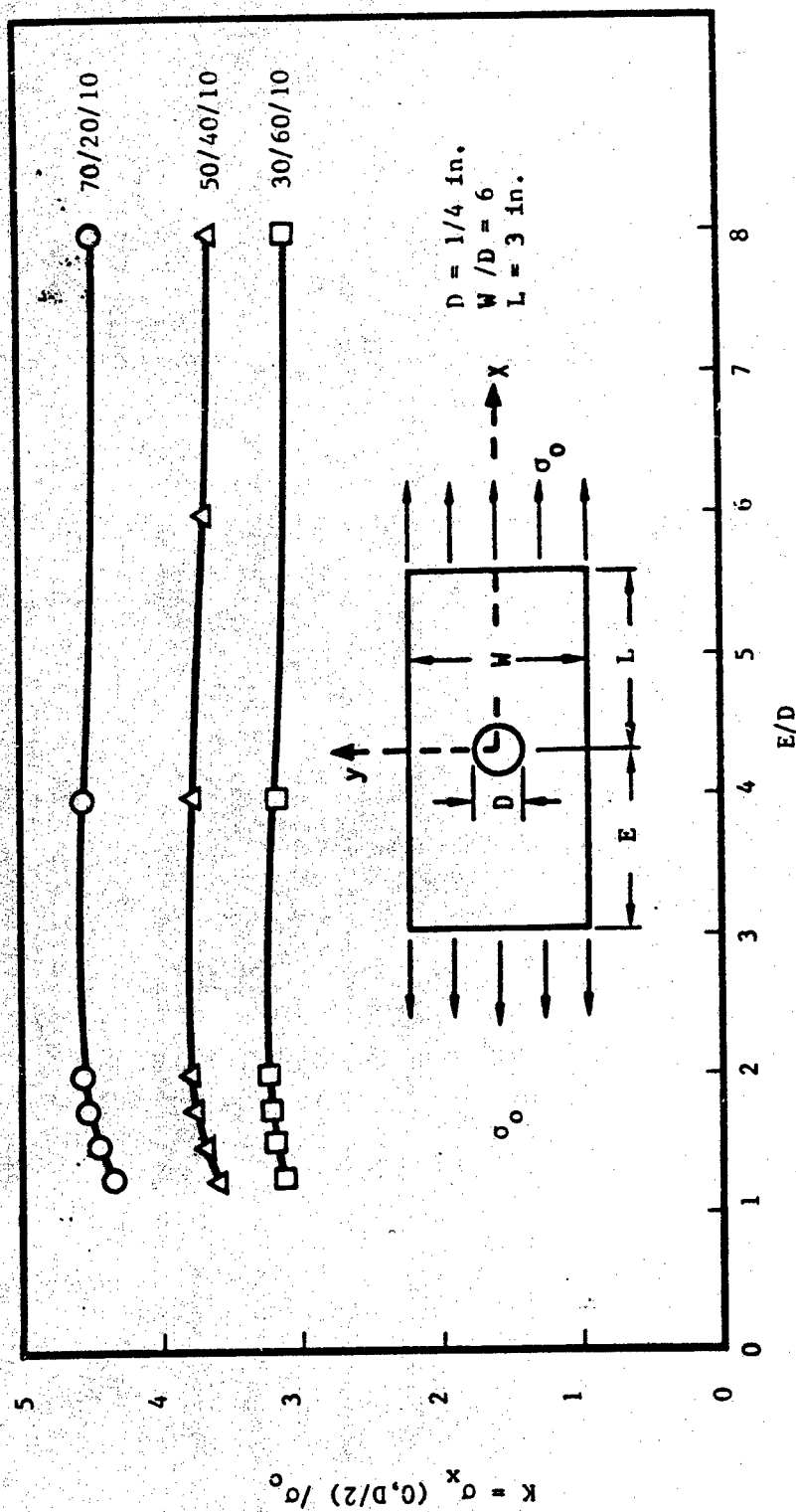
Figure 2-6. Effect of Edge Distance (E/D Ratio) on Stress Concentration.

24
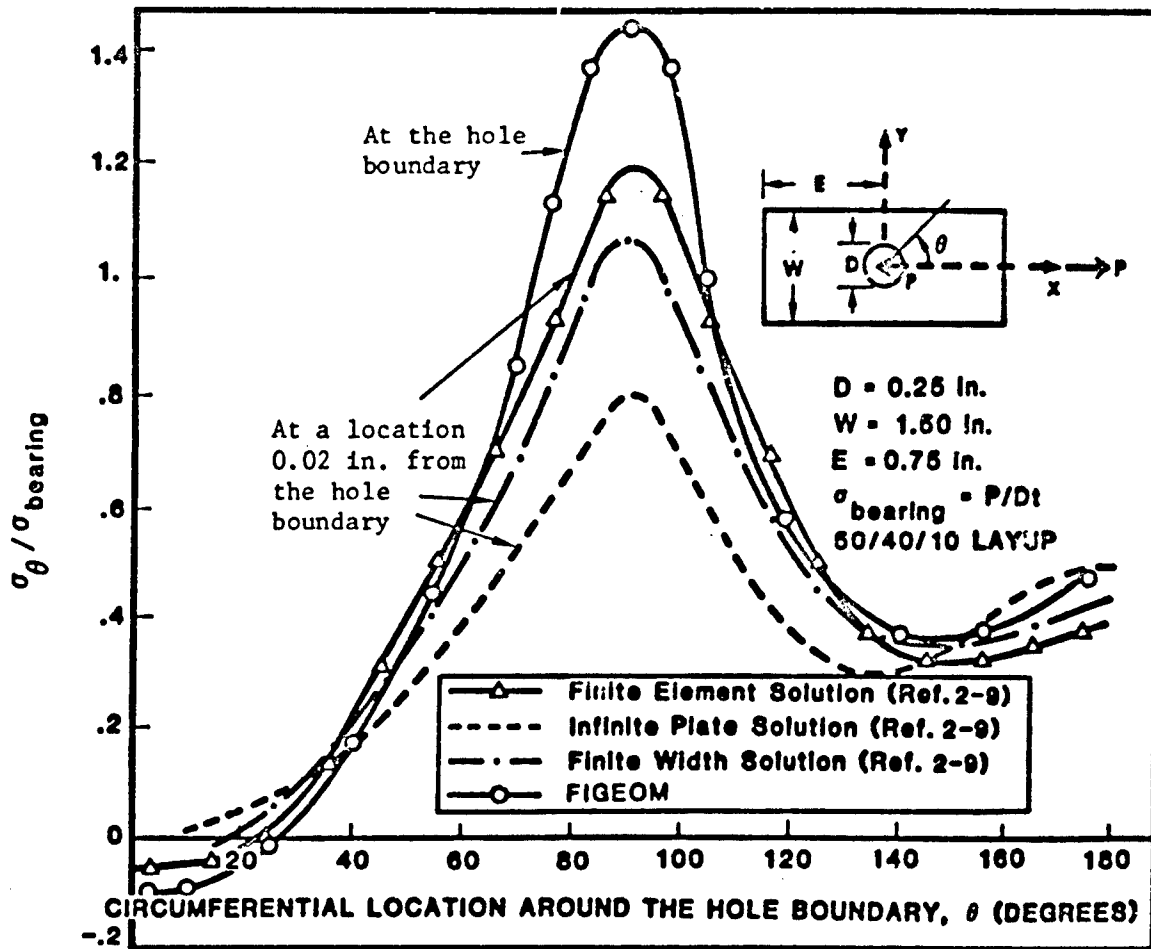
Figure 2-7. Effect of E/D = 3 and W/D = 6 on the σ_θ Variation with θ.
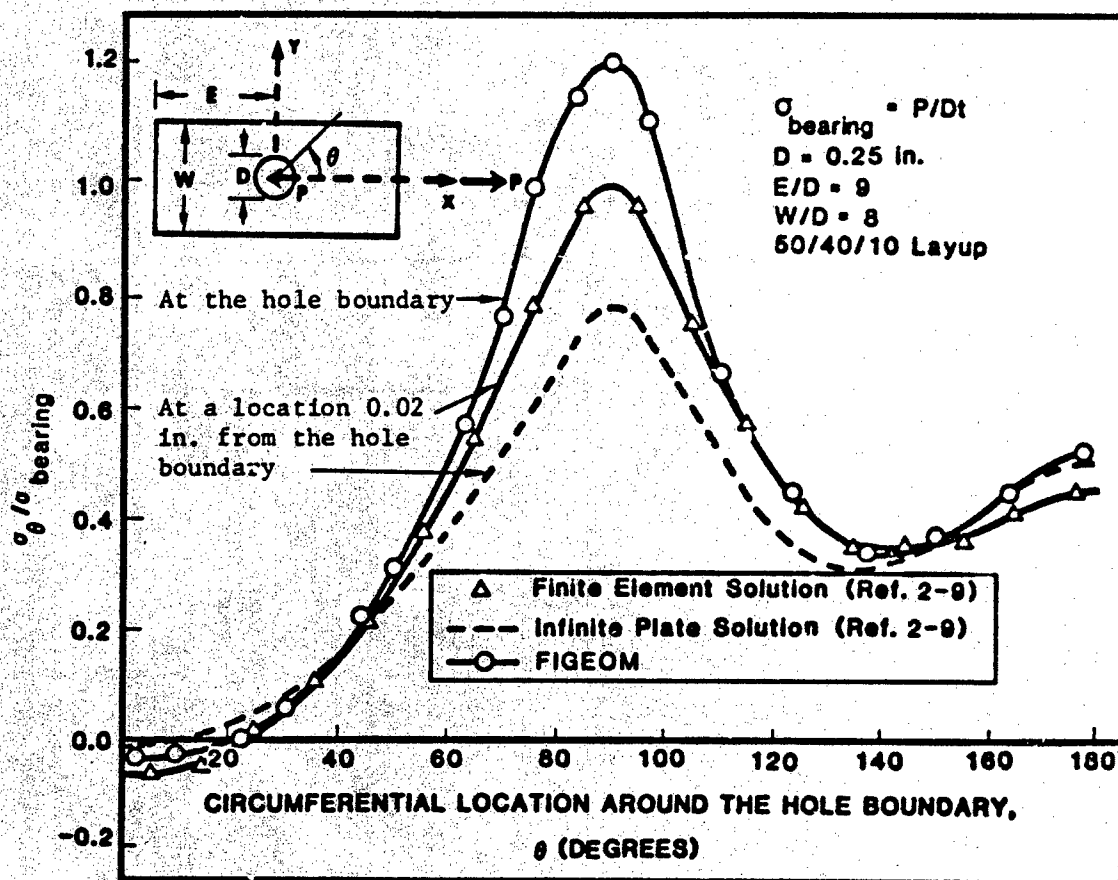
Figure 2-8. Effect of E/D = 9 and W/D = 8 on the σ_θ Variation with θ.
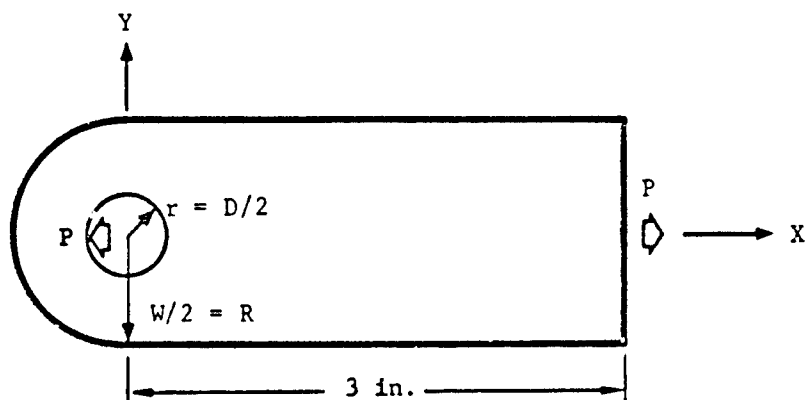
50/40/10 laminate; h = 0.119 in.; double shear load
transfer to 0.155 in. Al plates; P/Wh = 1 ksi
D = 1/4 in.; σ_{brg} = P/Dh = W/D ksi
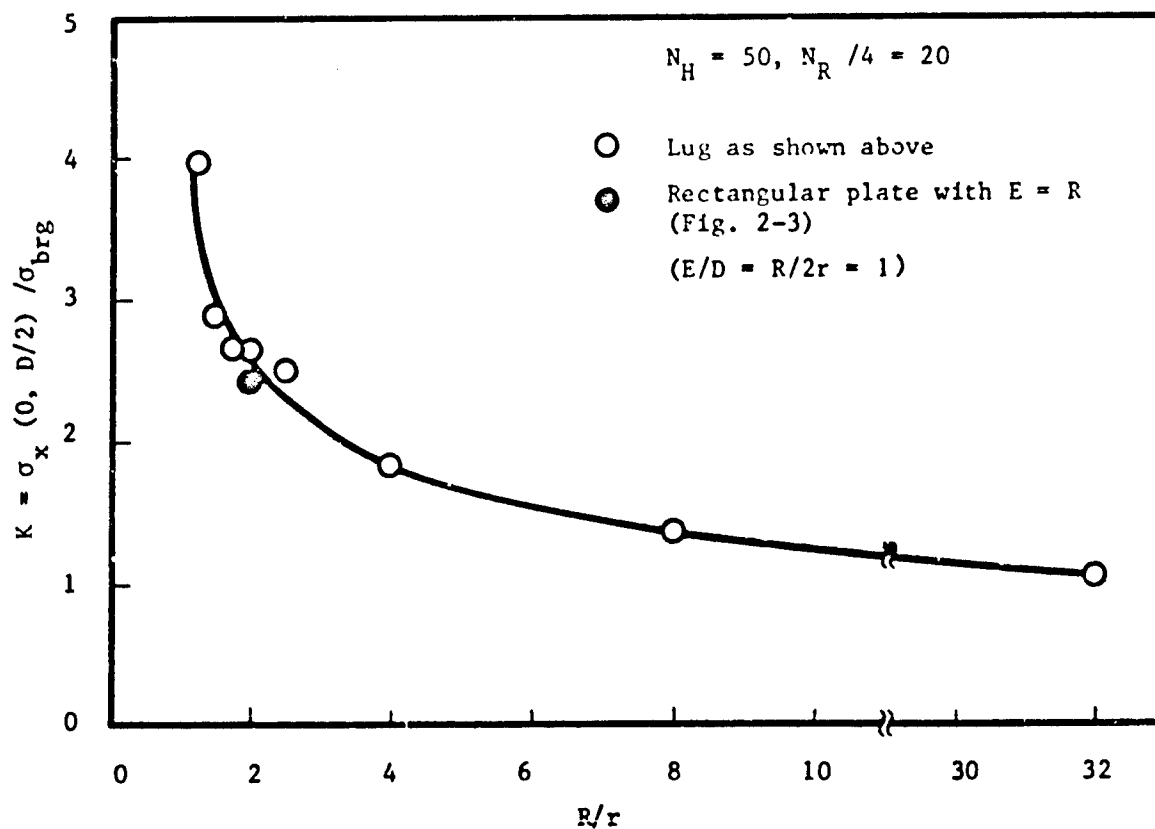
Figure 2-9. Effect of Lug Geometry on Stress Concentration.

The difference between the total applied load and the fastener load is referred to as the by-pass load. This example represents an isolated fastener location in a plate that is mechanically fastened to another using many bolts (see Figure 1-1). Results for three laminates, with D = 1/4 inch, E/D = 5 and W/D = 8, are presented in Figure 2-10. Presented results indicate that the stress concentration increases when the fractional bolt bearing load is increased. The predicted linear increase in K with an increase in the fractional bolt load provides an explanation for the linear strength reduction with the bolt load fraction observed in Reference 2-10.

2.10   Summary

A two-dimensional analysis (FIGEOM) for finite anisotropic plates with loaded or unloaded holes, developed in Reference 2-1, was discussed. The analysis uses a boundary collocation technique and computes the solution in a least squares sense. Examples were presented to demonstrate the capability of the analysis in computing the effect of plate geometry on the stress concentration at the boundary of the loaded or unloaded holes. Computed solutions were compared with infinite plate solutions to demonstrate the significant increase in the stress concentration when the outer plate boundaries are moved closer to the hole.

The major limitation of the FIGEOM computer code is its approximation of the fastener/plate contact stress distribution. Though the contact stress distribution and the contact region depend on the laminate layup, FIGEOM assumes a cosinusoidal bearing stress distribution over half the hole boundary. Nevertheless, the developed analysis is a significant improvement over the infinite plate analysis presented in Reference 2-9.

28
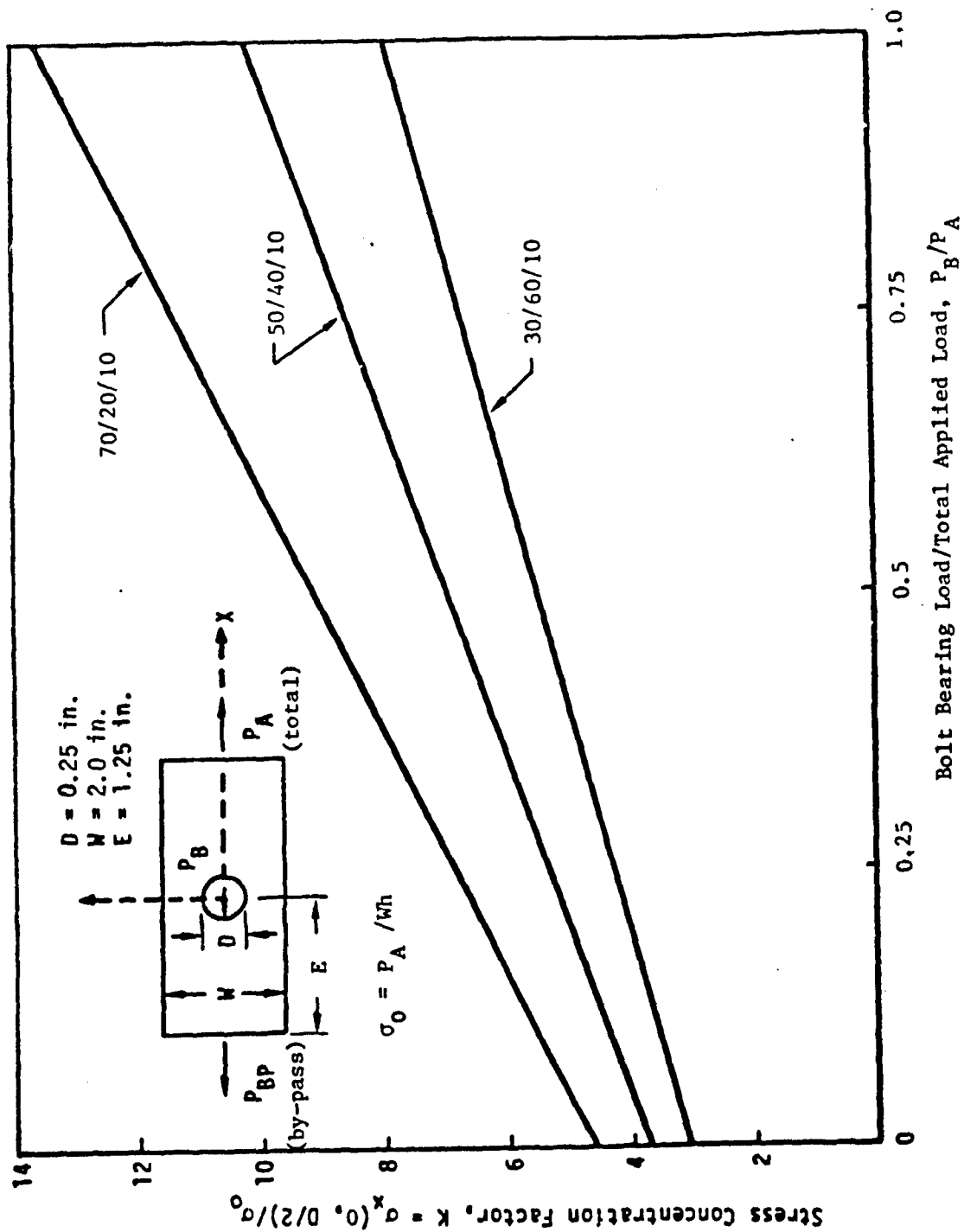
Figure 2-10. Effect of Partial Loading of the Hole on Stress Concentration.

SECTION 3

FASTENER ANALYSIS

3.1 Introduction

In the computation of the two dimensional stress state in a bolted plate, it is generally assumed that the fastener is rigid and that the fastener plate displacement due to inplane loads does not vary in the plate thickness direction (see Section 2). In most of the practical situations, this assumption is not valid, and the stress field at the fastener location is complex and three dimensional in nature. The three dimensional stress field at the fastener location in a bolted metal or composite plate is influenced by many factors: (1) fastener size, (2) fastener stiffness, (3) fastener end constraints, (4) fastener torque, (5) hole clearance, (6) properties of the bolted plates, (7) stacking sequence of the bolted laminate, (8) load eccentricity induced by joint configuration, etc.

Figures 3-1 and 3-2 illustrate the difference between a double lap and a single lap joint configuration. The single lap configuration, due to the eccentricity in the load path, will affect the local stress field more significantly. This effect is further influenced by the fastener properties. If the fastener modulus is large compared to the bolted plate modulus, and the fastener diameter is large compared to the plate thickness, the fastener bending and shear stiffnesses will be large enough to cause it to act like a rigid fastener. Otherwise, fastener bending and shear deformation will influence the local stress field significantly (see Figure 3-3).

Fastener end constraints also have a significant effect on the local stress state. Figure 3-4 shows three situations of interest. The protruding head fastener with a large applied torque value (Figure 3-4a) essentially creates a nearly fixed end boundary condition (constraint). A pin permits free rotation at the boundary (Figure 3-4c), and a highly torqued countersunk fastener creates nearly fixed and nearly free constraints at the nut and head locations, respectively (Figure 3-4b). Intermediate torque values can be represented by elastic constraint equations that quantify constraints between fixed and free conditions.

30
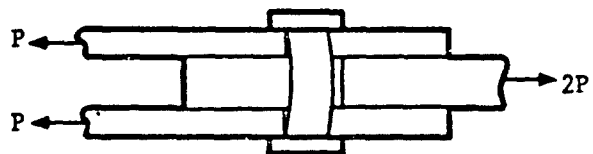
Figure 3-1. A Double Lap Configuration.
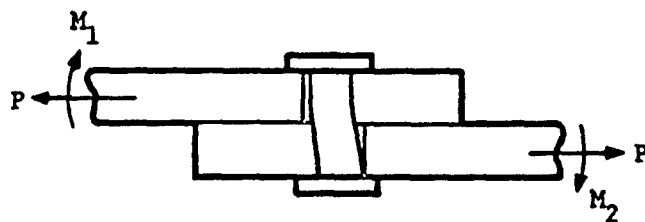
Figure 3-2. A Single Lap Configuration.

31

EI, AG are large compared to
plate EA value

P ←   → P

$E_X \approx 10$ Msi

Steel

|← D →|

h

D/h >>1
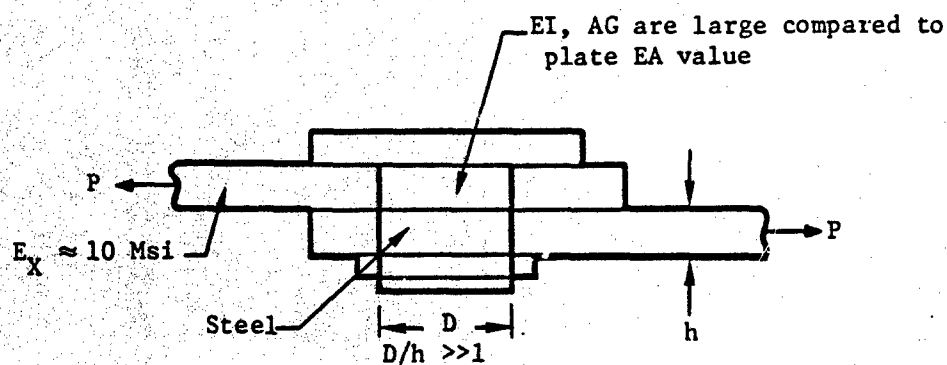
(a) Rigid Fastener -- negligible fastener bending &
        shear deformation

EI and AG are comparable
to plate EA

P ←   → P
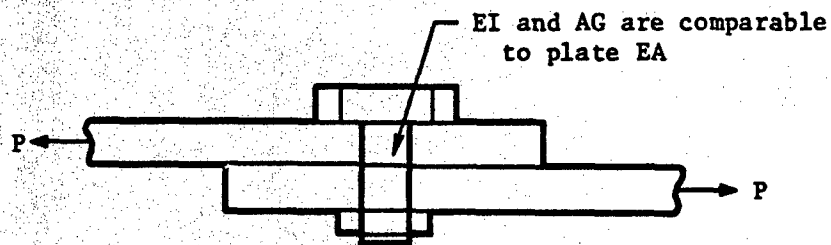
(b) Flexible Fastener -- Measurable fastener bending
        and shear deformation

EA - plate axial stiffness

EI - fastener bending stiffness

GA - fastener shear stiffness

Figure 3-3. Typical Rigid and Flexible Fasteners.

32
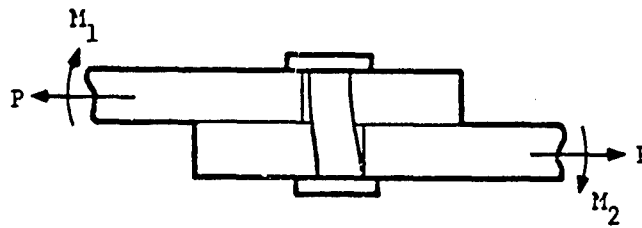
(a) Fixed - Fixed Conditions (Protruding head fastener --
high torque-up)
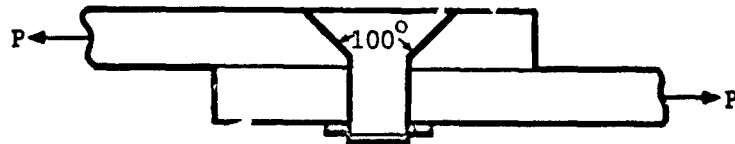
(b) Fixed - Free conditions (countersunk fastener, — high
torque-up)

(c) Free-Free Conditions (pin)

Figure 3-4. A Single Lap Configuration with Various
End Constraints on the Fastener.

Hole clearance effects are also obvious from Figure 3-4. In the case of a free pin, for example, an initial hole clearance will cause the pin to rotate in place or "cock " when a load is applied. If a protruding head fastener is used, the friction due to the applied torque is overcome prior to fastener cocking (rigid body rotation).

If the fastener bending and shear deformation effects are not negligible or if fastener rotation is induced by any of the discussed factors, the local stress field will be affected by the stacking sequence of the bolted laminate. This is due to the non-uniform strain distribution in the thickness direction of the bolted plate.

The following subsections present details of an analysis that was developed to predict the three dimensional stress state at a fastener location in a bolted laminated or metallic plate. The discussed analysis is similar in approach to that in References 3-1 to 3-3. But, while the analysis in References 3-1 to 3-3 is restricted to bolted metallic plates, the analysis developed in this program is applicable to metallic and laminated anisotropic plates.

3.2 Summary of Approach

A brief summary of the analytical approach is presented with the aid of Figure 3-5. For a single lap joint configuration subjected to a tensile load (Figure 3-5a), a typical fastener/bolted plate displacement variation is shown in Figure 3-5(b). The distribution of the contact force is influenced by the many factors discussed in Section 3.1, and is not a continuous function along the fastener axial direction (or the plate thickness direction) for a laminated bolted plate. Figure 3-5(b) shows a typical contact force distribution in bolted metallic plates. The resultant of the contact force distribution will be equal to the applied load (P) in magnitude, but will not, in general, lie along the line of action of P. This is because its line of action is determined based on moment equilibrium considerations. A free body diagram of the fastener will include contact forces that are opposite in sense to those shown in Figure 3-5(c). The spring constants represent the resistance offered by the bolted plate to fastener displacement. In a laminated plate, spring constants vary from ply to ply and are dependent on ply

34
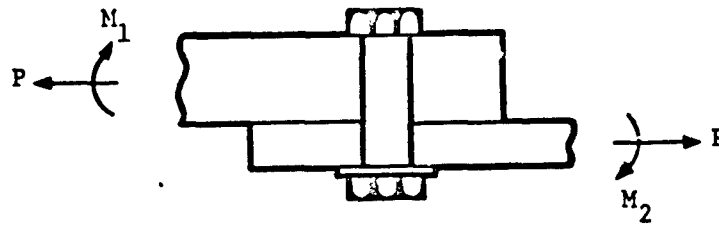
(a) Single Lap Bolted Joint
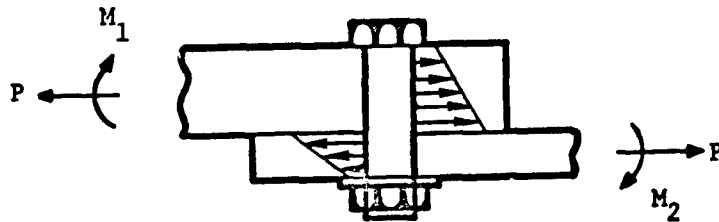
(b) Typical Fastener/Plate Displacement
     Variation
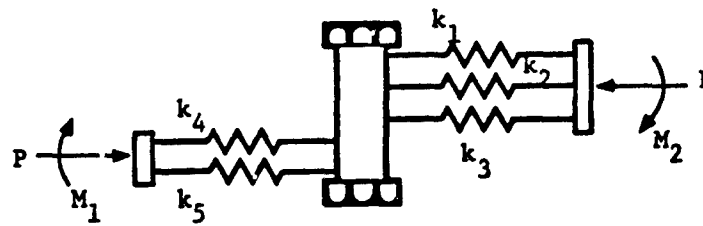
(c) Mathematical Representation

Figure 3-5. Representation of a Single Lap Configuration
             by an Equivalent Fastener Problem.

35

fiber orientations. In a metallic plate, the spring constant will be invariant in the thickness direction. The various springs, with appropriate constants assigned to each, mathematically replace the bolted plates by an elastic foundation whose modulus is piecewise uniform in general.

The three dimensional stress field at the fastener location is, therefore, computed by obtaining the solution to a mathematical problem that represents the fastener as a beam resting on an elastic foundation with piecewise uniform moduli that represent the various plies in a bolted laminate. The fastener is modeled as a Timoshenko beam to account for bending and shear deformation effects. The foundation is represented by a general bilinear contact load versus deflection curve, to account for a reduced ply stiffness after an initial damage (local failure) is precipitated. At the head and nut locations of the fastener, rotational constraints are introduced. These constraints are influenced by the applied torque and the size of the washers, if any. Fastener torque also introduces friction forces on the bolted plates, reducing the load transferred directly by the fastener. If either of the bolted plates is a laminate, its stacking sequence will influence the fastener displacement, and hence the load distribution in the thickness direction.

The governing differential equation for the fastener displacement is solved after the derivatives are replaced by appropriate differences. The finite difference formulation of the problem facilitates fast and accurate computations via an easily automated solution procedure. For a symmetric double lap configuration, symmetry conditions at the center replace the nut location boundary conditions used otherwise. Solutions are obtained over the region of contact in each plate, and continuity conditions are enforced where the two plates are in contact. The following sub-sections present details of the analysis.

3.3 Governing Differential Equation

The fastener is modeled as a Timoshenko beam to account for shear deformation effects. Figure 3-6 shows the deformed state of an infinitesimal segment of the fastener, and Figure 3-7 presents the assumed sign conventions

36
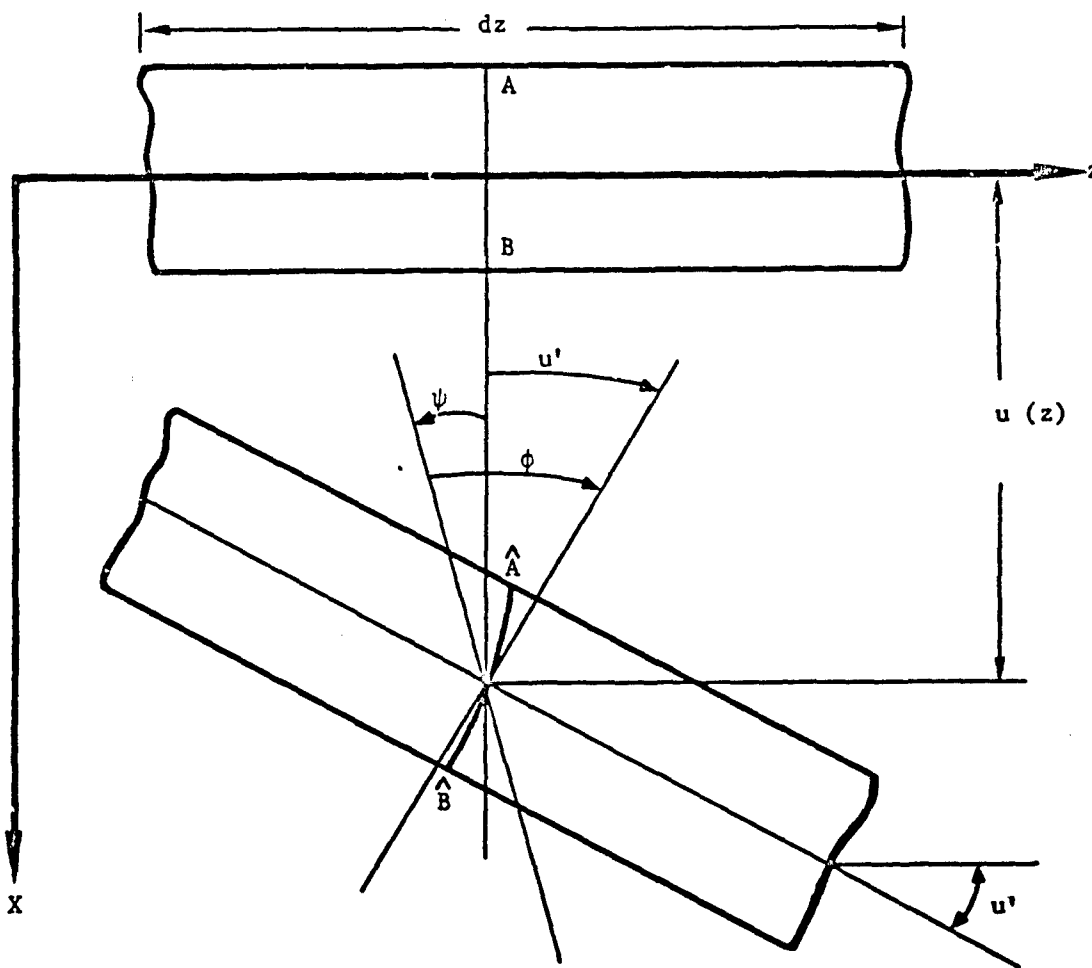
Figure 3-6. Deformation of an Infinitesimal Beam Element.
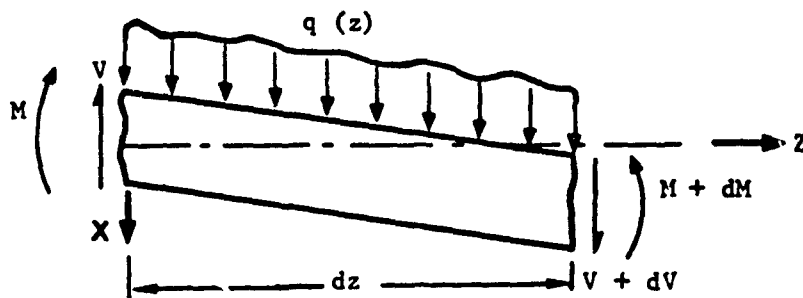
Figure 3-7. Positive Shear and Moment Conventions.

37

for transverse shear (V) and bending moment (M) in the fastener. The coordinates along the fastener axis and the loading direction (in the plane of the bolted plate) are labeled z and x, respectively. Under load, a plane section AB deforms to the form $\widehat{AB}$ shown in Figure 3-6. In doing so, the cross-section undergoes a translational displacement u(z) in the x direction, a bending rotation $\psi(z)$, and shear deformation. While ψ is not a function of x, the shear strain due to V is, due to the variation of the transverse shear stress (τ_{zx}) in the x direction. This results in the curved shape for $\widehat{AB}$. Representing the average cross-sectional shear distortion (rotation) by the symbol ϕ, the following relationship is assumed (Timoshenko beam theory):

$$V = \int \tau_{zx} \, dA = \lambda G A \phi \qquad (3-1)$$

where A is the fastener cross-sectional area, G is its shear modulus, and λ is a shear correction factor accounting for nonlinear τ_{zx} distribution in the x direction. The total rotation of the section AB is denoted by u', where the prime denotes differentiation with respect to z. From Figure 3-6, it follows that:

$$u' = \phi - \psi \qquad (3-2)$$

The bending moment at any z location is expressed as follows:

$$M = \int \sigma_z \, x dA = \int (E \, \epsilon_z) \, x dA = \int E(x\psi') \, x dA = EI\psi' \qquad (3-3)$$

where σ_z is the fastener bending stress, ϵ_z is the axial strain in the fastener due to bending, E is the fastener Young's modulus, and I is the moment of inertia of the fastener cross-section about the y axis (normal to the yz plane).

If the fastener is subjected to a distributed transverse load q(z), force and moment equilibrium considerations yield the following relationship (see Figure 3-7):

38

$$V' = -q, \text{ and} \qquad (3\text{-}4)$$

$$M' = V \qquad (3\text{-}5)$$

Again, primes denote differentiation with respect to z. Equations 3-1 to 3-5 yield the following relationships for M, V and ψ:

$$M = -EI\left[u'' + q/(\lambda GA)\right] \qquad (3\text{-}6)$$

$$V = -EI\left[u''' + q'/(\lambda GA)\right] \qquad (3\text{-}7)$$

$$\psi = -(EI/\lambda GA)\left[u''' + q'/(\lambda GA)\right] - u' \qquad (3\text{-}8)$$

Equations 3-4 and 3-5 may be combined to yield the following equilibrium equation:

$$M'' = -q \qquad (3\text{-}9)$$

Substituting Equation 3-6 into the above equation, the following governing equation is obtained:

$$u'''' + q''/(\lambda GA) - q/(EI) = 0 \qquad (3\text{-}10)$$

This equation, where $q = q(z)$, governs the displacement of the fastener. $u'''' = d^4u/dz^4$ and $q'' = d^2q/dz^2$.

3.4 Nonlinear Foundation Behavior

The effect of the bolted plate (metallic or laminated) on the fastener displacement is represented by the transverse loading term $q(z)$ in the Equation 3-10. The $q(z)$ term is, in turn, linearly related to the fastener displacement $u(z)$ through the foundation modulus $k(z)$. For the more general laminated foundation, the foundation modulus varies from ply to ply, and is uniform within a ply. $k(z)$ is, therefore, piecewise uniform.

In the developed analysis, every ply is also assumed to be a bilinear elastic (Hencky) material (see Figure 3-8). This representation of the ply behavior permits the prediction of a local damage in the ply (when $u = u_o$)

39
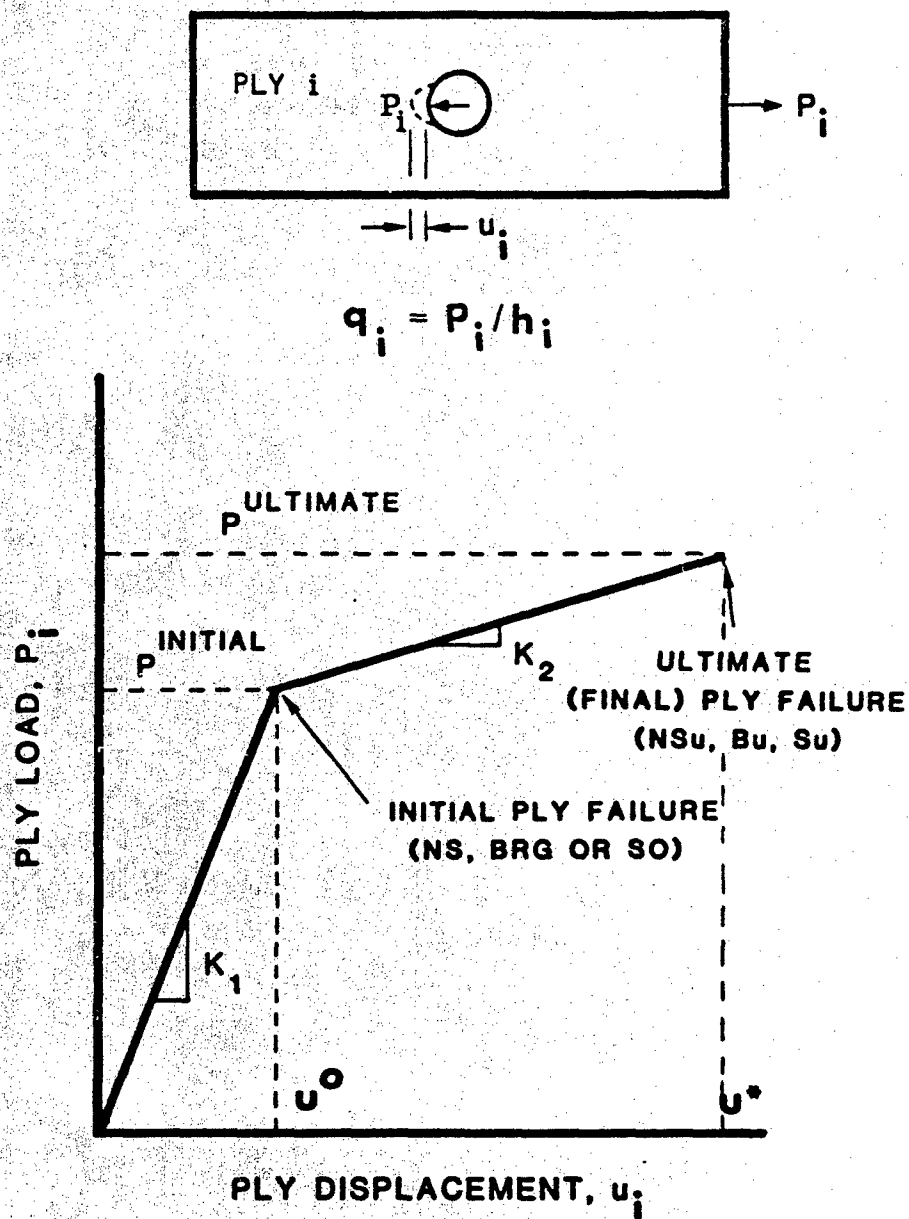
Figure 3-8. Bilinear Elastic Behavior of a Ply.

40

that is not catastrophic. The ply modulus is k_1 for $0 < u < u_o$. Depending on the type of damage predicted in the ply, its modulus (k_2) beyond $u = u_o$ is set to be greater than, equal to or less than zero. If $k_2 > 0$, the ply exhibits a hardening behavior; if $k_2 < 0$, it exhibits a softening behavior; and if $k_2 = 0$, the ply is an elastic-perfectly plastic material. When u takes the value of u* (Figure 3-8), the ply loses its load-carrying capability. At this load level, the ply is assumed to have failed totally and its modulus and load are reset to zero. Adjacent unfailed plies share the load that is released by the totally failed ply.

The general ply load versus displacement behavior (Figure 3-8) is expressed mathematically as:

$$q(z) = -ku - \overline{ku} \qquad (3-11)$$

where, $\quad k = k_1$ for an undamaged ply

$k = k_2 = \alpha k_1$ for a partically damaged ply

$k = 0$ for a totally damaged ply

$\overline{k} = k_1 - k_2 = (1-\alpha)k_1$ for a partically damaged ply

$\overline{k} = 0$ for a totally damaged ply

$\overline{u} = 0$ for an undamaged ply

$\overline{u} = u_o$ for a partially or totally damaged ply

(k_1, u_o, k_2 and u* or $P_{ultimate}/P_{initial}$) fully define the general ply behavior. The computation of k_1 for the various plies is discussed in the following sub-section. u_o and u* are dependent on the failure criteria used to predict partial and total ply damage. $k_2 = \alpha k_1$ will be established by assigning α values for the various partial damage types. If the ply behavior can be adequately represented by a linear elastic approximation, a simplified form of Equation 3-11 may be used.

3.5 Computation of Initial Foundation Moduli (k_1) for the Various Ply Types

If a bolted plate is a laminate, the various fiber orientations in its lay-up determine the number of ply types in the laminate, assuming all plies to be made of the same material. A metallic bolted plate has only one ply type. The initial foundation modulus (k_1 in Figure 3-8) for each ply type

41

is computed by considering a situation where the local three dimensional stress field can be approximated by a two dimensional stress field. This is done by assuming that the fastener is rigid in bending ($EI \rightarrow \infty$) and in shear ($GA \rightarrow \infty$), and that the load is transferred in a symmetrical double lap configuration. In this situation, the inplane strains do not vary in the thickness direction when only inplane loads are present. This strain field and the corresponding stress state in each ply are computed using the FIGEOM computer code (Reference 2-1).

An effective fastener displacement in the load direction (x) is obtained prior to computing k_1 for the various ply types. This is accomplished by equating the total work done by the fastener-imposed radial bearing stresses around the hole boundary (ΣW_i) to the expression $(1/2) P \delta_{eff}$, where P is the total fastener load and δ_{eff} is the effective fastener displacement in the load (x) direction:

$$\delta_{eff} = \sum_{i=1}^{n} W_i / \sum_{i=1}^{n} F_{xi}$$

$$= \left[1/2 \sum_{i=1}^{n} \sigma_{ri} hR \, \Delta\theta_i \, u_{ri} \right] / \left[\frac{1}{2} \sum_{i=1}^{n} \sigma_{ri} hR \Delta\theta_i \, \text{Cos}(\theta_i + 0.5\Delta\theta_i) \right] \quad (3\text{-}12)$$

where n is the number of collocation points around the hole boundary, and Figure 3-9 describes the various quantities that are present in Equation 3-12. R is the radius of the hole and h is the total plate thickness.

The strains corresponding to a fastener load of P are invariant in the plate thickness direction. Using the appropriate stiffness matrix for each ply type and these strains, ply stresses are computed at each collocation point. Stresses in rectangular coordinates (x,y) are transformed to stresses in polar coordinates (R, θ) using appropriate transformation relationships. The load (P_{xj}) in the jth ply, in the load direction, is computed as follows (see Figure 3-10):

$$W = \frac{1}{2} \sum_{i=1}^{n} \sigma_{ri} h R \Delta\theta_i u_{ri}$$
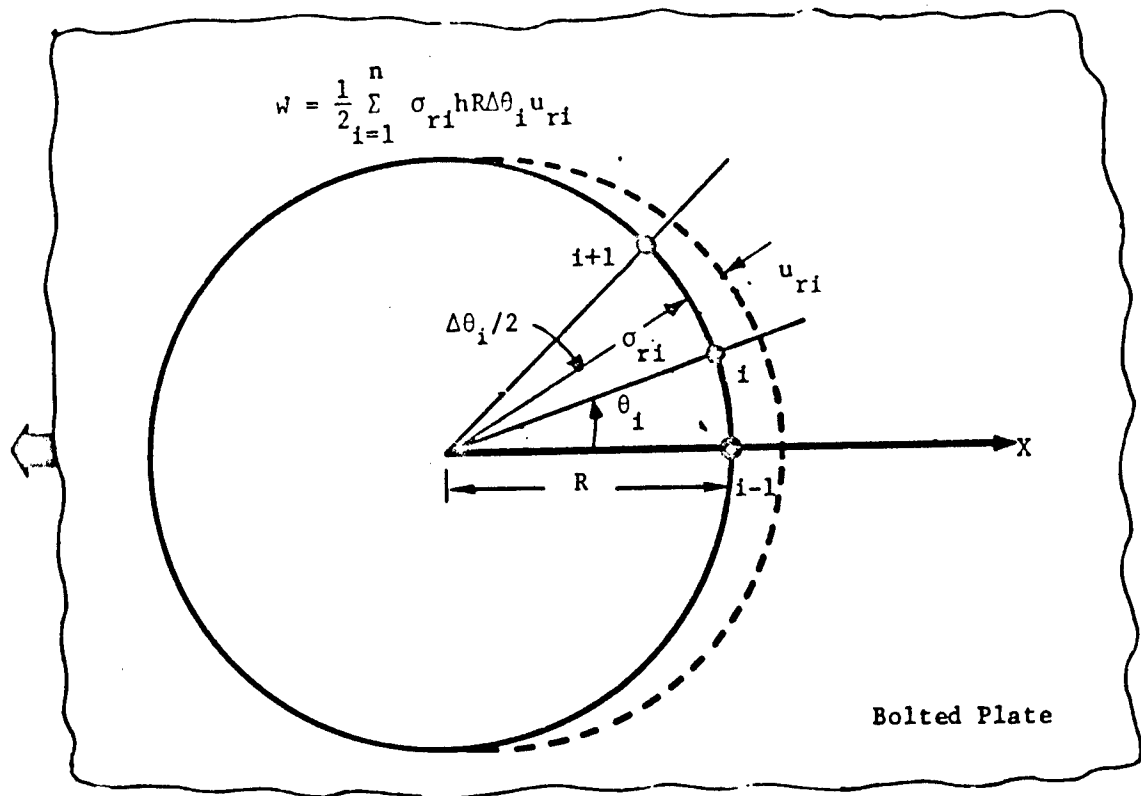
Figure 3-9. Computation of Work Done by the Fastener Bearing Stress

$$P_{xj} = \sum_{i=1}^{n} \sigma_{ri} h_j R\Delta\theta_i \cos(\theta_i + 0.5\,\Delta\theta_i) - \sum_{i=1}^{n} \tau_{r\theta i} h_j R\Delta\theta_i \sin(\theta_i + 0.5\,)$$
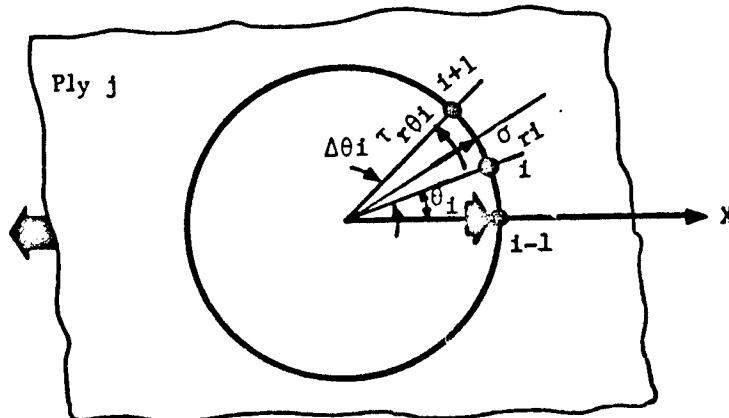
Figure 3-10. Computation of Ply Load.

$$P_{xj} = \sum_{i=1}^{n} \sigma_{ri} h_j R \, \Delta\theta_i \, \text{Cos} \, (\theta_i + 0.5 \, \Delta\theta_i) -$$

$$(3-13)$$

$$\sum_{i=1}^{n} T_{r\theta i} h_j R \, \Delta\theta_i \, \text{Sin} \, (\theta_i + 0.5 \, \Delta\theta_i)$$

The initial foundation modulus (k_1) for the j th ply type is then computed using the following relationship:

$$k_1^j = P_{xj} / (h_j \delta_{eff})$$

$$(3-14)$$

where δ_{eff} and P_{xj} are defined in Equations 3-12 and 3-13, respectively, and h_j is the thickness of the j th ply type.

3.6 Boundary and Continuity Conditions

The boundary and continuity conditions on a fastener that bolts two plates in a single lap configuration are shown in Figure 3-11. The portion of the fastener in each plate is shown separately. The load (P) in each plate is enforced as a shear boundary condition at the interfacial location, to satisfy force equilibrium requirement. The shear force values at the outer boundaries (the head and nut locations of the fastener) are set equal to zero, since the load transfer is effected between these locations. At the interface between the bolted plates, continuity of the bending slope and the bending moment are enforced. Continuity of displacement is not enforced at this location. This is because u (z) represents the fastener/ plate displacement, and undergoes a finite discontinuity across this interfacial location in the joint.

At the fastener head location, the head type and the presence of washers, if any, influence the constraint against free rotation. A washer and a nut offer a similar constraint at the other boundary. The constraints at the fastener head and nut locations can be generalized as shown in Figure 3-11, where R_1 and R_2 quantify the elastic restraint. For a pin-connected joint (Figure 3-4c), for example, R_1 and R_2 are set equal to zero.
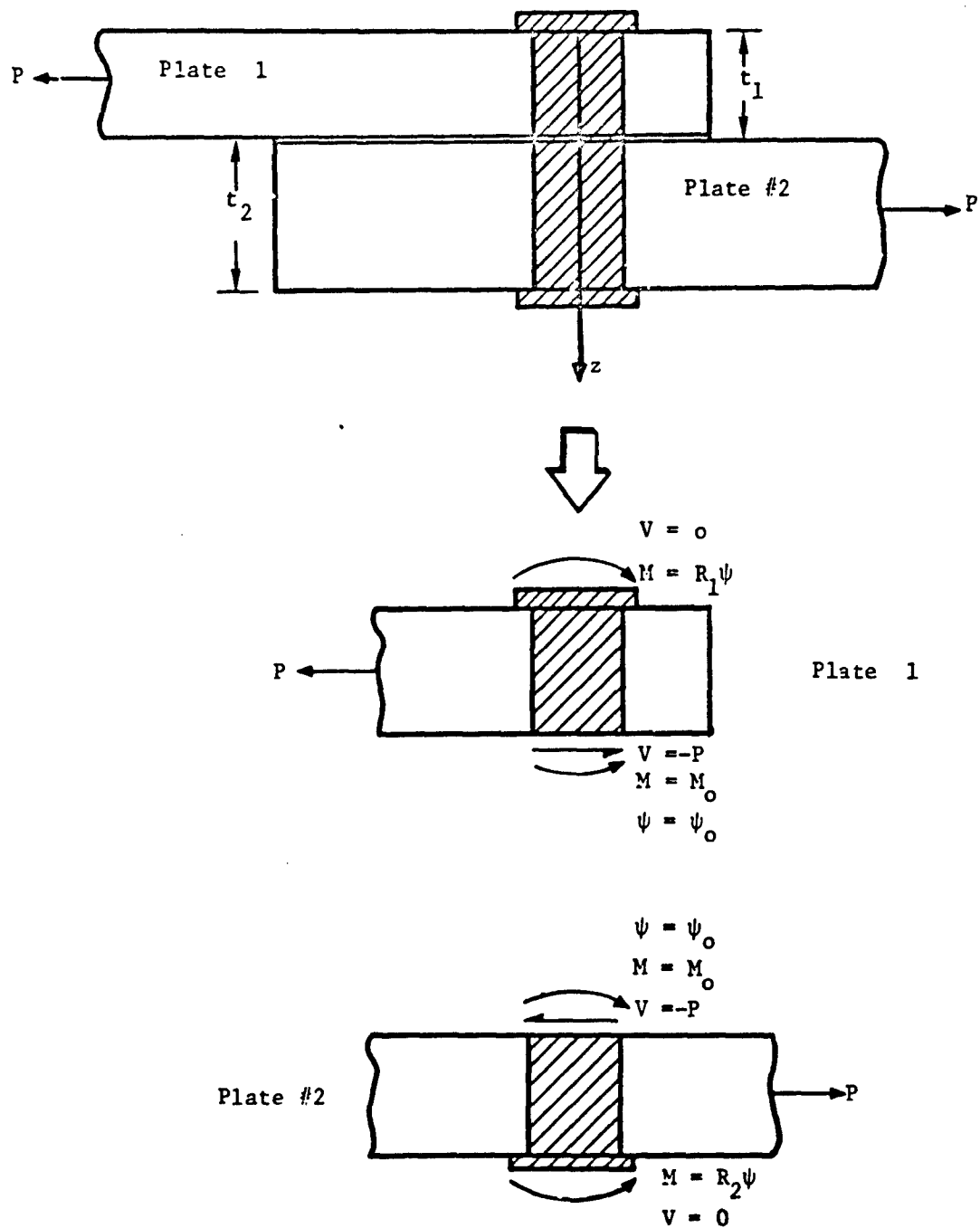
Figure 3-11. Boundary and Continuity Conditions for a
Typical Single Lap Joint.

For a countersunk fastener, R_1 is set equal to zero (at the head location). Fastener torque influences R_1 and R_2 values significantly. If a protruding head fastener is highly torqued (Figure 3-4a), R_1 and R_2 values become very large ($\rightarrow \infty$), and tend to reduce the bending slope to zero at the head and nut locations.

Reference 3-5 presents an elasticity analysis that could be useful in the determination of the rotational constant R in $M = R\psi$. The analysis assumes a rigid circular disk to be supported by a transversely isotropic half space, and subjected to a transverse load and a bending moment. The derived expression for R is:

$$R = 8Gr_o^3/(3\phi_o) \tag{3-15}$$

where G is the transverse shear modulus of the half space, r_o is the radius of the disk, and ϕ_o is a dimensionless constant that varies from 0.7 for an isotropic space to 1.0 for a highly anisotropic space. In a practical joint, an annular disk (washer) is supported by a foundation of finite thickness and the expression in equation 3-15 is not directly applicable. An empirical expression will, therefore, be derived for R, based on a correlation between analysis and experiment. This expression will relate R to the washer diameter and the fastener torque.

Load transfer in a symmetric double lap configuration yields the boundary, symmetry and continuity conditions shown in Figure 3-12. The boundary conditions at the fastener head location, and the shear and continuity conditions at the interface between adjacent plates, are identical to those discussed earlier (see Figure 3-11). The assumption of a symmetric double shear situation requires the imposition of the symmetry conditions shown in Figure 3-12. Symmetry introduces a zero shear and a zero bending slope condition at the midplane of plate 2. It is noted that only half the fastener is analyzed for a symmetric double shear situation.

A total of 8 boundary/continuity/symmetry conditions are identified for each joint configuration -- the single lap joint in Figure 3-11, and
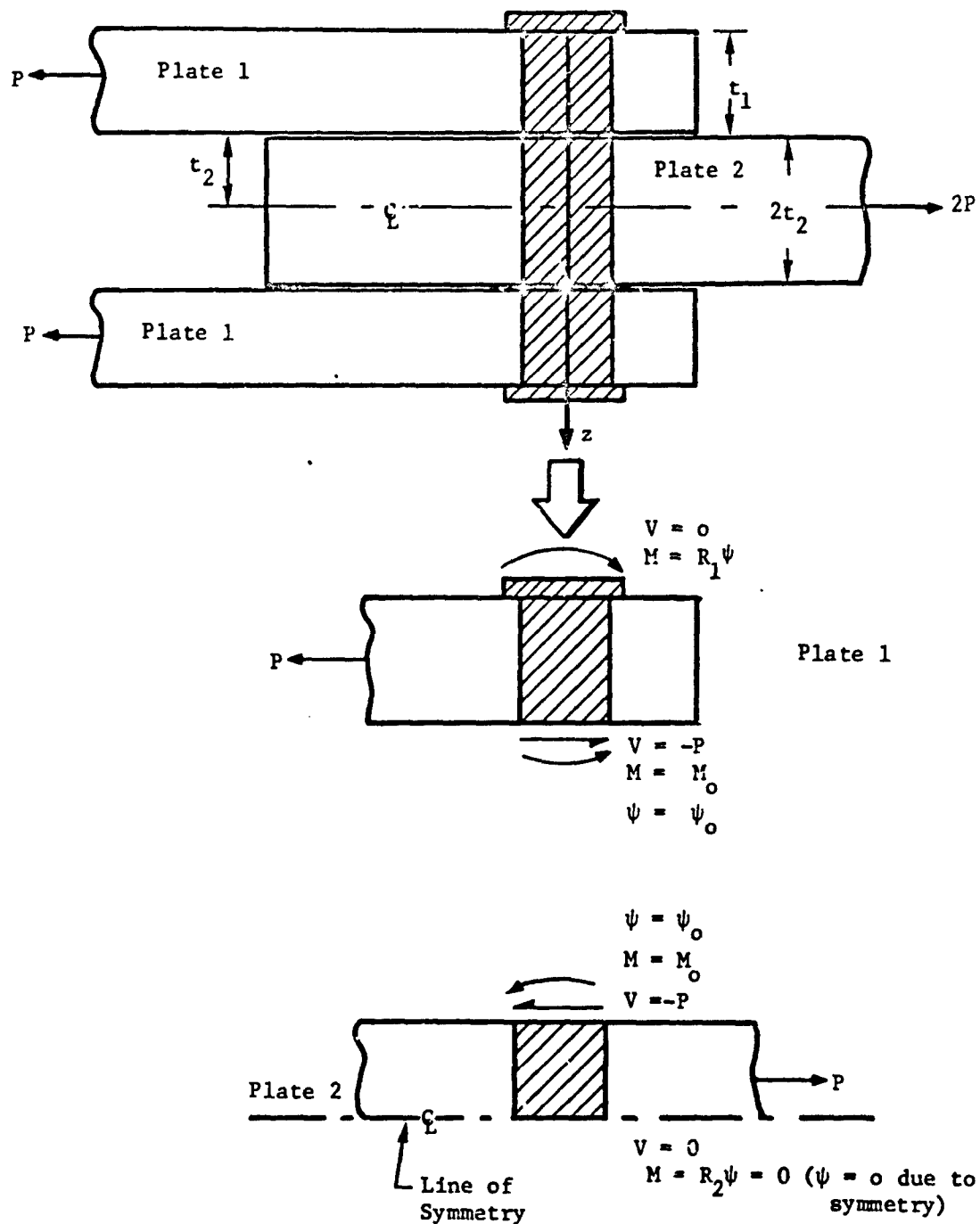
Figure 3-12. Boundary and Continuity Conditions for a Typical Double Lap Joint.

the double lap joint in Figure 3-12. For the single lap joint (Figure 3-11), the 8 conditions are:

$V = 0$ and $M = R_1\psi$ at the fastener head location

$V = -P$ at the plate 1/plate 2 interface, in the plate 1 region

$V = -P$ at the plate 1/plate 2 interface, in the plate 2 region

M at the plate 1/plate 2 interface in the plate 1 region = M at the plate 1/plate 2 interface in the plate 2 region   (3-16)

ψ at the plate 1/plate 2 interface in the plate 1 region = ψ at the plate 1/plate 2 interface in the plate 2 region

$V = 0$ and $M = R_2\psi$ at the nut location

For the double lap joint (Figure 3-12), the first 6 conditions are the same as above. The last two conditions at the nut location are replaced by the following conditions at the midplane of plate 2:

$V = 0$ and $M = 0$ ($\psi = 0$) at the midplane of plate 2 (plane of symmetry)

(3-17)

3.7   Finite Difference Formulation of the Problem

The governing equation for the fastener/plate displacement (Equation 3-10) contains expressions that are dependent on the relationship between the ply load and the ply displacement (Equation 3-11). Incorporation of Equation (3-11) into Equation (3-10) will result in a fourth order, ordinary differential equation for $u(z)$ with variable coefficients (because k is a function of z). A finite difference approximation of the governing equation (and the boundary and continuity conditions) is adopted to obtain the fastener/plate displacement and the corresponding fastener load distribution in the thickness direction of the bolted plates. This provides a rapidly executable solution scheme that can be economically executed many times to predict progressive failures in bolted joints. Details of the finite difference formulation of the problem are presented below.
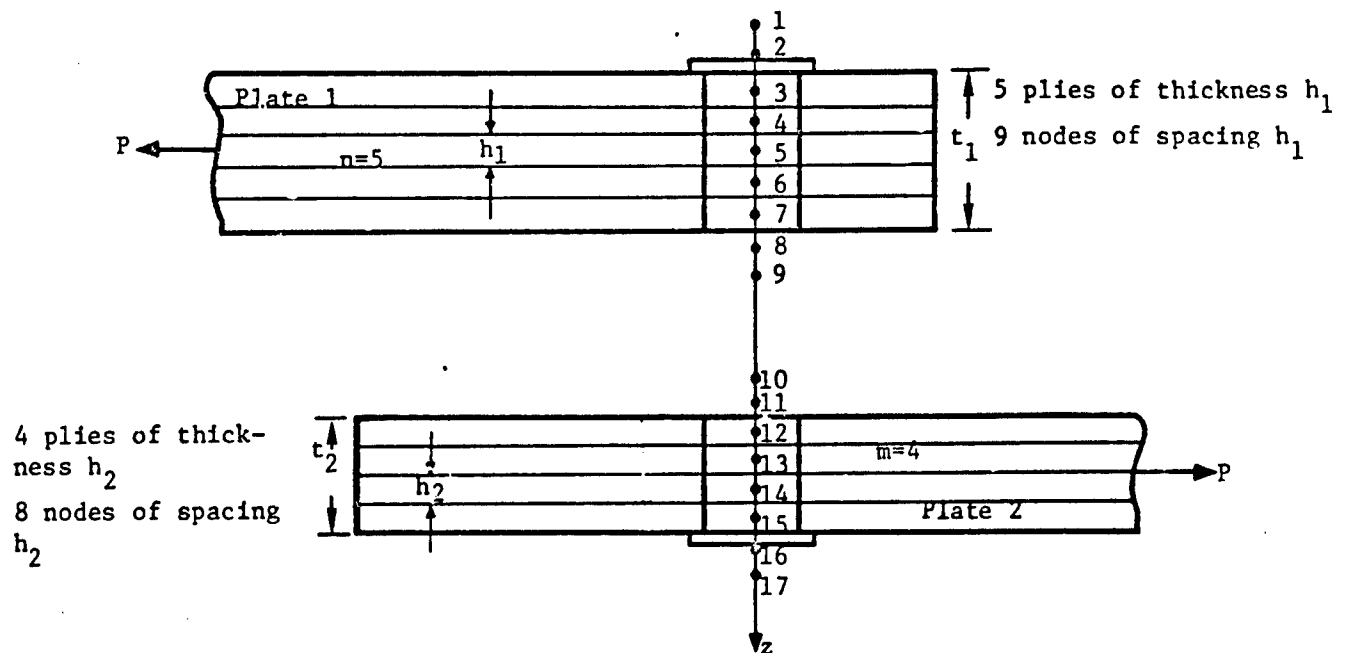
Figure 3-13.   An Example of the Node Layout and Numbering
Scheme in a Single Lap Shear Joint Configuration.
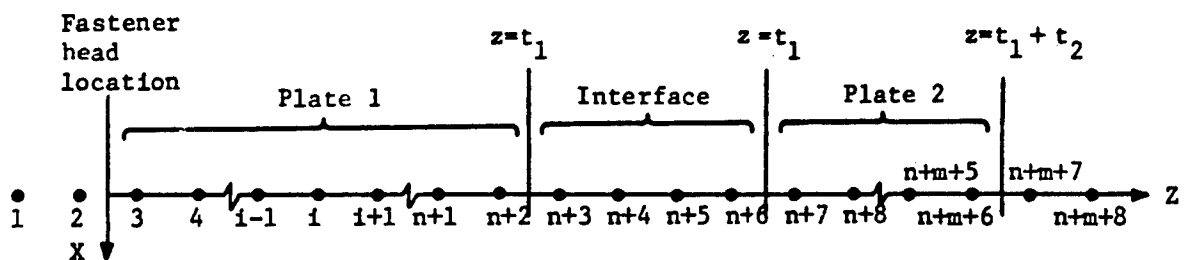
Figure 3-14.   A General Node Arrangement with n Nodes in Plate 1
and m Nodes in Plate 2.

49

3.7.1 Nodal Discretization of the Fastener

Figure 3-13 describes how the continuous fastener is discretized
to a finite number of nodal points. In the chosen example, plates 1 and
2 are assumed to be 5-ply and 4-ply laminates, respectively, bolted together
in a single lap configuration. The portion of the fastener in each plate
is represented by equally-spaced nodes located at the ply midplanes. If
either plate is metallic, it is divided into m or n number of plies of the
same properties. To enable the use of a central difference scheme for
the governing equation and the boundary conditions, two 'false' nodes are
assumed to be present on either side of a plate. In the example in Figure
3-13, a total of 17 nodes is assumed. Nine of these are h_1 apart in the
plate 1 region, and the remaining eight are h_2 apart in the plate 2 region.
Nodes 1, 2, 8 and 9 are 'false' nodes corresponding to the portion of
the fastener in plate 1, and nodes 10, 11, 16 and 17 are 'false' nodes
corresponding to the plate 2 region.

In a symmetric double lap joint (see Figure 3-12), the fastener is
discretized only up to the plane of symmetry (midplane of plate 2). In
this case, m in Figure 3-13 represents half of the number of plies in
plate 2.

In the example in Figure 3-13, $m + n + 8$ nodes are present. Of these,
$m + n$ are 'physical' nodes, and 8 are 'false' nodes. The enforcement of
the governing equation at the 'physical' nodes yields $m + n$ equations.
The imposition of the boundary/continuity/symmetry conditions yields 8
equations (see Section 3.6). These $m + n + 8$ equations provide the
solutions for the $m + n + 8$ nodal displacements.

The properties of a ply are represented by an equivalent stiffness
at the corresponding node in this approach. The computed nodal displace-
ments are used in the calculation of the average ply loads. When a ply
failure is predicted, the corresponding nodal stiffness is modified to
appropriately represent this failure.

50

3.7.2 Central Difference Expressions

Assume that the nodes in a region are separated by a distance h. In this case $\Delta z = h$ for the region, and the derivatives of the nodal displacements with respect to z may be approximated by the following central difference expressions, at node i:

$$2hu_i' = -u_{i-1} + u_{i+1}$$

$$h^2 u_i'' = u_{i-1} - 2u_i + u_{i+1}$$

$$2h^3 u_i''' = -u_{i-2} + 2u_{i-1} - 2u_{i+1} + u_{i+2}$$

$$h^4 u_i'''' = u_{i-2} - 4u_{i-1} + 6u_i - 4u_{i+1} + u_{i+2}$$

$$(3-18)$$

The error in the above approximations is of the order of h^2. In the example in Figure 3-13, plate 1 is divided into n plies that are h_1 in thickness, and plate 2 is divided into m plies that are h_2 in thickness. h_1 and h_2 must be of the same order of magnitude.

It is noted that the difference approximations of derivatives to the fourth order (Equations 3-18) involve a maximum of two nodes on either side of the node where the derivative is approximated. The enforcement of the governing equation at every physical node, therefore, requires two 'false' nodes on either side of each plate (see Figure 3-13). The boundary/continuity/ symmetry conditions are enforced at the first or the last nodal location in each plate. Referring to these conditions in Equations 3-16 and 3-17, and to their relationships to derivatives to the third order of the nodal displacement (Equations 3-6 to 3-8), it is seen that these conditions also require the two 'false' nodes on either side of each plate. A general node arrangement for an n-ply plate bolted to an m-ply plate is shown in Figure 3-14. A total of 8 'false' nodes are required for the discussed finite difference formulation.

The 'false' nodes are assumed to be mirror reflections about the first physical node at every boundary. Referring to Figure 3-14, node 2 is assumed to have the properties (stiffness) of node 4, and node 1 is assumed to be iden-

tical to node 5. Likewise, nodes n+3, n+4, n+5, n+6, m+n+7 and m+n+8 are mirror reflections of nodes n+1, n, n+9, n+8, m+n+5 and m+n+4, respectively.

A central difference approximation of the governing equation is obtained by incorporating Equation 3-18, and similar difference expressions for Equation 3-11, into Equation 3-10. The following difference expressions are used in the process:

$$h^4 u^{iv} = u_{i-2} - 4 u_{i-1} + 6u_i - 4 u_{i+1} + u_{i+2}$$

$$q_i = -k_i u_i - \bar{k}_i \bar{u}_i \tag{3-19}$$

$$h^2 q_i'' = q_{i-1} - 2 q_i + q_{i+1}$$

$$= (-k_{i-1} u_{i-1} - \bar{k}_{i-1} \bar{u}_{i-1}) - 2(-k_i u_i - \bar{k}_i \bar{u}_i) + (-k_{i+1} u_{i+1} - \bar{k}_{i+1} \bar{u}_{i+1})$$

$$= -k_{i-1} u_{i-1} + 2k_i u_i - k_{i+1} u_{i+1} - \bar{k}_{i-1} \bar{u}_{i-1} + 2\bar{k}_i \bar{u}_i - \bar{k}_{i+1} \bar{u}_{i+1}$$

Substituting the above expressions into Equation 3-10, the governing equation at the ith node becomes:

$$u_{i-2} - (4 + \frac{h^2 k_{i-1}}{\alpha \lambda GA}) u_{i-1} + (6 + \frac{2h^2 k_i}{\alpha \lambda GA} + \frac{h^4 k_i}{\alpha EI}) u_i$$

$$-(4 + \frac{h^2 k_{i+1}}{\alpha \lambda GA}) u_{i+1} + u_{i+2} = (\frac{h^2 \bar{k}_{i-1}}{\alpha \lambda GA}) \bar{u}_{i-1}$$

$$-(\frac{2}{\lambda GA} + \frac{h^2}{\alpha EI}) h^2 \bar{k}_i \bar{u}_i + (\frac{h^2 \bar{k}_{i+1}}{\alpha \lambda GA}) \bar{u}_{i+1} \tag{3-20}$$

$\alpha = 1$ for plate 1, and $\alpha = 2$ for plate 2. For the ith ply, the values of $k, \bar{k}$ and $\bar{u}$ are determined by its state of damage (see Equation 3-11).

Equations 3-6 to 3-8 express the fastener bending moment, transverse shear and the bending slope, respectively, in terms of u and q derivatives. Central difference expressions for M, V and ψ yield the following boundary/continuity/symmetry conditions:

At z=0 (fastener head location / top of the joint)

(i) $V_1 = 0$:

$$-u_1 + (2 + \frac{h_1^2 k_2}{\lambda GA}) u_2 - (2 + \frac{h_1^2 k_4}{\lambda GA}) u_4 + u_5 = 0 \qquad (3\text{-}21)$$

(ii) $M_1 = R_1 \psi_1$:

$$R_1 u_1 - (2 R_1 - 2h_1 \lambda GA - h_1^2 R_1 \frac{\lambda GA}{EI} + \frac{h_1^2 R_1 k_2}{\lambda GA}) u_2$$

$$-(4h_1 \lambda GA + 2h_1^3 k_3) u_3$$

$$-(-2R_1 - 2h_1 \lambda GA + \frac{h_1^2 R_1 \lambda GA}{EI} - \frac{h_1^2 R_1 k_4}{\lambda GA}) u_4$$

$$-R_1 u_5 = 2h_1^3 \bar{k}_3 \bar{u}_3 \qquad (3\text{-}22)$$

At z=t_1 (joint interface between plates 1 and 2)

(iii) $V_1 = -P$:

$$u_n - (2 + \frac{h_1^2 k_{n+1}}{\lambda GA}) u_{n+1} + (2 + \frac{h_1^2 k_{n+3}}{\lambda GA}) u_{n+3} - u_{n+4} =$$

$$\frac{-2h_1^3 P}{EI} \qquad (3\text{-}23)$$

(iv) $\psi_1 = \psi_2$:

$$u_n - (2 + \frac{h_1^2 k_{n+1}}{\lambda GA} - \frac{h_1^2 \lambda GA}{EI}) u_{n+1} + (2 + \frac{h_1^2 k_{n+3}}{\lambda GA} -$$

$$\frac{h_1^2 \lambda GA}{EI}) u_{n+3} - u_{n+4} - h_{12}^3 u_{n+5} + h_{12}^3 (2 + \frac{h_2^2 k_{n+6}}{\lambda GA} -$$

$$\frac{h_2^2 \lambda GA}{EI}) u_{n+6} - h_{12}^3 (2 + \frac{h_2^2 k_{n+8}}{\lambda GA} - \frac{h_2^2 \lambda GA}{EI}) u_{n+8} + h_{12}^3 u_{n+9} = 0$$

$$(3\text{-}24)$$

where $h_{12} = h_1/h_2$

(v) $\underline{M_1 = M_2}$:

$$u_{n+1} - (2 + \frac{h_1^2 k_{n+2}}{\lambda GA}) u_{n+2} + u_{n+3} - h_{12}^2 u_{n+6}$$

$$+ h_{12}^2 (2 + \frac{h_2^2 k_{n+7}}{\lambda GA}) u_{n+7} - h_{12}^2 u_{n+8} = \frac{h_1^2}{\lambda GA} (\bar{k}_{n+2} \bar{u}_{n+2} - \bar{k}_{n+7} \bar{u}_{n+7})$$

$$\text{(3-25)}$$

(vi) $\underline{V_2 = -P}$

$$u_{n+5} - (2 + \frac{h_2^2 k_{n+8}}{\lambda GA}) u_{n+6} + (2 + \frac{h_2^2 k_{n+8}}{\lambda GA}) u_{n+8} - u_{n+9} =$$

$$\frac{-2h_2^3 P}{EI} \qquad \text{(3-26)}$$

At $z = t_1 + t_2$ (fastener nut location/bottom of the joint)

(vii) $\underline{V_2 = 0}$:

$$-u_{n+m+4} + (2 + \frac{h_2^2 k_{n+m+5}}{\lambda GA}) u_{n+m+5} - (2 + \frac{h_2^2 k_{n+m+7}}{\lambda GA}) u_{n+m+7} +$$

$$u_{n+m+8} = 0 \qquad \text{(3-27)}$$

(viii) $\underline{M_2 = R_2 \psi_2}$

$$R_2 u_{n+m+4} - (2R_2 - 2h_2 \lambda GA - \frac{R_2 h_2^2 \lambda GA}{EI} + \frac{h_2^2 R_2 k_{n+m+5}}{\lambda GA}) u_{n+m+5}$$

$$-(4h_2 \lambda GA + 2h_2^3 k_{n+m+6}) u_{n+m+6} - (-2R_2 - 2h_2 \lambda GA + \frac{h_2^2 R_2 \lambda GA}{EI} -$$

$$\frac{h_2^2 R_2 k_{n+m+7}}{\lambda GA}) u_{n+m+7} - R_2 u_{n+m+8} = 2h_2^3 \bar{k}_{n+m+6} \bar{u}_{n+m+6} \qquad \text{(3-28)}$$

54

3.8 Solution Procedure

The governing Equation 3-20 is enforced at the n+m 'physical' nodes. Equations 3-21 to 3-28 are enforced at the boundary nodes (identified in Figure 3-14 as nodes 3 and n+2 in plate 1, and nodes n+7 and m+n+6 in plate 2). This provides a system of m+n+8 equations that determine the through-the-thickness fastener displacement. Figure 3-15 shows a matrix representation of the problem defined in Figure 3-13 (n=5, m=4). The functions $f(\overline{u}_i)$ are set equal to zero until the ply corresponding to mode i is damaged.

The system of m+n+8 equations, in general, is solved for the nodal displacements by using a standard matrix decomposition or matrix inversion routine. It is seen, from Figure 3-15, that the coefficient matrix to be inverted is banded in nature. A special purpose Gaussian triangularization computer code was developed to solve for the nodal displacements. When the coefficient matrix size is large, this provides an economical means of obtaining solutions, especially when the solution procedure is repeated many times to predict progressive failures in the bolted plates.

The finite difference formulation of the fastener analysis has been programmed to be the FDFA computer code. Convergence studies on the analysis, correlation of FDFA predictions with available analytical solutions, and sample predictions using FDFA are presented below.

3.9 Convergence Study on the Fastener Analysis (FDFA)

The number of actual plies in a bolted laminate determines the number of nodes in the portion of the fastener within that laminate. A physical ply can also be divided equally into two or more plies of smaller thicknesses, to improve the accuracy of the solution. Referring to Figure 3-13, if plate 1 is a laminate with n plies, the portion of the fastener within plate 1 can be divided into $\ell \times n$ segments that are $t_1/(\ell \times n)$ in thickness, where ℓ is any integer ≥ 1. In Figure 3-13, n = 5 and ℓ = 1.

The effect of the number of nodes per bolted plate on the displacement solution was studied by considering a steel-to-steel bolted joint example. The steel plates were 0.125 inch in thickness, and transferred a tensile load

55

The Matrix Equation (Figure 3-15)

$$
\begin{bmatrix}
c_{1,1} & c_{1,2} & c_{1,3} & c_{1,4} & c_{1,5} & 0 & & & & & & & & & & & \\
c_{2,1} & c_{2,2} & c_{2,3} & c_{2,4} & c_{2,5} & 0 & & & & & & & & & & & \\
c_{3,1} & c_{3,2} & c_{3,3} & c_{3,4} & c_{3,5} & 0 & & & & & & & & & & & \\
0 & c_{4,2} & c_{4,3} & c_{4,4} & c_{4,5} & c_{4,6} & 0 & & & & & & & & & & \\
0 & 0 & c_{5,3} & c_{5,4} & c_{5,5} & c_{5,6} & c_{5,7} & 0 & & & & & & & & & \\
0 & 0 & c_{6,4} & c_{6,5} & c_{6,6} & c_{6,7} & c_{6,8} & 0 & & & & & & & & & \\
0 & 0 & 0 & c_{7,5} & c_{7,6} & c_{7,7} & c_{7,8} & c_{7,9} & & & & & & & & & \\
0 & 0 & 0 & c_{8,5} & c_{8,6} & c_{8,7} & c_{8,8} & c_{8,9} & & & & & & & & & \\
0 & 0 & 0 & c_{9,5} & c_{9,6} & c_{9,7} & c_{9,8} & c_{9,9} & c_{9,10} & c_{9,11} & c_{9,12} & c_{9,13} & c_{9,14} & & & & \\
0 & 0 & 0 & 0 & c_{10,6} & c_{10,7} & c_{10,8} & c_{10,9} & c_{10,10} & c_{10,11} & c_{10,12} & c_{10,13} & & & & & \\
& & & & & & & & c_{11,10} & c_{11,11} & c_{11,12} & c_{11,13} & c_{11,14} & 0 & & & \\
& & & & & & & & c_{12,10} & c_{12,11} & c_{12,12} & c_{12,13} & c_{12,14} & 0 & & & \\
& & & & & & & & c_{13,11} & c_{13,12} & c_{13,13} & c_{13,14} & c_{13,15} & 0 & & & \\
& & & & & & & & & c_{14,12} & c_{14,13} & c_{14,14} & c_{14,15} & c_{14,16} & 0 & & \\
& & & & & & & & & & & c_{15,13} & c_{15,14} & c_{15,15} & c_{15,16} & c_{15,17} & \\
& & & & & & & & & & & c_{16,13} & c_{16,14} & c_{16,15} & c_{16,16} & c_{16,17} & \\
& & & & & & & & & & & c_{17,13} & c_{17,14} & c_{17,15} & c_{17,16} & c_{17,17} &
\end{bmatrix}
\begin{bmatrix}
u_1 \\ u_2 \\ u_3 \\ u_4 \\ u_5 \\ u_6 \\ u_7 \\ u_8 \\ u_9 \\ u_{10} \\ u_{11} \\ u_{12} \\ u_{13} \\ u_{14} \\ u_{15} \\ u_{16} \\ u_{17}
\end{bmatrix}
=
\begin{bmatrix}
0 \\
f_2(\bar{u}_3) \\
f_3(\bar{u}_2,\bar{u}_3,\bar{u}_4) \\
f_4(\bar{u}_3,\bar{u}_6,\bar{u}_5) \\
f_5(\bar{u}_4,\bar{u}_5,\bar{u}_6) \\
f_6(\bar{u}_5,\bar{u}_6,\bar{u}_7) \\
f_7(\bar{u}_6,\bar{u}_7,\bar{u}_8) \\
-2h_1^3 P/EI \\
0 \\
0 \\
-2h_2^3 P/EI \\
f_{12}(\bar{u}_{11},\bar{u}_{12},\bar{u}_{13}) \\
f_{13}(\bar{u}_{12},\bar{u}_{13},\bar{u}_{14}) \\
f_{14}(\bar{u}_{13},\bar{u}_{14},\bar{u}_{15}) \\
f_{15}(\bar{u}_{14},\bar{u}_{15},\bar{u}_{16}) \\
0 \\
f_{17}(\bar{u}_{15})
\end{bmatrix}
$$

Row labels (left of matrix):

$V_1(0)=0$

$M_1(0)=R_1\psi_1(0)$

Governing Equations

$V_1(t_1)=-P$

$\psi_1(t_1)=\psi_2(t_1)$

$M_1(t_1)=M_2(t_1)$

$V_2(t_1)=-P$

Governing Equations

$V_2(t_1+t_2)=0$

$M_2(t_1+t_2)=R_2\psi_2(t_1+t_2)$

Figure 3-15. The Matrix Equations for n=5 and m=4 (see Figure 3-13).

56

in a single lap configuration via a 0.25 inch diameter steel bolt. The steel bolt was assumed to have a modulus (E) of 30 x 10^6 and a Poisson's ratio (2) of 0.30. The steel plates were assumed to have an effective modulus of 7.68 x 10^6 psi, and the bolt was assumed to be free to rotate at the head and nut locations (zero moment or pin conditions). Figure 3-16 shows the predicted fastener/plate displacement variation through the thickness of plate 1, for an applied load of 1000 lbs, when the number of nodes in plate 1 is increased from 5 to 40. It is seen that beyond 20 nodes, the displacement distribution is relatively unaffected.

Figure 3-17 presents the fastener/plate displacement distribution through the thickness of plate 1, when the 1 kip load transfer is affected in a double lap configuration. In this case, the properties were assumed to be the same as those in Figure 3-16, and plate 2 was 0.25 inch in thickness. The results in Figure 3-17 also indicate that beyond 20 nodes, the displacement solution is relatively unaffected.

It is therefore necessary to divide a metallic plate into at least 20 identical "plies" to obtain a converged displacement solution, which ensures an accurate prediction of the load distribution in the thickness direction. In laminated (non-metallic) plates, a minimum of 30 nodes per plate is required to obtain accurate solutions.

3.10 Comparison of FDFA Predictions with Available Analytical Solutions

Harris and Ojalvo (Reference 3-1) have obtained analytical solutions for metal-to-metal load transfer in single and double shear configurations, when the boundary conditions at the fastener head and nut locations are restricted to zero moment (free pin) or zero slope (rigid head or nut). Predictions made by the finite difference fastener analysis (FDFA) code in SASCJ were compared with the results in Reference 3-1 to establish the validity of FDFA.

The first example selected for the correlation study is a single shear situation with no rotational constraint (zero moment or free pin condition) at the fastener head and nut locations. The bolted plates are 0.125 inch thick steel plates, and are assumed to have an effective modulus of 7.68 x 10^6 psi. The steel fastener is 0.25 inch in diameter, with E = 30 x 10^6 psi and ν = 0.3. The fastener is assumed to be a flexural beam in one case (rigid in shear), a shear beam in the second case (rigid in bending), and a completely
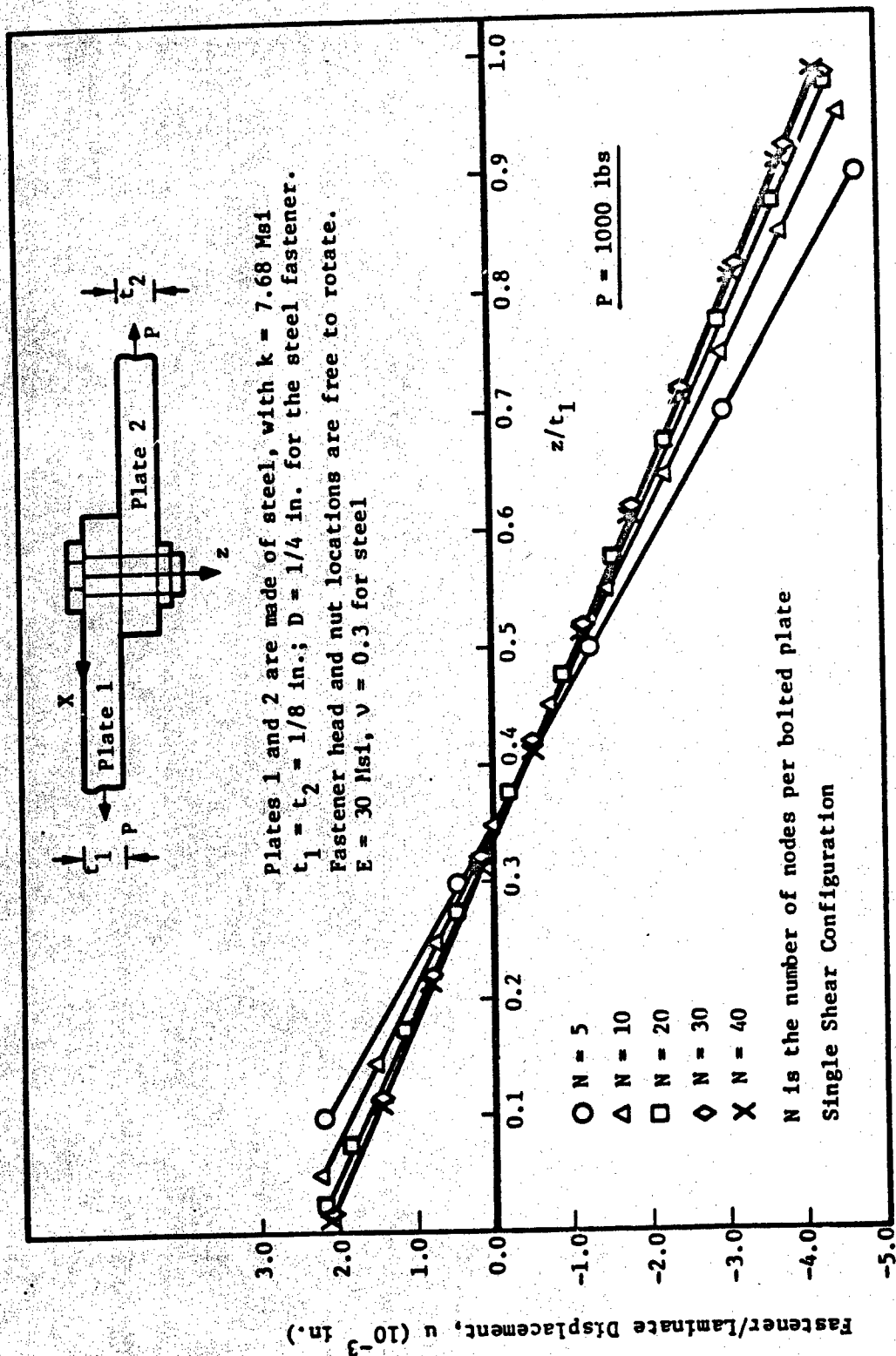
Figure 3-16. The Effect of Nodes Per Bolted Plate on the Convergence of the FDFA Displacement Solution for a Single Shear Situation.
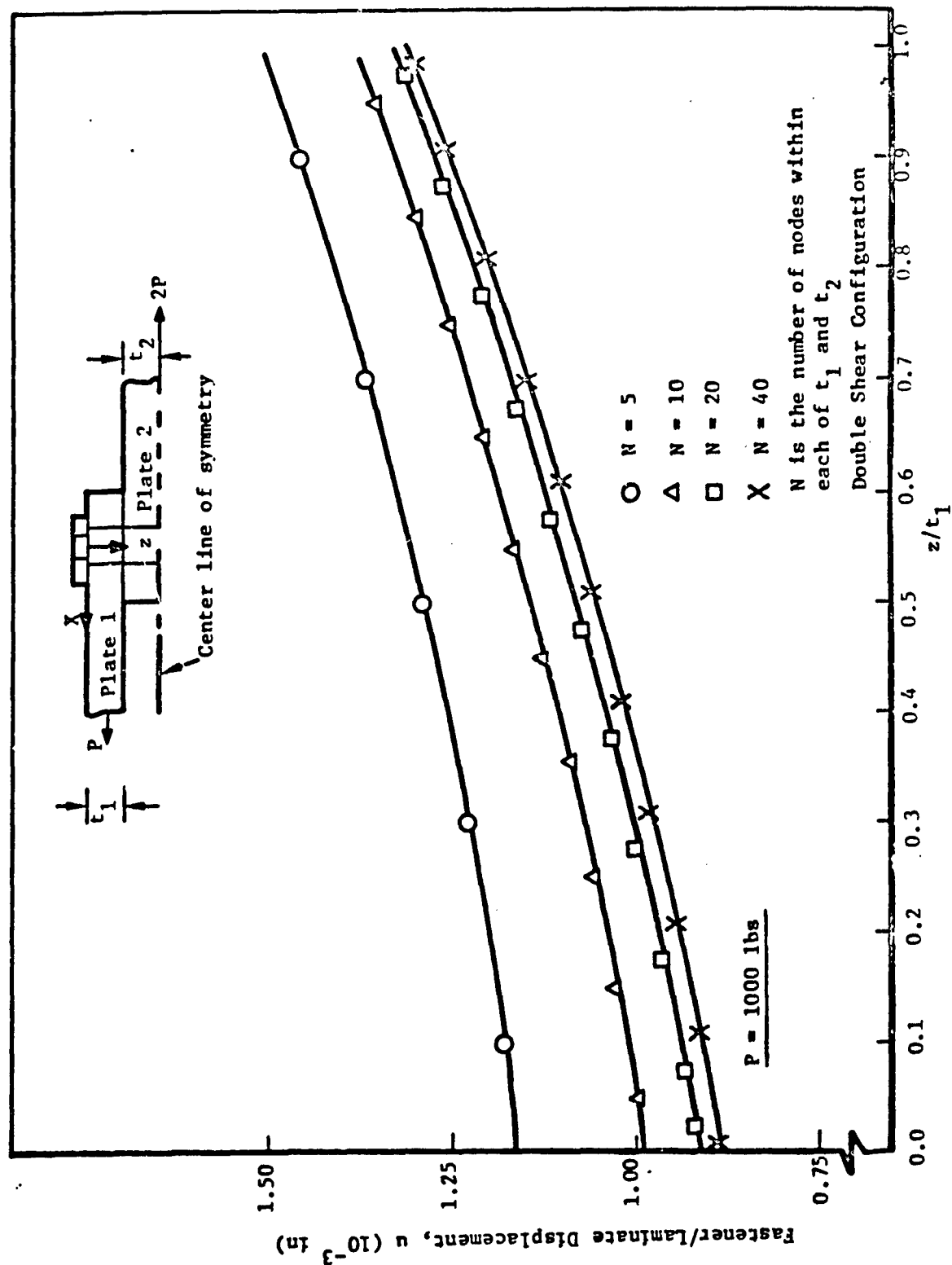
Figure 3-17. The Effect of Nodes per Bolted Plate on the Convergence of the FDFA
Displacement Solution for a Double Shear Situation

59

rigid beam in the third case. For the flexural beam, the analysis in Reference 3-1 set GA to be infinite in magnitude, and FDFA assumed λGA to be 10^{10} lbs. For the shear beam, FDFA assumed EI (infinity in Reference 3-1) to be 10^{10} lb-in^2. For the completely rigid beam, the analysis in Reference 3-1 set EI and GA to be infinity, and FDFA set E to be 3×10^{12} psi. A comparison between the predictions made by FDFA and the analysis in Reference 3-1 is presented in Table 3-1. Refer to Figure 3-11 for the definition of z/t_1, where t_1 is the thickness of the top plate (plate 1), and z is measured from the fastener head location (top of plate 1) toward the nut location. For the steel plates, the loading rate (q in lbs/inch) is expressed by $q = -ku$ (see Equation 3-11), where k is the effective modulus of the plate material and u is the fastener/plate displacement. The quantity qt_1/P represents a load interaction parameter which provides a measure of the deviation in the through-the-thickness load distribution from the uniform value of unity corresponding to a two-dimensional analysis of the plate. P is the applied load on the steel plates (see Figure 3-11).

Table 3-1 indicates that the FDFA predictions are within 5 percent of the analytical predictions made in Reference 3-1. It is noted that rigidity in shear or bending, or both, is only approximated by the FDFA code. The representation of the rigidities by numbers larger than those shown in Table 3-1 will result in numerical problems that result from an ill-conditioned coefficient m___ ___ ____ r the unknown displacements. Nevertheless, FDFA predictions and those base. the analysis in Reference 3-1 demonstrate an excellent agreement (erroi 5%), validating the FDFA code. It is also noted that the three types of rigidity yield approximately the same results using either analysis.

The second example selected for the correlation study is the same as the first example, but the fastener head and nut locations are assumed to be rigidly constrained (zero bending slope). Table 3-2 presents the comparison between predictions made by FDFA and the analysis in Reference 3-1. Again, the difference between the two sets of results is less than 5 percent and the two types of rigidities yield approximately the same results.

The last example considered for the validation of the FDFA code is a double shear situation where two 0.0625 inch thick steel plates (labeled 1 in Figure 3-12) transfer the applied load to a 0.125 inch thick steel plate

60

TABLE 3-1. COMPARISON BETWEEN FDFA AND THE ANALYSIS IN REFERENCE 3-1 FOR A SINGLE SHEAR SITUATION WITH NO ROTATIONAL CONSTRAINT AT THE FASTENER HEAD AND NUT LOCATIONS.

| Flexure Beam (Rigid in Shear) | | | | Shear Beam (Rigid in Bending) | | | | Completely Rigid Beam | | | |
| Ref. 3-1 (GA→∞) | | FDFA ($\lambda GA=10^{10}$ lbs) | | Ref. 3-1 (EI→∞) | | FDFA ($EI=10^{10}$ lb–in^2) | | Ref. 3-1 (EI, λGA→∞) | | FDFA ($E=3\times10^{12}$ psi) | |
z/t_1	qt_1/P	z/t_1	qt_1/P	z/t_1	qt_1/P	z/t_1	qt_1/P	z/t_1	qt_1/P	z/t_1	qt_1/P
0.0	-1.998	0.0167	-2.059	0.0	-1.992	0.0167	-2.053	0.0	-2.000	0.0167	-2.119
0.1	-1.389	0.05	-1.846	0.1	-1.392	0.05	-1.838	0.1	-1.400	0.05	-1.901
0.2	-0.800	0.15	-1.207	0.2	-0.795	0.15	-1.199	0.2	-0.800	0.15	-1.249
0.3	-0.201	0.25	-0.567	0.3	-0.200	0.25	-0.563	0.3	-0.200	0.25	-0.596
0.4	0.399	0.35	0.073	0.4	0.395	0.35	0.072	0.4	0.400	0.35	0.056
0.5	0.998	0.45	0.713	0.5	0.990	0.45	0.707	0.5	1.000	0.45	0.708
0.6	1.599	0.55	1.353	0.6	1.588	0.55	1.343	0.6	1.600	0.55	1.361
0.7	2.199	0.65	1.994	0.7	2.190	0.65	1.984	0.7	2.200	0.65	2.013
0.8	2.800	0.75	2.636	0.8	2.796	0.75	2.630	0.8	2.800	0.75	2.665
0.9	3.401	0.85	3.277	0.9	3.410	0.85	3.284	0.9	3.400	0.85	3.318
1.0	4.003	0.95	3.919	1.0	4.032	0.95	3.947	1.0	4.000	0.95	3.970
		0.983	4.133			0.983	4.171			0.983	4.188

Steel plates 1 and 2 are 0.125 inch in thickness, with an effective modulus of 7.8×10^6 psi.

The steel fastener is 0.25 inch in diameter, with $E = 30 \times 10^6$ psi and $\nu = 0.3$.

61

TABLE 3-2. COMPARISON BETWEEN FDFA AND THE ANALYSIS IN REFERENCE 3-1 FOR A SINGLE SHEAR SITUATION WITH RIGID CONSTRAINTS AT THE FASTENER HEAD AND NUT LOCATIONS.

Shear Beam (Rigid in Bending)				Completely Rigid Beam			
Ref. 3-1 $(EI \to \infty)$		FDFA $(EI=10^5 \text{lb-in}^2)$		Ref. 3-1 $(EI, \lambda 6A \to \infty)$		FDFA $(E= 3\times10^{12}\text{psi})$	
z/t_1	qt_1/p	z/t_1	qt_1/p	z/t_1	qt_1/p	z/t_1	qt_1/p
0.0	0.961	0.0167	0.988	0.0	1.000	0.0167	1.031
0.1	0.962	0.05	0.989	0.1	1.000	0.05	1.031
0.2	0.966	0.15	0.991	0.2	1.000	0.15	1.031
0.3	0.972	0.25	0.996	0.3	1.000	0.25	1.032
0.4	0.980	0.35	1.005	0.4	1.000	0.35	1.032
0.5	0.990	0.45	1.016	0.5	1.000	0.45	1.033
0.6	1.029	0.55	1.030	0.6	1.000	0.55	1.034
0.7	1.018	0.65	1.048	0.7	1.000	0.65	1.036
0.8	1.036	0.75	1.068	0.8	1.000	0.75	1.037
0.9	1.056	0.85	1.091	0.9	1.000	0.85	1.039
1.0	1.078	0.95	1.118	1.0	1.000	0.95	1.040
		0.983	1.127			0.983	1.041

Steel plates 1 and 2 are 0.125 inch in thickness, with an effective modulus of 7.68×10^6 psi.

The steel fastener is 0.25 inch in diameter, with $E = 30 \times 10^6$ psi and $\nu = 0.3$.

62

(labeled 2 in Figure 3-12) via a 0.25 inch diameter steel fastener. The
fastener is assumed to be completely rigid (EI and GA $\rightarrow \infty$), and is assumed to be
free to rotate at the head and nut locations (zero moment conditions). The
FDFA code represented a rigid fastener by increasing its modulus from
30×10^6 to 30×10^{10} psi. The analysis in Reference 3-1 predicted a uniform
load distribution ($qt_1/P = 1$ for $0 < z/t_1 < 1$). The FDFA code also predicted
a uniform load distribution ($qt_1/P = 1.034$ for $0 < z/t_1 < 1$), and indicated
a 3% error in the recovery of the applied load.

The FDFA code, therefore, predicts accurately the closed form solutions
for the discussed joint situations. The error in the FDFA predictions is
restricted to within 5 percent, and the FDFA code is also applicable in
situations where closed form solutions are difficult to obtain. These
include non-metallic bolted plates, and general elastic constraints at the
fastener head and nut locations.

3.11 Effect of Single and Double Shear Load Transfer on the Through-the-Thickness
Load Distribution

The difference in the through-the-thickness load distributions between
single and double shear load transfer situations is demonstrated in Figure 3-18.
In this case, the bolted plates are made of steel, and the 1/4 inch diameter
steel fastener is assumed to be free to rotate at the head and nut locations.
The load intensity in a ply is quantified by -ku (lbs/in), and the load
intensity for a uniform distribution is expressed as P/t_1 (lbs/in) for the top
plate (plate 1). The load intensity ratio - kut_1/P, therefore, is a measure
of the variation from the uniform distribution. Figure 3-18 indicates that the
load intensity ratio varies between -2 and 4 for the single shear situation,
and is approximately 1 (near uniform distribution) for the double shear
situation.

If the fastener head and nut locations are constrained against rotation
(zero bending slope), the single shear situation also results in a near uniform
load distribution (see Table 3-2). In practical joints, rotational constraints
at the fastener head and nut locations are introduced by the washers, and are
influenced by the fastener torque (see Section 3.6). Regardless of what the
empirical elastic constraint equations are at these locations ($M = R\psi$), the
load intensity ratio will be approximately unity in practical situations, and

63
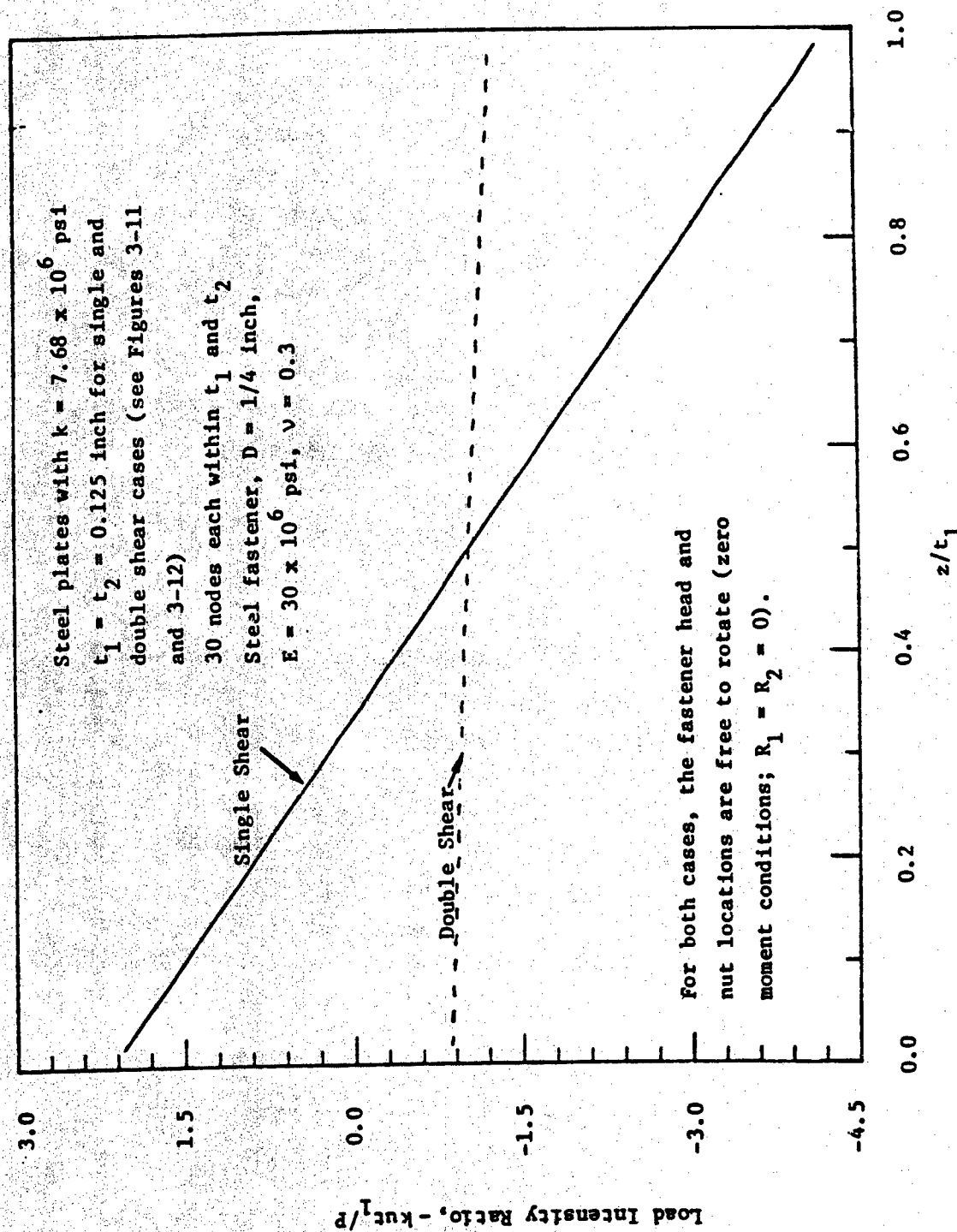
Figure 3-18. Effect of Single and Double Shear Load Transfer on the Through-the-Thickness Load Distribution.

64

will not vary as much as in the situation considered in Figure 3-18. An exception is a flush-head or countersunk fastener in which the head is practically unconstrained against rotation. But, the FDFA code is currently restricted to protruding head fasteners.

3.12 Effect of Fastener Size

The effect of fastener size on the through-the-thickness load distribution is shown in Figure 3-19. The example assumes two 0.125 inch thick steel plates to be joined by a steel fastener in a single shear configuration. The head and nut locations of the fastener are assumed to be unrestrained (zero moment conditions). Figure 3-19 indicates that for D/t_1 values that are greater than or equal to unity, the fastener size has a negligible effect on the through-the-thickness load distribution. For $D/t_1 \geq 1$, the load intensity ratio varies from -2 to 4 as z/t_1 varies from 0 to 1. But, for D/t_1 values that are less than unity, the fastener bending and shear effects increase with a decrease in D/t_1. For $D/t_1 = 1/4$, for example, the load intensity ratio varies from near 0 to 10 as z/t_1 varies from 0 to 1. In these situations, the large fastener displacements generally result in fastener failures.

3.13 Effect of Fastener Material

Three fastener materials were considered for this study -- steel, titanium and aluminum. The effect of the material on the through-the-thickness load distribution (load intensity ratio) is presented in Figures 3-20 to 3-22. When D/t_1 is greater than or equal to unity, the material has a negligible effect on the load distribution. In this case, the fastener behaves like a rigid fastener, and the differences among the moduli of the three materials have no effect on the load distribution. But, when D/t_1 is less than unity (1/2 in Figure 3-21, and 1/4 in Figure 3-22), the fastener flexibility is influenced significantly by the modulus of the material. In this case, the material with the lowest modulus (aluminum in the chosen example) yields the largest load intensity ratio.

3.14 Effect of Stacking Sequence on Through-the-Thickness Load Distribution

When one of the bolted plates is a laminate, the stacking sequence influences the ply load distribution and consequently the joint strength. To illustrate this, selected composite-to-aluminum tests from Reference 3-6 are considered. The selected test cases involve 50/40/10, AS1/3501-6 graphite/
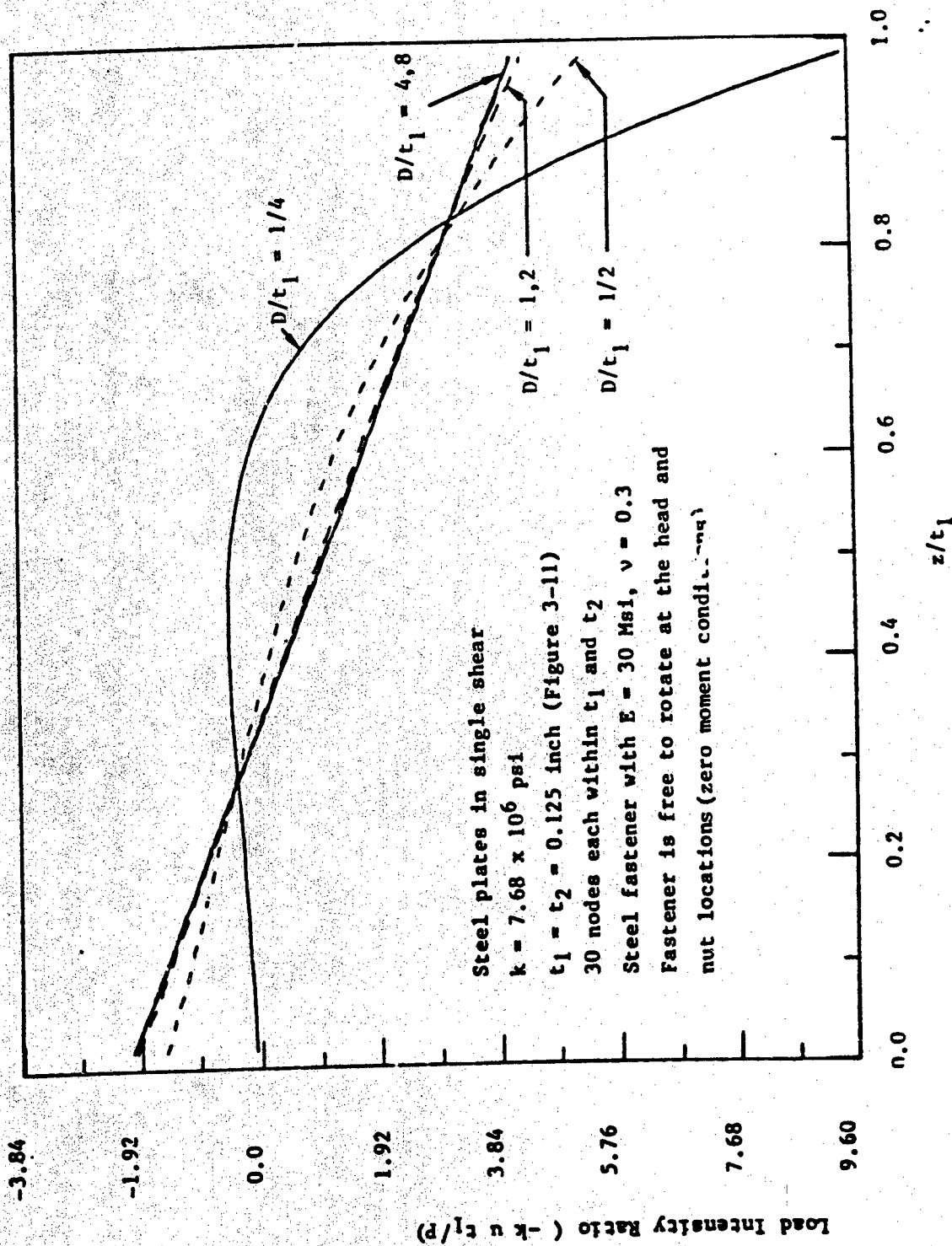
Figure 3-19.   Effect of Fastener Size on the Through-The Thickness Load Distribution.

Steel plates in single shear

k = 7.68 x 10^6 psi

t_1 = t_2 = 0.125 inch (Figure 3-11)

30 nodes each within t_1 and t_2

Steel fastener with E = 30 Msi, ν = 0.3

Fastener is free to rotate at the head and
nut locations (zero moment condi...ng)

D/t_1 = 1/4

D/t_1 = 4,8

D/t_1 = 1,2

D/t_1 = 1/2

z/t_1

Load Intensity Ratio (-k u t_1/P)

66
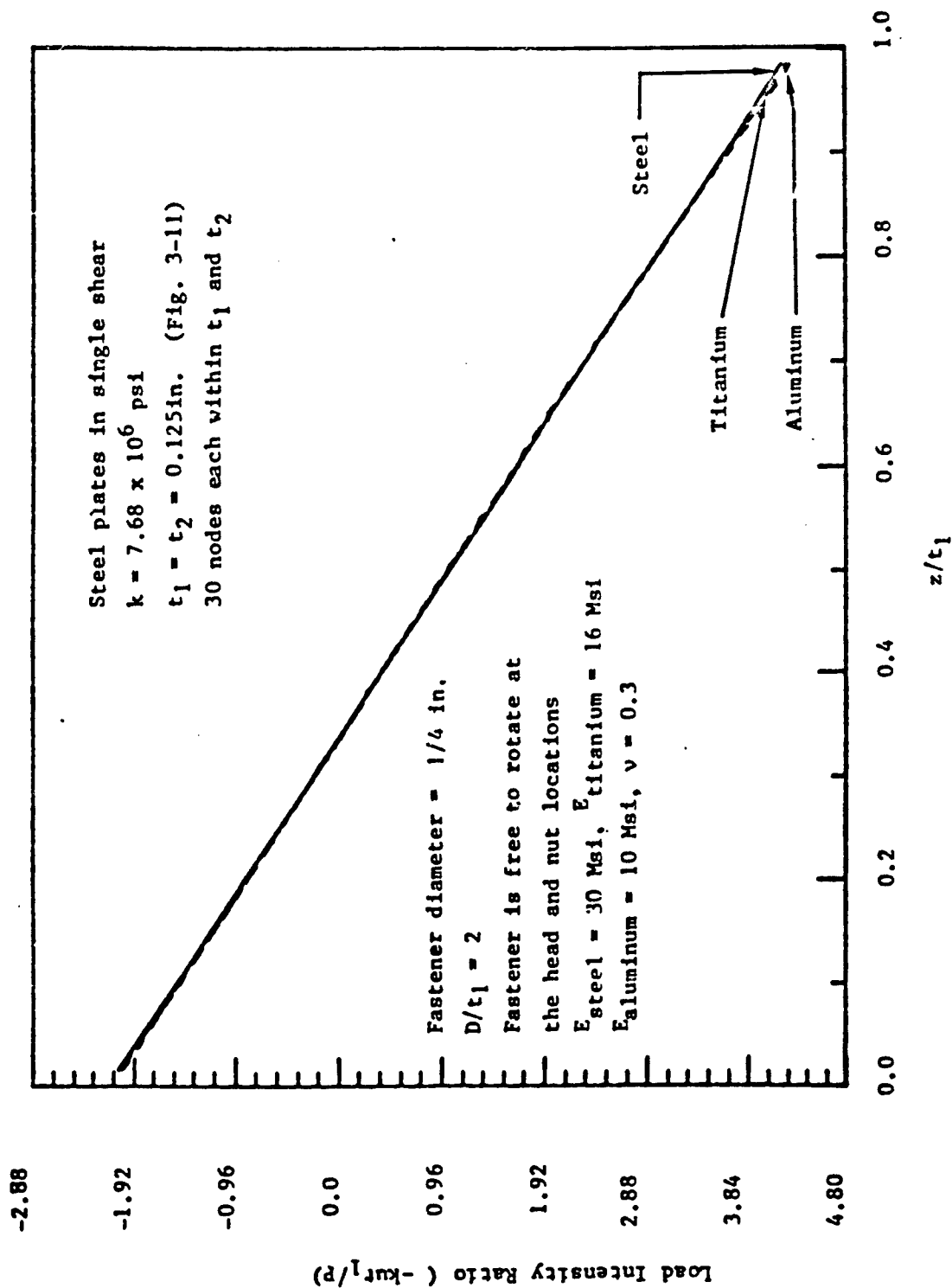
Figure 3-20. Effect of Fastener Material when $D/t_1 = 2$

The chart shows:

Steel plates in single shear

$k = 7.68 \times 10^6$ psi

$t_1 = t_2 = 0.125$in. (Fig. 3-11)

30 nodes each within t_1 and t_2

Fastener diameter = 1/4 in.

$D/t_1 = 2$

Fastener is free to rotate at the head and nut locations

$E_{steel} = 30$ Msi, $E_{titanium} = 16$ Msi

$E_{aluminum} = 10$ Msi, $\nu = 0.3$

Vertical axis: Load Intensity Ratio ($-kut_1/P$)

Horizontal axis: z/t_1

67
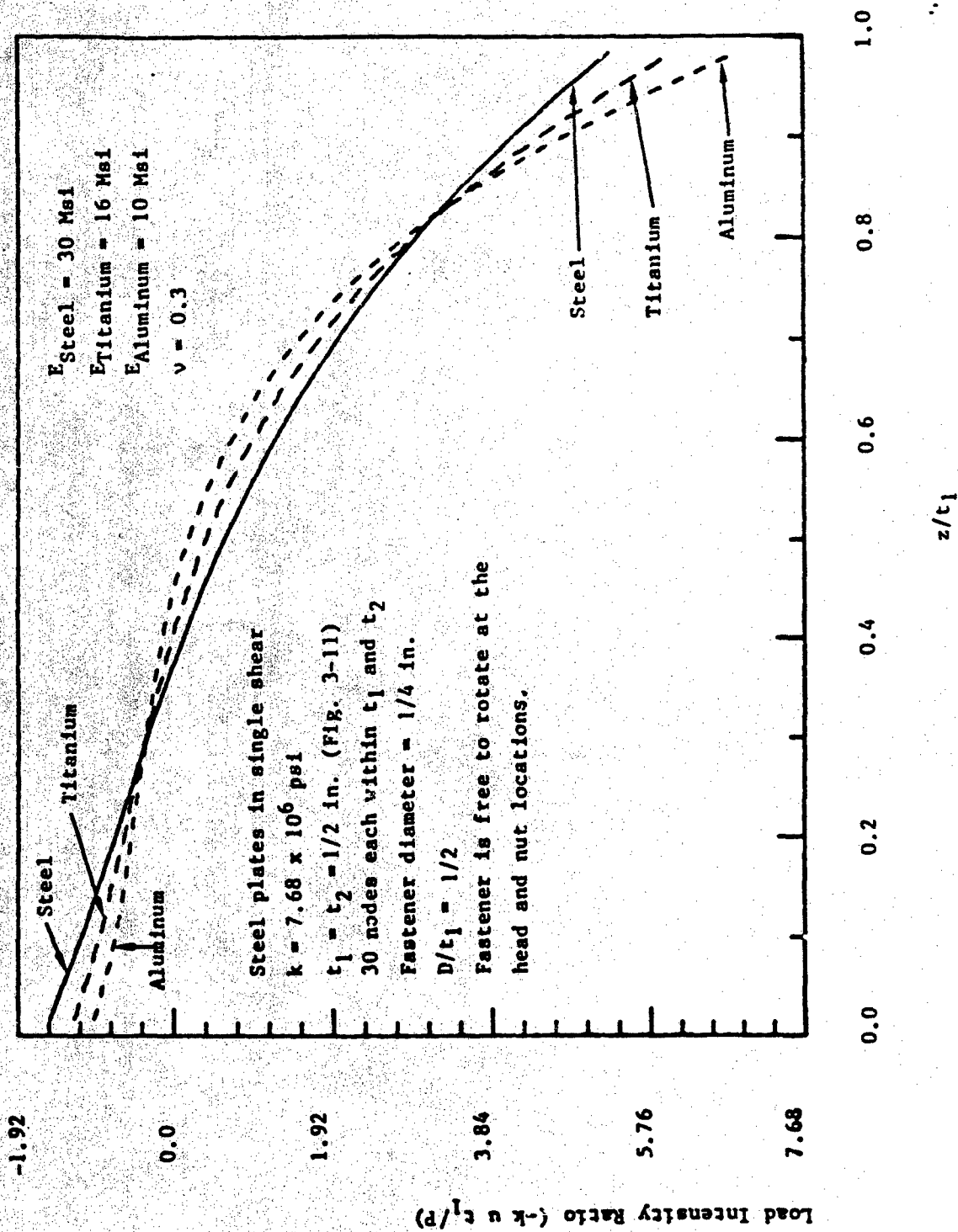
Figure 3-21. Effect of Fastener Material when $D/t_1 = 1/2$

Steel

Titanium

Aluminum

$E_{Steel} = 30$ Msi
$E_{Titanium} = 16$ Msi
$E_{Aluminum} = 10$ Msi
$\nu = 0.3$

Steel plates in single shear
$k = 7.68 \times 10^6$ psi
$t_1 = t_2 = 1/2$ in. (Fig. 3-11)
30 nodes each within t_1 and t_2
Fastener diameter = 1/4 in.
$D/t_1 = 1/2$
Fastener is free to rotate at the
head and nut locations.

z/t_1

Load Intensity Ratio $(-k \, u \, t_1/P)$

Aluminum

Titanium

Steel

Titanium

Aluminum

Steel plates in single shear

$k = 7.68 \times 10^6$ psi

$t_1 = t_2 = 0.125$ in. (Fig. 3-11)

30 nodes each within t_1 and t_2

Fastener diameter = 1/32 in. $(D/t_1 = 1/4)$

Fastener is free to rotate at the head and nut locations.

$E_{Steel} = 30$ Msi, $E_{Titanium} = 16$ Msi

$E_{Aluminum} = 10$ Msi, $\nu = 0.3$

z/t_1

0.0 0.2 0.4 0.6 0.8 1.0

Load Intensity Ratio $(-k\,u\,t_1/P)$

-2.4 0.0 2.4 4.8 7.2 9.6 12.0 14.4

Figure 3-22. Effect of Fastener Material when $D/t_1 = 1/4$

epoxy laminates of three different stacking sequences. The laminates are 0.119 inch in thickness, contain 20 plies, and are bolted to 0.31 inch thick aluminum plates with 0.25 inch diameter, protruding head, steel fasteners. The load transfer occurs in a single shear configuration (Figure 3-11).

The variation in the ply loads with a change in the laminate stacking sequence was predicted using the FDFA code. The aluminum plate was divided into 30 layers of identical properties ($E = 10$ Msi, $\nu = 0.3$). Each ply in the laminate was divided equally into two layers of identical properties. The 20-ply laminate was, therefore, modeled as a 40-ply plate with the following properties: $E_{11} = 18.5$ Msi, $E_{22} = 1.9$ Msi, $\nu_{12} = 0.3$ and $G_{12} = 0.85$ Msi. The aluminum and composite plates were assumed to be 2 inches long and 1 inch wide, with the 0.25 inch diameter hole at the center ($E/D = W/D = 4$). The effective foundation modulus for each ply type (fiber orientation) was computed as described in Section 3.5. This yielded an effective foundation modulus (k) of 28.8 Msi for aluminum, 30.5 Msi for the 0° AS1/3501-6 ply, 19.2 Msi for the + or -45° AS1/3501-6 ply, and 4.76 Msi for the 90° AS1/3501-6 ply. The elastic constraints at the fastener head and nut locations were assumed to be of the form shown in Equation 3-16, and the disk radius in Equation 3-15 was assumed to be 1/8 inch.

Using the above input data, FDFA predicted the ply load distributions in 50/40/10 layups of three different stacking sequences -- $[(45/0/-45/0)_2/0/90]_s$, $[0_3/\pm45/0_2/\pm45/90]_s$ and $[90/\pm45_2/0_5]_s$. Figure 3-23 shows how different the ply loads are when the stacking sequence is varied. This also has a direct influence on the joint strength.

70

Figure 2-23. Ply Loads in AS1/3501-6 Graphite/Epoxy Laminates with a 50/40/10 Layup and Different Stacking Sequences, When Bolted to Aluminum Plates in a Single Shear Configuration.

71

Figure 3-23. Ply Loads in AS1/3501-6 Graphite/Epoxy Laminates with a 50/40/10 Layup and Different Stacking Sequences, When Bolted to Aluminum Plates in a Single Shear Configuration (Continued).

The figure contains the following annotations:

Composite-to-aluminum load transfer in single shear.

Plate 1: Aluminum; $t_1 = 0.31$ in.

Plate 2: $\left[0_3/\pm45/0_2/\pm45/90\right]_s$ AS1/3501-6; $t_2 = 0.119$ in. Plate 2 has a 50/40/10 layup.

30 nodes within t_1.
40 nodes within t_2.

Applied Load = 1 kip
Steel fastener
D = 1/4 in.
Torque = 0 in-lbs
Elastic constraints at the head and nut locations

Axis labels:
Ply Loads in the Laminate (lbs)
z/t_2
Ply Number

Figure 3-23. Ply Loads in ASI/3501-6 Graphite/Epoxy Laminates with a 50/40/10 Layup and Different Stacking Sequences, When Bolted to Aluminum Plates in a Single Shear Configuration (Concluded).

SECTION 4

STRENGTH ANALYSIS OF SINGLE FASTENER JOINTS IN COMPOSITE STRUCTURES

4.1   Introduction

The two-dimensional anisotropic plate analysis described in Section 2 (FIGEOM) and the finite difference fastener analysis described in Section 3 (FDFA) are incorporated into a failure procedure to develop a strength analysis for single fastener joints in composite structures. A general fastener location in a bolted structure (see Figure 1-1) involves the type of loading shown in Figure 4-1. The general situation can be analyzed as a superposition of an unloaded hole situation and a fully-loaded hole situation, as shown in Figure 4-1. The unloaded hole case is analyzed using the two-dimensional plate analysis (FIGEOM), and does not involve the fastener analysis (FDFA). The fully-loaded hole situation involves both the analyses, and Section 4-2 describes the failure procedure for this case.

The loaded hole situation is analyzed using a progressive failure procedure that predicts local ply failures and delaminations until the bolted plate cannot carry any additional applied load. The employed ply failure criteria and the delamination criterion are discussed in Sections 4.4 and 4.5, respectively. The strength analysis has been programmed to be the SASCJ (Strength Analysis of Single Fastener Composite Joints) computer code. Sample strength predictions using SASCJ are presented in Section 5.

4.2   Strength Analysis Procedure for Fully-Loaded Holes

The strength of laminates with fully-loaded holes is predicted using the procedure outlined in Figure 4-2. A two-dimensional stress analysis (FIGEOM), accounting for finite dimensions of the bolted plates, is initially performed on each bolted plate. Computed plate stresses are used to calculate the effective moduli of the various ply types in each bolted plate (see Section 3.5). The inplane strains computed by the FIGEOM code are used to obtain the stress state in each ply. The ply stresses around the hole boundary are integrated to yield the bearing load in each ply (see Section 3.5). The inplane stresses in each ply, per unit bearing load, are incorporated into selected failure criteria to compute the ply (bearing) loads corresponding
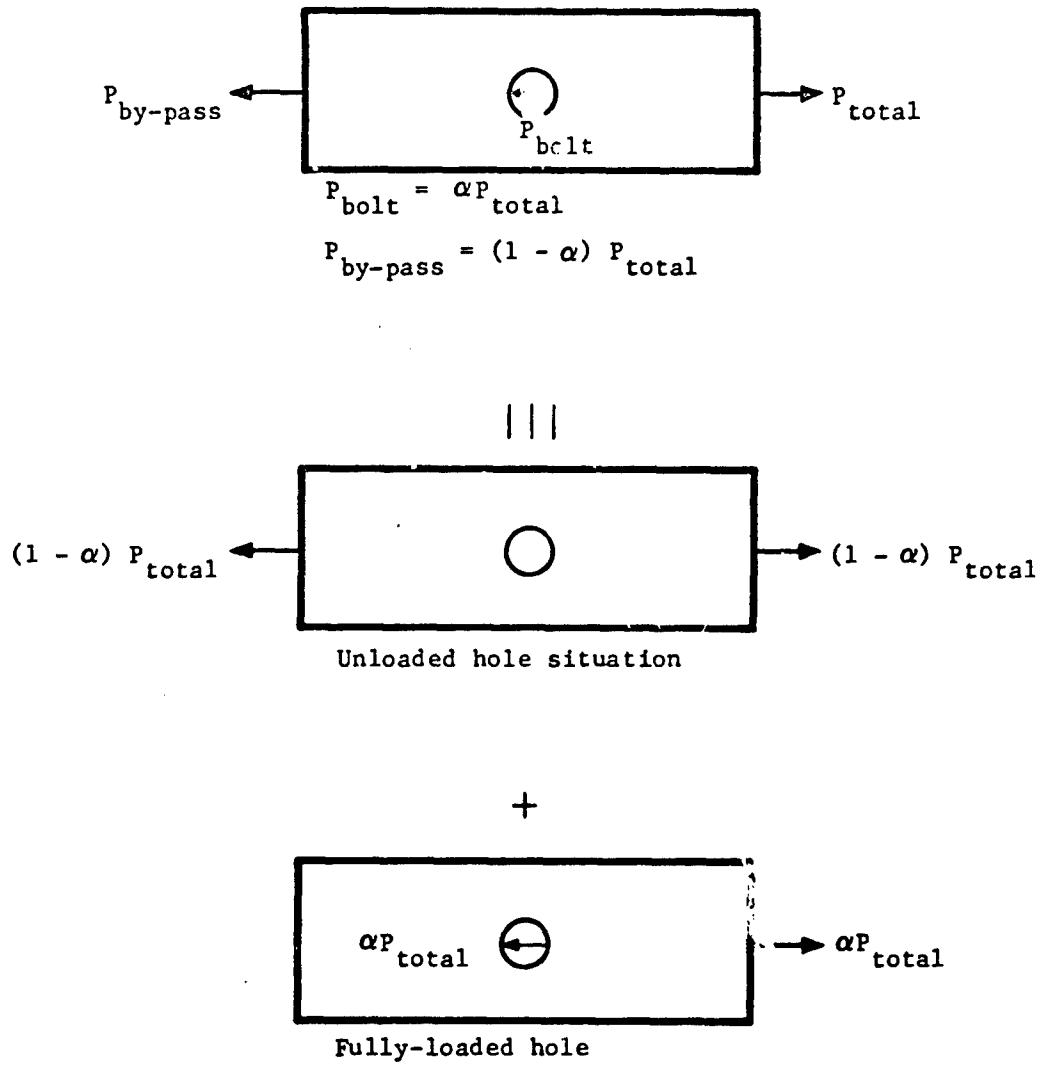
Figure 4-1. Schematic Representation of a General Single Fastener Situation as a Superposition of Unloaded and Fully-Loaded Hole Situations.
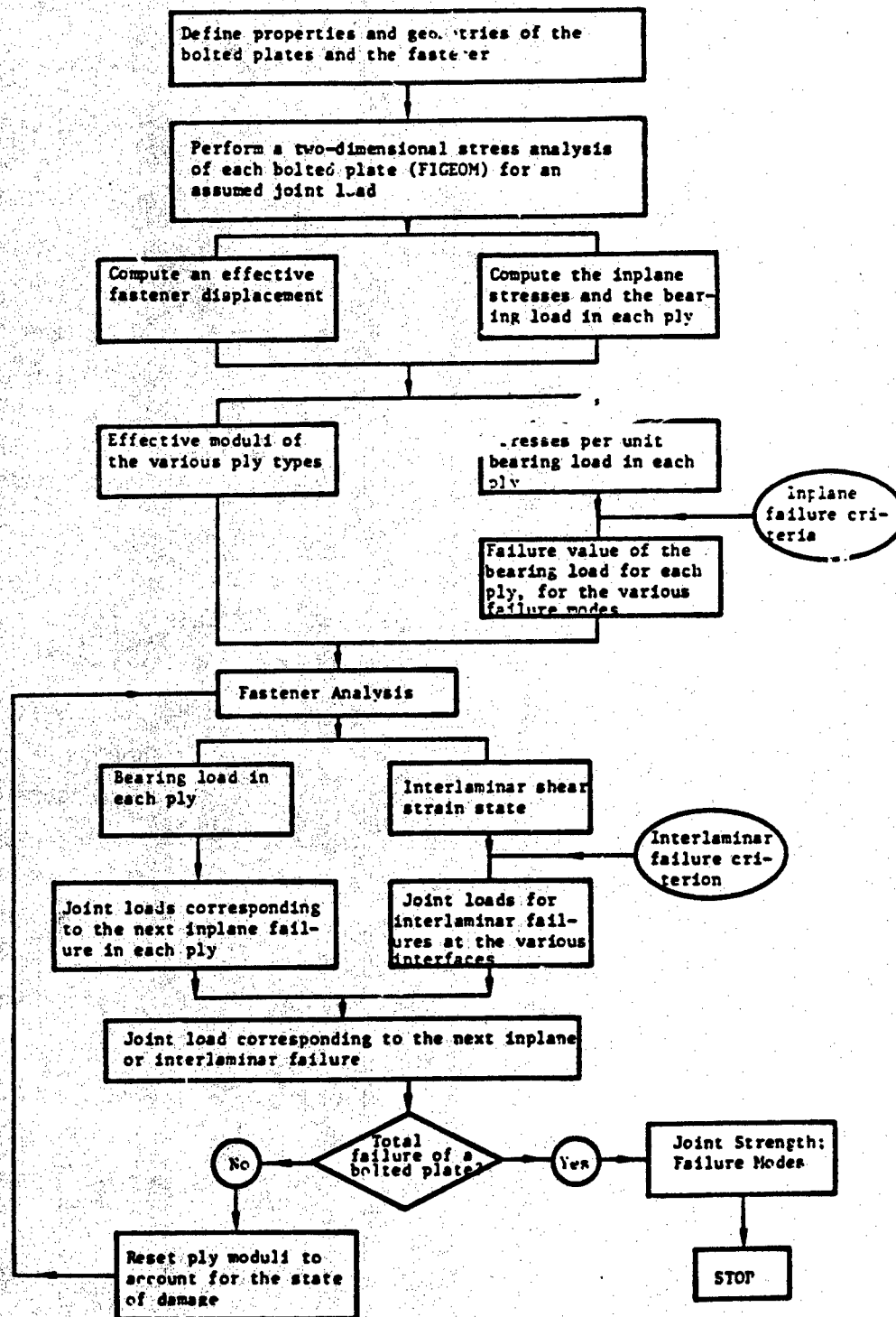
Figure 4-2. Flowchart for the Strength Analysis of
Laminates with Fully-Loaded Holes.

76

to the various inplane failure modes. The selected failure criteria are presented in Section 4.4.

The effective moduli and the ply bearing loads corresponding to the various failure modes, for all the plies in each bolted plate, are incorporated into the fastener analysis described in Section 3. The initial fastener analysis on the undamaged plates assumes the $\bar{u}$ terms for all the plies to be zero (see Equations 3-?? to 3-28), and computes the distribution of the applied bearing load among the various plies. Comparing these ply loads with the stored failure values for inplane ply failures, the joint load corresponding to the earliest ply failure is obtained. The fastener analysis also computes approximate shear strain values at the interfacial locations between adjacent plies. Incorporating these into an interlaminar failure criterion, the joint load corresponding to the earliest interlaminar failure (delamination) is obtained. The smaller of the two joint loads, corresponding to the earliest inplane and interlaminar failures, determines the first failure in a bolted plate and the corresponding joint load value.

The effective moduli of the damaged plies are reset to appropriately represent the predicted failure modes. The revised moduli are incorporated into the fastener analysis, and the procedure is repeated to predict the next failure mode and the corresponding joint load. When any ply is predicted to fail totally, the analysis computes the redistribution of the corresponding joint load among the remaining effective plies, and determines if any other concomitant ply failure is precipitated. This process is repeated until one of the bolted plates becomes ineffective in transferring the applied load (joint failure).

The SASCJ computer code is restricted to protruding head type fasteners, and assumes that fastener failure is precluded. It can analyze any combination of laminated and metallic plates, bolted together in a single lap or double lap configuration.

4.3   Strength Analysis Procedure for Partially-Loaded Holes

A general fastener location in a bolted plate transfers a fraction (α) of the total applied load via the fastener, the remainder ($1-\alpha$) being by-passed to the next fastener location (see Figures 1-1 and 4-1). In this

77

case, the stress state at the fastener location is computed as a superposition of the stress states corresponding to the unloaded and fully-loaded hole situations. Figure 4-3 presents a schematic representation of how the averaged stresses are obtained to predict net section, shear-out and bearing failures in the plies using average stress failure criteria (see Section 4.4). For a unit applied load, the averaged stresses in the laminate with an unloaded hole, when subjected to a load of $(1-\alpha)$, and the averaged stresses in the laminate with a fully loaded hole, when subjected to a load of α, are computed separately and added. Incorporating the combined averaged stresses into the appropriate failure criteria, the applied load corresponding to a ply failure is computed.

In the case of fully-loaded holes, progressive failure prediction involves the repetition of the fastener analysis with revised ply properties after every ply failure. The two-dimensional analysis (FIGEOM) is only carried out once (see Section 4.2). But, in the case of partially-loaded holes, a ply failure will affect the unloaded and the fully-loaded hole contributions to the local stresses. Hence, progressive failure prediction in the partially-loaded case involves repeating FIGEOM and FDFA analyses after total ply failures.

4.4   Inplane Failure Criteria

The SASCJ code permits the user to select any of the following five failure criteria for the prediction of ply failures based on inplane stresses and strains: (1) point stress failure criterion, (2) average stress failure criterion, (3) maximum (fiber directional) strain criterion, (4) Hoffman criterion, and (5) Tsai-Hill criterion. The first two criteria predict three modes of failure in each ply--net section, shear-out and bearing. The maximum strain criterion predicts ply failure based on fiber directional strain. The Hoffman and Tsai-Hill criteria predict ply failure accounting for biaxial stress interaction that is ignored by the first three criteria.

The point stress failure criterion predicts net section, shear-out and bearing failures when the appropriate stress components at selected locations attain unnotched specimen failure values (see Figure 4-4). a_o^{ns}, a_o^{so} and a_o^{brg} are called characteristic distances (see Reference 4-1). When $\sigma_x(0, D + a_o^{ns})$ exceeds the unnotched tensile or compressive strength of the ply, as appropriate,
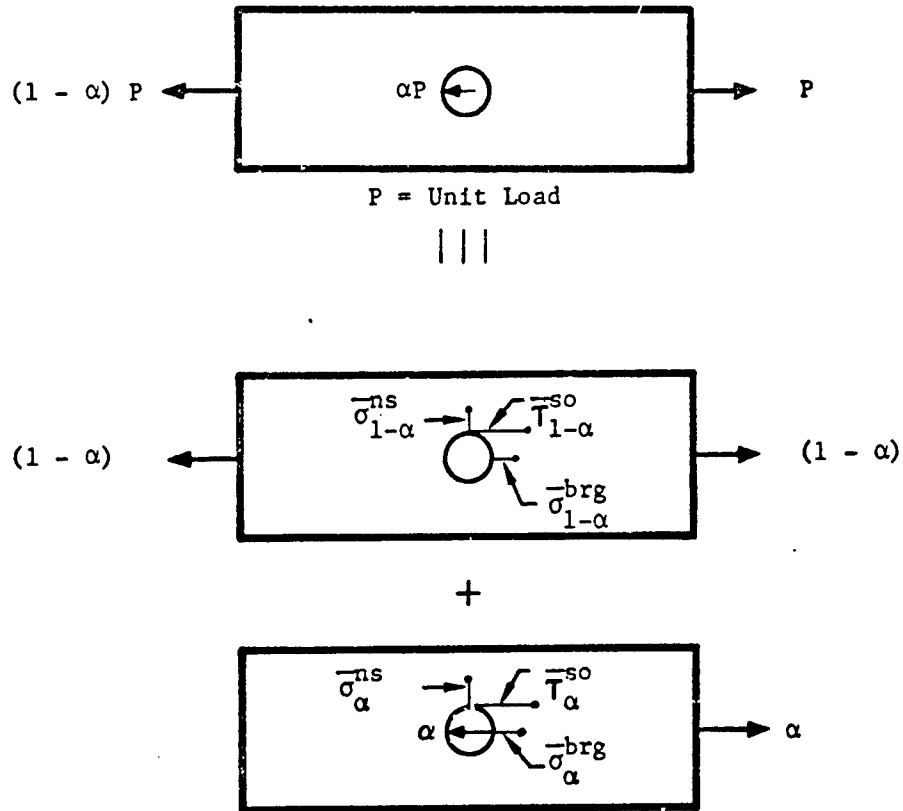
$$\overline{\sigma}^{ns} = \int_{D/2}^{D/2 + d_{ons}} \sigma_x(o,y)\, dy \qquad = \qquad \overline{\sigma}^{ns}_{1-\alpha} + \overline{\sigma}^{ns}_{\alpha}$$

$$\overline{\tau}^{so} = \int_{0}^{d_{oso}} \tau_{xy}(x, D/2)\, dx \qquad = \qquad \overline{\tau}^{so}_{1-\alpha} + \overline{\tau}^{so}_{\alpha}$$

$$\overline{\sigma}^{brg} = \int_{D/2}^{D/2 + d_{obrg}} \sigma_x(x,o)\, dx \qquad = \overline{\sigma}^{brg}_{1-\alpha} + \overline{\sigma}^{brg}_{\alpha}$$

Figure 4-3. Strength Analysis of Laminates with Partially-Loaded Holes using Average Stress Failure Criteria.

The σ_x value at this location determines net section failure

The τ_{xy} value at this location determines shear-out failure

a_o^{ns} a_o^{so}

a_o^{brg}

The σ_x value at this location determines bearing failure
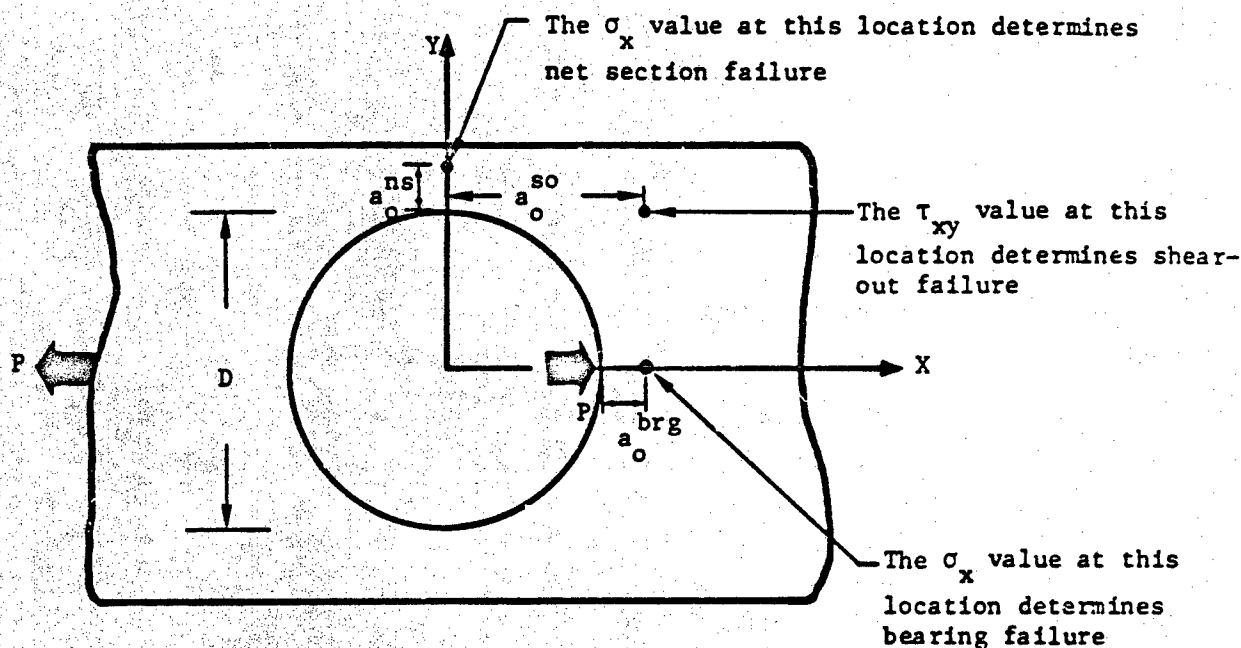
Figure 4-4. The Characteristic Distances used in the Point Stress Failure Criteria

$$\int_{D/2}^{D/2 + d_{ons}} \sigma_x(o,y)\,dy \text{ determines net section failure}$$

$$\int_{o}^{d_{oso}} \tau_{xy}(x,D/2)\,dx$$
determines shear-out failure

d_o^{ns} d_o^{so}

d_o^{brg}

$$\int_{D/2}^{D/2 + d_{obrg}} \sigma_x(x,0)\,dx$$
D/2
determines bearing failure
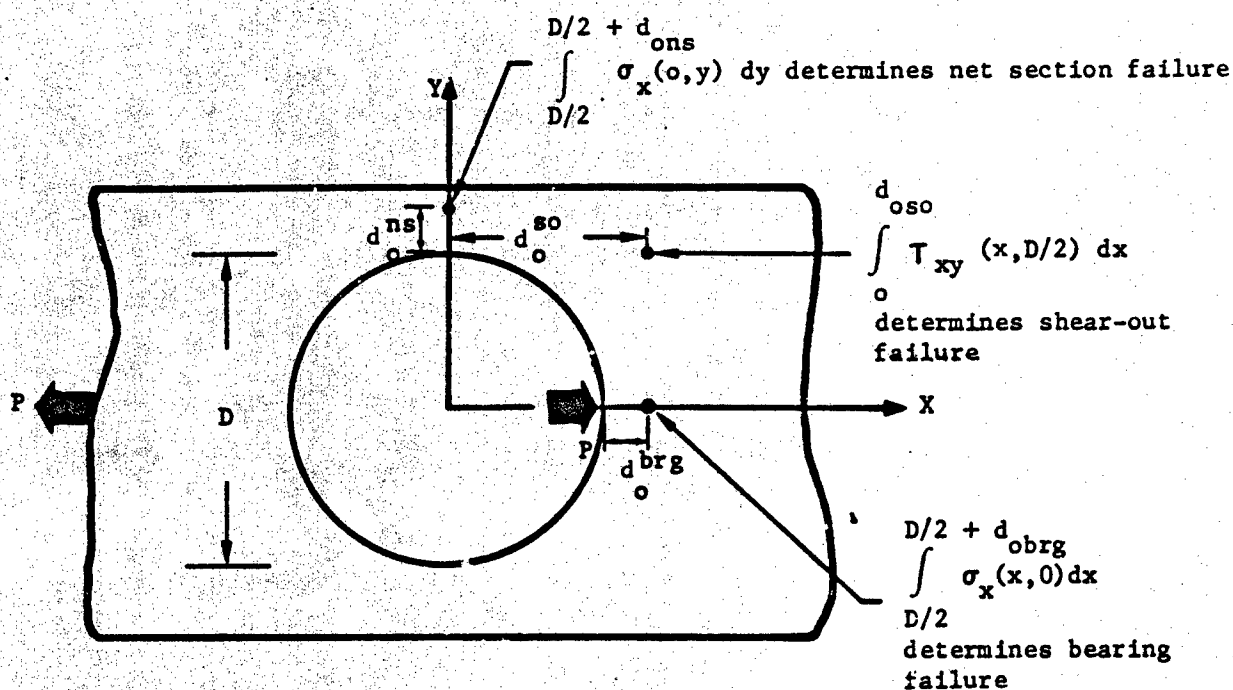
Figure 4-5. The Characteristic Distances Used in the Average Stress Failure Criteria.

80

a net section ply failure is predicted. When $\sigma_x(D + a_o^{brg}, 0)$ exceeds the un-notched compressive strength of the ply, a bearing mode of ply failure is predicted. When τ_{xy} (a_o^{so}, D/2) exceeds the unnotched ply shear strength, a shear-out mode of ply failure is predicted. The average stress failure criterion predicts these failures based on averaged values of the mentioned stress components over selected characteristic distances (d_o^{ns}, d_o^{so}, and d_o^{brg}) that are larger in magnitude compared to those used in conjunction with the point stress criterion (see References 4-2 and 4-3, and Figure 4-5)

Of the three ply failure modes, only the net section mode causes the ply to become almost ineffective (total failure). The bearing mode of failure causes the ply to suffer a reduction in its effective modulus without losing its load-carrying capacity. The shear-out mode of failure causes a ply to become ineffective only when it is delaminated from the adjacent plies (see Section 4.5). When a ply suffers any of the above failures, its load versus deflection response is at the knee of the bilinear representation in Figure 3-8. The damaged ply can carry additional load until total ply failure is precipitated. The SASCJ computer code auto-matically stores the damage state in every ply in the bolted plates, and re-assigns values for ply moduli to appropriately represent predicted ply failures. When a ply suffers total failure, its modulus is set equal to zero (see Equation 3-11), and the redistribution of the joint load among the remaining plies is computed. A typical overall load versus deflection behavior of the joint is shown in Figure 4-6, indicating the effects of local and total ply failures.

The maximum strain (fiber directional), Hoffman and Tsai-Hill criteria are applied along a path that is concentric to the fastener hole, at a characteristic distance (a_o) from the hole boundary (see Figure 4-7 and Reference 4-4). The location along this path where the selected criterion is satisfied determines the failure location. The maximum strain criterion predicts fiber failure in a ply (total ply failure) when its fiber directional strain exceeds the failure value (ε_{11}^{tu} or ε_{11}^{cu}).

81
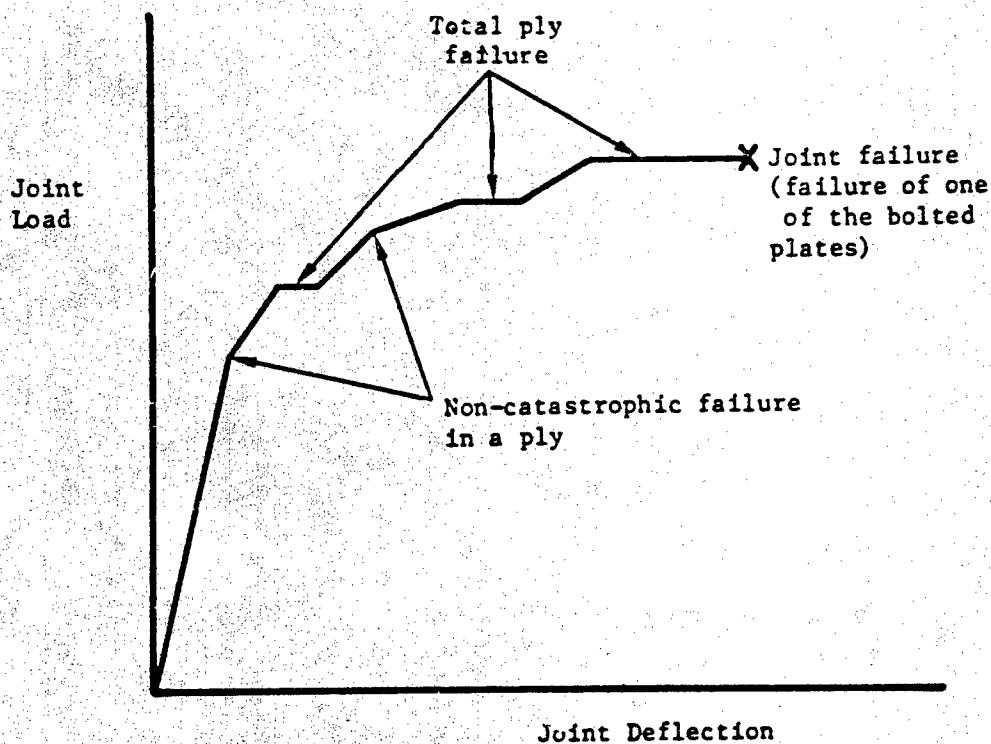
Figure 4-6. A Schematic Representation of the Overall Load Versus Deflection Response of the Joint.
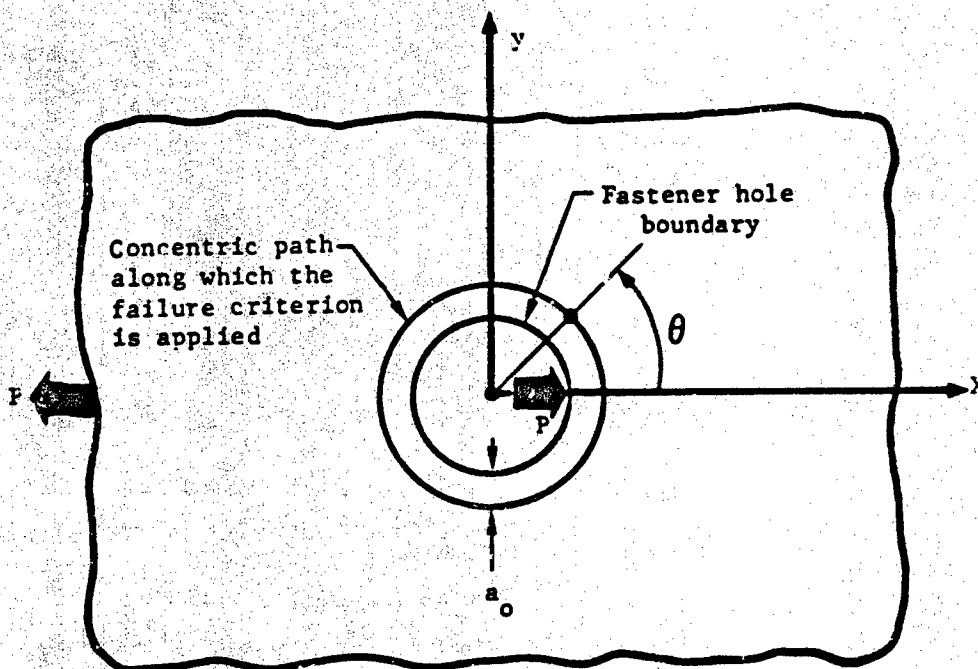
Figure 4-7. The Characteristic Distance (a_o) Defining the Region Where the Maximum Strain, Hoffman or Hill Criterion is Applied.

The Hoffman failure criterion, based on inplane ply stresses, states that total ply failure will occur when the failure index (H) in the following equation reaches a value of unity:

$$(\sigma_1^2 - \sigma_1\sigma_2)/X_cX_t + \sigma_1(X_c-X_t)/X_cX_t + \sigma_2^2/Y_cY_t + \sigma_2(Y_c-Y_t)/Y_cY_t +$$

$$\sigma_6^2/S^2 = H \qquad\qquad (4-1)$$

In the above equation, σ_1, σ_2 and σ_6 are the ply stresses in the fiber coordinate system, X_t and X_c are the uniaxial tensile and compressive material strengths along the fiber direction (1), Y_t and Y_c are the uniaxial tensile and compressive material strength perpendicular to the fiber direction (2), and S is the material shear strength in the 1-2 plane.

In the SASCJ code, the Hoffman criterion is applied along a path that is concentric to the fastener hole, defined by the characteristic distance a_o (see Figure 4-7). At selected points along this path, the following expressions for the failure value of the ply load (P_f) are computed:

$$P_f = (-b \pm \sqrt{b^2-4ac})/2a$$

where

$$a = \left[(\sigma_1^2-\sigma_1\sigma_2)/X_cX_t + \sigma_2^2/Y_cY_t + \sigma_6^2/S^2\right]/P_i^2$$

$$b = \left[(X_c-X_t)\sigma_1/X_cX_t + (Y_c-Y_t)\sigma_2/Y_cY_t\right]/P_i \qquad\qquad (4-2)$$

$$c = -1, \text{ and}$$

$$P_i = \text{ply load at which } \sigma_1, \sigma_2 \text{ and } \sigma_6 \text{ are computed}$$

The location where the smallest non-negative value for P_f is computed identifies the failure initiation point.

The Hoffman criterion predicts total ply failure and the failure location, but does not identify the mode of failure. The failure location, though, generally indicates the possible failure mode. Referring to Figure 4-7, if failure is predicted near $\theta=0°$, a bearing mode of failure is suspected. If the failure location is near $\theta=90°$, a net section mode

83

of failure is suspected. And, intermediate values of θ indicate a shear-out mode of failure. The Tsai-Hill criterion can be obtained from Equation 4-1 by setting $X_c = X_t$ and $Y_c = Y_t$. This criterion, therefore, does not account for different strengths under tension and compression. The ply failure load (P_f) in this case is computed to be $1/\sqrt{a}$ (see Equation 4-2).

4.5 <u>Interlaminar Failure Criterion</u>

Delamination between plies is predicted by incorporating computed shear strains at the interfacial locations into a maximum shear strain criterion. At the interface betwen plies i and j, for example, the shear strain is computed to be:

$$\gamma_{xz}^{i-j} = (u_i - u_j) / h_\alpha \tag{4-3}$$

where h_α is the ply thickness in the plate containing plies i and j. This expression for the shear strain is approximate. Plies i and j are assumed to delaminate when γ_{xz}^{i-j} exceeds a failure value. The failure value for γ_{xz} will be determined by correlating predictions with observations for a sample test case.

SECTION 5

STRENGTH PREDICTIONS USING THE SASCJ CODE

5.1   Introduction

The developed strength analysis for laminated and metallic plates
(SASCJ code) requires as input a few failure parameters and post-failure ply
property degradations (see Section 4). Section 5.3 describes how these
quantities are determined. Subsequently, the validity of the SASCJ code is
established by comparing its strength predictions with experimental measure-
ments (see Sections 5.4 to 5.6). Test results from Reference 5-1 are used
in the determination of the mentioned input properties and for establishing
the validity of the SASCJ code. Figures 5-1 and 5-2 present the geometries
of the bolted laminated and metallic plates used in Reference 5-1. Table 5-1
lists the various static tests conducted in Reference 5-1.

5.2   Initial Studies On Failure Parameters For Laminates With
Unloaded (Open) Holes

The strength of laminates with unloaded or loaded holes has hitherto
been predicted based on a one-step procedure. The laminate or the individual
lamina stresses or strains are incorporated into a selected failure criterion
to predict the laminate strength. The procedure does not go beyond the first
ply failure when lamina stresses or strains are used to predict laminate
strength. This strength prediction procedure results in failure parameters that
are dependent on the laminate layup, and requires modificaiton of lamina
properties to preclude "non-critical" failures. Examples are presented below.

Consider a laminate with an unloaded (open) 5/16 in. diameter hole
subjected to static tensile or compressive loading. At the laminate level,
the two-dimensional laminate stress state around the fastener hole is in-
corporated into a selected failure criterion to predict the laminate strength.
The point stress and average stress failure criteria have been used before for
this problem (see References 5-2 to 5-4). The characteristic distances for
net section, bearing and shear-out failures, respectively, that make SASCJ
predictions agree with the measured tensile strengths, for three laminate
layups, are presented in Figure 5-3. The axial tensile and compressive
strengths, and the shear strengths, of the laminate layups were computed

85
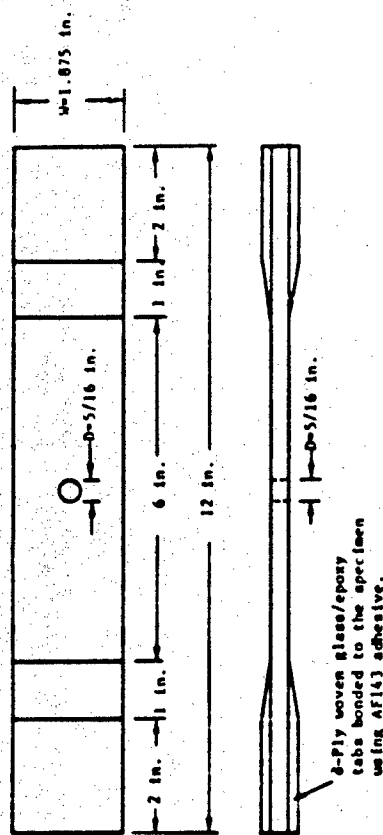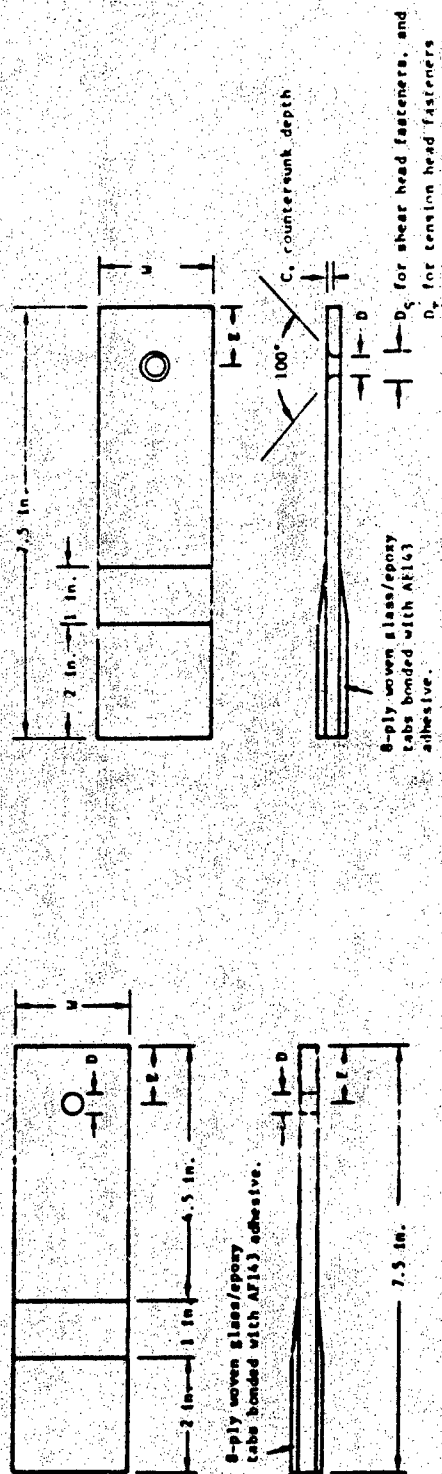
Figure 5-1. Laminated Specimen Geometries Used in Reference 5-1.

ALUMINUM BLOCK TYPE	D	W	E	t_1	t_2	L	a
A	.250	1.500	1.8	0.31	0.73	6.60	1.8
B	.313	1.875	1.8	0.31	0.73	6.60	1.8
C	.500	3.000	1.8	0.31	0.73	6.60	1.8
D	.750	4.500	2.0	0.31	0.73	7.50	2.5
E	.313	0.625	1.8	0.31	0.73	6.60	1.8
F	.313	1.250	1.8	0.31	0.73	6.60	1.8
G	.313	2.500	1.8	0.31	0.73	6.60	1.8
H	.500	3.000	2.0	0.50	1.22	7.00	2.0
I	.750	4.500	2.5	0.68	1.69	9.00	2.5
J	.313	1.875	2.0	0.16	--	6.00	--

All dimensions in inches

Single Shear Tests

A to I

Double Shear Tests

J
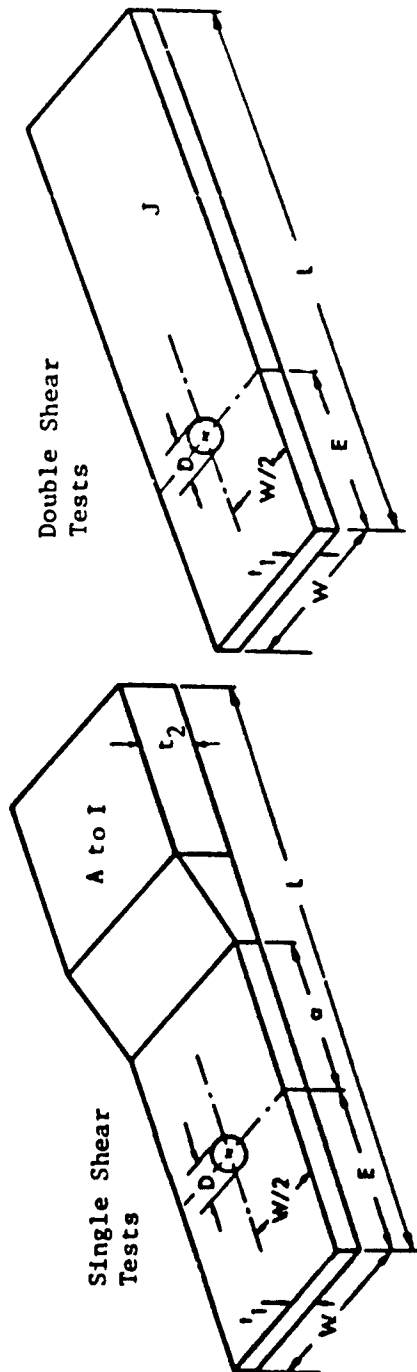
Figure 5-2. Metal Plate Dimensions Used in Reference 5-1.

TABLE 5-1. STATIC TESTS CONDUCTED IN REFERENCE 5-1.

TEST CASE	NUMBER OF PLIES	DIAMETER D (in)	EDGE DIST E(in)	WIDTH W(in)	FASTENER PART NUMBER	FASTENER DESCRIPTION	TYPE OF LOADING	BEARING/ TOTAL LOAD RATIO	SPECIMEN IDENTIFICATION	ALUM. BLOCK TYPE	CSK. DEPTH	REMARKS
1	20	0.25	0.75	1.50	51B464-4A8	--	Tension	1	1.A73;1.B73;1.C73	A	--	--
2	20	0.3125	0.9375	1.875	51B464-5A8	--	Tension	1	1.A1;1.B21;1.C41	B	--	--
3	20	0.50	1.50	3.00	51B464-8A8	--	Tension	1	1.A75;1.B75;1.C75	C	--	--
4	20	0.75	2.25	4.50	51B464-12A8	--	Tension	1	1.A77;1.B77;1.C77	D	--	--
5	20	0.25	0.75	1.50	51B464-4A8	--	Comp.	1	1.A74;1.B74;1.C74	A	--	--
6	20	0.3125	0.9375	1.875	51B464-5A8	--	Comp.	1	1.A2;1.B22;1.C42	B	--	--
7	20	0.50	1.50	3.00	51B464-8A8	--	Comp.	1	1.A76;1.B76;1.C76	C	--	--
8	20	0.75	2.25	4.50	51B464-12A8	--	Comp.	1	1.A78;1.B78;1.C78	D	--	--
9	20	0.3125	0.4688	1.875	51B464-5A8	--	Tension	1	1.A3;1.B23;1.C43	B	--	E/D=1.5
10	20	0.3125	0.7031	1.875	51B464-5A8	--	Tension	1	1.A4;1.B24;1.C44	B	--	E/D=2.25
11	20	0.3125	1.25	1.875	51B464-5A8	--	Tension	1	1.A5;1.B25;1.C45	B	--	E/D=4.0
12	20	0.3125	1.5625	1.875	51B464-5A8	--	Tension	1	1.A6;1.B26;1.C46	B	--	E/D=5.0
13	20	0.3125	0.4688	1.875	51B464-5A8	--	Tension	1	2.1;2.21;2.31	B	--	E/D=1.5
14	20	0.3125	1.5625	1.875	51B464-5A8	--	Tension	1	2.2;2.22;2.32	B	--	E/D=5.0
15	20	0.3125	0.9375	1.875	51B335-9	Csk-T	Tension	1	2.3;2.23;2.33	B	.10	--
16	20	0.3125	0.9375	1.875	51B581-5A8	Csk-S	Tension	1	2.4;2.24;2.34	B	.07	--
17	20	0.3125	0.4688	1.875	51B464-5A8	--	Tension	1	3.1;3.21;3.31	B	--	E/D=1.5
18	20	0.3125	1.5625	1.875	51B464-5A8	--	Tension	1	3.2;3.22;3.32	B	--	E/D=5.0
19	20	0.3125	0.9375	1.875	51B335-9	Csk-T	Tension	1	3.3;3.23;3.33	B	.10	--
20	20	0.3125	0.9375	1.875	NAS1581V5-8	Ti-Csk-S	Tension	1	3.4;3.24;3.34	B	.07	--
21	20	0.3125	0.9375	1.875	51B464-5A8	--	Tension	1	2.5;2.25;2.35	B	--	--
22	20	0.3125	0.9375	1.875	51B464-5A8	--	Tension	1	3.5;3.25;3.35	B	--	--
23	20	0.3125	0.9375	1.875	51B464-5A8	--	Comp.	1	2.6;2.26;2.36	B	--	--
24	20	0.3125	0.9375	1.875	51B464-5A8	--	Comp.	1	3.6;3.26;3.36	B	--	--
25	20	0.3125	0.9375	0.625	51B464-5A8	--	Tension	1	1.A71;1.B65;1.C71	E	--	W/D=2
26	20	0.3125	0.9375	1.250	51B464-5A8	--	Tension	1	1.A67;1.B71;1.C66	F	--	W/D=4
27	20	0.3125	0.9375	2.50	51B464-5A8	--	Tension	1	1.A69;1.B67;1.C69	G	--	W/D=8
28	20	0.3125	0.9375	1.875	51B335-9	Csk-T	Tension	1	1.B36;1.B13;1.C2	B	.10	--
29	20	0.3125	0.9375	1.875	51B5851-5-8	Csk-S	Tension	1	1.A20;1.B12;1.C3	B	.07	--
30	20	0.3125	0.9375	0.625	51B464-5A8	--	Comp.	1	1.A72;1.B66;1.C72	E	--	W/D=2
31	20	0.3125	0.9375	1.250	51B464-5A8	--	Comp.	1	1.A70;1.B68;1.C70	F	--	W/D=4
32	20	0.3125	0.9375	2.5	51B464-5A8	--	Comp.	1	1.A68;1.B70;1.C68	G	--	W/D=8
33	20	0.3125	0.9375	0.625	51B464-5A8	--	Tension	1	2.40;2.48;2.56	E	--	W/D=2
34	20	0.3125	0.9375	1.250	51B464-5A8	--	Tension	1	2.41;2.49;2.57	F	--	W/D=4

NOTE: All test cases have E/D=3, W/D=6, protruding head steel fasteners torqued to 100 in-lbs, room-temperature dry test conditions and single-lap configuration, unless specified otherwise.
CSK-T = Tension Head Countersink   218W = 218 F, Wet   OH = Open Hole   Ti = Titanium
CSK-S = Shear Head Countersink   RTW = Room Temp. Wet   DL = Double Lap   Al = Aluminum

88

TABLE 5-1. STATIC TESTS CONDUCTED IN REFERENCE 5-1 (Continued)

TEST CASE	NUMBER OF PLIES	DIAMETER D (in)	EDGE DIST E(in)	WIDTH W (in)	FASTENER PART NUMBER	FASTENER DESCRIPTION	TYPE OF LOADING	BEARING/TOTAL LOAD RATIO	SPECIMEN IDENTIFICATION	ALUM. BLOCK TYPE	CSK DEPTH	REMARKS
35	20	0.3125	0.9375	2.50	51B464-5A8	--	Tension	1	2.42;2.50;2.58	6	--	W/D-8
36	20	0.3125	0.9375	1.875	51B335-9	Csk-T	Tension	1	2.43;2.51;2.59	8	.10	218W
37	20	0.3125	0.9375	1.875	NAS1155V8	Ti;Csk-T	Tension	1	2.44;2.52;2.60	8	.10	218W
38	20	0.3125	0.9375	0.625	51B164-5A8	--	Comp.	1	2.45;2.53;2.61	E	--	W/D-2 218W
39	20	0.3125	0.9375	1.250	51B464-5A8	--	Comp.	1	2.46;2.54;2.62	F	--	W/D-4 218W
40	20	0.3125	0.9375	1.875	51B464-5A8	--	Comp.	1	2.47;2.55;2.63	8	--	218W
41	20	0.3125	0.9375	0.625	51B464-5A8	--	Tension	1	3.40;3.48;3.56	E	--	W/D-2
42	20	0.3125	0.9375	1.250	51B464-5A8	--	Tension	1	3.41;3.49;3.57	F	--	W/D-4
43	20	0.3125	0.9375	2.50	51B464-5A8	--	Tension	1	3.42;3.50;3.58	6	--	W/D-8
44	20	0.3125	0.9375	1.875	51B335-9	Csk-T	Tension	1	3.43;3.51;3.59	8	.10	218W
45	20	0.3125	0.9375	1.875	NAS1155V8	Ti;Csk-T	Tension	1	3.44;3.52;3.60	8	.10	218W
46	20	0.3125	0.9375	0.625	51B464-5A8	--	Comp.	1	3.45;3.53;3.61	E	--	W/D-2 218W
47	20	0.3125	0.9375	1.250	51B464-5A8	--	Comp.	1	3.46;3.54;3.62	F	--	W/D-4 218W
48	20	0.3125	0.9375	1.875	51B464-5A8	--	Comp.	1	3.47;3.55;3.63	8	--	218W
49	20	0.3125	0.9375	1.875	51B464-5A8	--	Tension	1	1.A7;1.B27;1.C47	8	--	Torque=0
50	20	0.3125	0.9375	1.875	51B464-5A8	--	Tension	1	1.A8;1.B28;1.C48	8	--	Torque=50
51	20	0.3125	0.9375	1.875	51B464-5A8	--	Tension	1	1.A9;1.B29;1.C49	8	--	Torque=150
52	20	0.3125	0.9375	1.875	51B464-5A8	--	Tension	1	1.A10;1.B30;1.C50	8	--	Torque=200
53	20	0.3125	0.9375	1.875	51B464-5A8	--	Comp.	1	1.A11;1.B31;1.C51	8	--	Torque=0
54	20	0.3125	0.9375	1.875	51B464-5A8	--	Comp.	1	1.B91;1.B45;1.A15	8	--	Torque=200
55	20	0.3125	0.9375	1.875	NAS1155V8	Ti;Csk-T	Tension	1	1.B92;1.B46;1.A16	8	.10	--
56	20	0.3125	0.9375	1.875	NAS1581V5-8	Ti;Csk-S	Tension	1	1.B93;1.B47;1.A17	8	.07	--
57	20	0.3125	0.9375	1.875	51B464-5A8	--	Tension	1	4.1;4.4;4.7	8	--	--
58	20	0.3125	0.9375	1.875	51B464-5A8	--	Tension	1	7.1;7.3;7.5	8	--	--
59	20	0.3125	0.9375	1.875	51B464-5A8	--	Tension	1	5.1;5.3;5.5	8	--	--
60	20	0.3125	0.9375	1.875	51B464-5A8	--	Tension	1	8.1;8.3;8.5	8	--	--
61	20	0.3125	0.9375	1.875	51B464-5A8	--	Tension	1	6.1;6.3;6.5	8	--	--
62	20	0.3125	0.9375	1.875	51B464-5A8	--	Tension	1	9.1;9.3;9.5	8	--	--
63	20	0.3125	0.9375	1.875	51B335-9	Csk-T	Tension	1	4.2;4.5;4.8	8	.10	--
64	20	0.3125	0.9375	1.875	NAS15E*V5-8	Ti;Csk-S	Comp.	1	1.A12;1.B32;1.C52	8	.07	--
65	20	0.3125	0.9375	1.875	ML22-10-9	Al	Tension	1	1.B83;1.B33;1.C83	8	--	--
66	20	0.3125	0.9375	1.875	ML23-10-8	Al;Csk-T	Tension	1	1.B84;1.B34;1.C56	8	.10	--
67	20	0.3125	0.9375	1.875	NAS1155V8	Ti;Csk-T	Comp.	1	1.B85;1.B35;1.C55	8	.10	--
68	20	0.3125	0.9375	1.875	NAS1155V8	Ti;Csk-T	Tension	1	4.3;4.6;4.9	8	.10	--

NOTE: All test cases have E/D=3, W/D=6, protruding head steel fasteners torqued to 100 in-lbs, room-temperature dry test
conditions and single-lap configuration, unless specified otherwise.
CSK-T = Tension Head Countersink   218F = 218°F, Wet   OH = Open Hole   Ti = Titanium
CSK-S = Shear Head Countersink   RTW = Room Temp. Wet   DL = Double Lap   Al = Aluminum

TABLE 5-1. STATIC TESTS CONDUCTED IN REFERENCE 5-1 (Concluded).

TEST CASE	NUMBER OF PLIES	DIAMETER D (in)	EDGE DIST E (in)	WIDTH W w (in)	FASTENER PART NUMBER	FASTENER DESCRIPTION	TYPE OF LOADING	BEARING/ TOTAL LOAD RATIO	SPECIMEN IDENTIFICATION	FLOW BLOCK TYPE	CSK. DEPTH	REMARKS
69	20	0.3125	0.9375	1.875	NAS1155VR	T1;Csk-T	Tension	1	7.2;7.4;7.6	B	.10	--
70	20	0.3125	0.9375	1.875	NAS1155VR	T1;Csk-T	Tension	1	2.7;2.27;2.37	B	.10	--
71	20	0.3125	0.9375	1.875	NAS1155VB	T1;Csk-T	Tension	1	3.7;3.27;3.37	B	.10	--
72	20	0.3125	0.9375	1.875	518335-P	Csk-T	Tension	1	1.886,1.A19,1C56	B	.10	RTW
73	20	0.3125	0.9375	1.875	NAS1155VB	T1;Csk-T	Tension	1	1.887,1.C54,1C57	B	.10	218W
74	20	0.3125	0.9375	1.875	518335-9	Csk-T	Tension	1	1.888;1.838;1.C58	B	.10	218W
75	20	0.3125	0.9375	1.875	518335-9	Csk-T	Comp.	1	1.089,1.839;1.C59	B	.10	218W
76	40	0.51	1.50	3.00	518330-13	Csk-T	Tension	1	10.1,10.3,10.5	M	.20	--
77	60	0.75	2.25	4.50	518464-12A18	--	Tension	1	11.1;11.3,11.5	T	--	--
78	40	0.50	1.50	3.0	518338-13	Csk-T	Tension	1	12.1,12.3,12.5	M	.20	--
79	60	0.75	2.25	4.5	518464-12A18	--	Tension	1	13.1;13.3,13.5	T	--	--
80	40	0.50	1.50	3.0	518338-13	Csk-T	Tension	1	14.1;14.3,14.5	M	.20	.
81	60	0.75	2.25	4.50	518464-12A18	--	Tension	1	15.1,15.3;15.5	T	--	--
82	20	0.3125	0.9375	1.875	518464-5A8	--	Tension	1	1.890;1.840;1.C60	J	--	DL
83	20	0.3125	0.9375	1.875	518464-5A8	--	Tension	1	2.8;2.28,2.38	J	--	DL
84	20	0.3125	0.9375	1.875	518464-5A8	--	Tension	1	3.8;3.28;3.38	J	--	DL
85	20	0.3125	0.9375	1.875	518464-5A8	--	Comp.	1	1.8104;1.814;1.A18	J	--	DL
86	20	0.3125	--	1.875	---	--	Tension	0	1.A84;1.850;1.A50	--	--	UM
87	20	0.3125	--	1.875	518464-5A8	--	Tension	0.167	1.A85;1.851;1.A51	--	--	--
88	20	0.3125	--	1.875	518464-5A8	--	Tension	0.287	1.A86;1.852;1.A52	--	--	--
89	20	0.3125	--	1.875	518464-5A8	--	Tension	0.375	1.A87;1.853;1.A53	--	--	--
90	20	0.3125	--	1.875	---	--	Tension	0	2.75;2.67;2.71	--	--	OH
91	20	0.3125	--	1.875	518335-9	Csk-T	Tension	0.167	2.64;2.68;2.72	--	.10	--
92	20	0.3125	--	1.875	518335-9	Csk-T	Tension	0.287	2.65;2.69;2.73	--	.10	--
93	20	0.3125	--	1.875	518335-9	Csk-T	Tension	0.375	2.66;2.70;2.74	--	.10	--
94	20	0.3125	--	1.875	---	--	Tension	0	3.75;3.67;3.71	--	--	OH
95	20	0.3125	--	1.875	NAS1581V5-6	Csk-S,T1	Tension	0.167	3.64;3.68;3.72	--	.07	--
96	20	0.3125	--	1.875	NAS1581V5-8	Csk-S,T1	Tension	0.287	3.65;3.69;3.73	--	.07	--
97	20	0.3125	--	1.875	NAS1581V5-8	Csk-S,T1	Tension	0.375	3.66;3.70;3.74	--	.07	--
98	20	0.3125	--	1.875	---	--	Comp.	0	1.A88;1.854;1.A54	--	--	OH
99	20	0.3125	--	1.875	518464-5A8	--	Comp.	0.2	1.A89;1.855;1.A55	--	--	--
100	20	0.3125	--	1.875	518464-5A8	--	Comp.	0.33	1.A90;1.856;1.A56	--	--	--
101	20	0.3125	--	1.875	---	--	Comp.	0	2.76;2.79;2.82	--	--	OH
102	20	0.3125	--	1.875	518335-9	Csk-T	Comp.	0.2	2.77;2.80;2.83	--	--	--
103	20	0.3125	--	1.875	518335-9	Csk-T	Comp.	0.33	2.78;2.81;2.84	--	.10	--
104	20	0.3125	--	1.875	--	--	Comp.	0	3.76;3.79;3.82	--	--	OH
105	20	0.3125	--	1.875	NAS1581V5-8	T1;Csk-S	Comp.	0.2	3.77;3.80;3.83	--	.07	--
106	20	0.3125	--	1.875	NAS1581V5-8	T1;Csk-S	Comp.	0.33	3.78;3.81;3.84	--	.07	--

NOTE: All test cases have E/D=3, W/D=6, protruding head steel fasteners torqued to 100 in-lbs, room-temperature dry test conditions and single-lap configuration, unless specified otherwise.
Csk-T = Tension Head Countersink   218f = 218°F, Wet   T1 = Titanium
Csk-S = Shear Head Countersink   RTW = Room Temp. Wet   Al = Aluminum
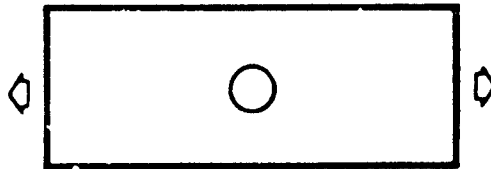
LAYUP[1]	TEST CASE (REF. 5-1)	AVERAGE FAILURE LOAD(KIPS) (REF. 5-1)	POINT STRESS CRITERION[2]	AVERAGE STRESS CRITERION[2]
50/40/10 [3]	86	12.9	a_{ons} = 0.024 in.	a_{ons} = 0.06 in.
70/20/10 [4]	90	20.8	a_{ons} = 0.047 in.	a_{ons} = 0.146 in.
30/60/10 [5]	94	10.3	a_{ons} = 0.024 in.	a_{ons} = 0.055 in.

[1] Percentages of $0°$, ±45 and $90°$ plies, respectively

[2] a_{OBRG} = 0.025 in. and a_{OSO} = 0.08 in. for every case

[3] X_t, X_c and S = 125, 150 and 45 ksi, respectively

[4] X_t, X_c and S = 165, 175 and 30 ksi, respectively

[5] X_t, X_c and S = 95, 108 and 60 ksi, respectively

Figure 5-3. Failure Parameters for the Laminate Level Prediction of Static Tensile Strengths of Laminates with Unloaded (Open) 5/16 Inch Diameter Holes.

using laminate theory and AS1/3501-6 properties from Reference 5-5. The characteristic distances that make SASCJ predictions agree with the measured compressive strengths are presented in Figure 5-4. Predictions in both cases are sensitive only to the a_{ons} value, since the laminates fail in a net section mode. The a_{ons} value for the average stress criterion is approximately 2.5 times the value for the point stress criterion, as observed in Reference 5-2. Note that a_{ons} for the highly fiber-dominated 70/20/10 layup is much larger than that for the 50/40/10 and 30/60/10 layups under tension.

The tensile and compressive strengths of the laminates with unloaded (open), 5/16 inch diameter holes can also be predicted at the lamina level, based on first ply failure. The point or the average stress criterion (see Figures 4-4 and 4-5), the Hoffman, Tsai-Hill or the maximum strain criterion (see Figure 4-7) may be used at the ply level. Laminate failure is assumed to be precipitated by the first major ply failure. When the Tsai-Hill criterion is used, matrix failures between fibers are precluded by setting the transverse tensile and compressive strength for the ply to be large (10^4 psi). When the maximum strain criterion is used, only the fiber directional strain is interrogated. When the point and average stress criteria are used, the strengths of the $\pm 45^{\circ}$ plies are increased to twice the actual values, and the transverse tensile strength is increased to preclude matrix failures between fibers in the 90° plies. Figures 5-5 and 5-6 present the characteristic distances that make SASCJ predictions agree accurately with the measured tensile and compressive strengths of three laminates with unloaded (open), 5/16 inch diameter holes.

The above examples clearly indicate the need for the progressive ply failure procedure incorporated in the SASCJ code. The one-step laminate level failure prediction leads to the dependence of the failure parameters on the laminate layup. The one-step ply level failure prediction requires the modification of actual lamina properties. The progressive failure procedure in SASCJ provides a means for using invariant failure parameters and ply property degradation rates to predict the strength of bolted laminates. An example is presented below.
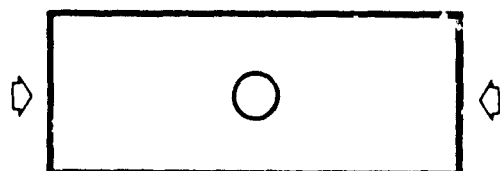
LAYUP[1]	TEST CASE (REF. G-1)	AVERAGE FAILURE LOAD(KIPS) (REF. 6-1)	POINT STRESS CRITERION[2]	AVERAGE STRESS CRITERION[2]
50/40/10 [3]	98	-13.4	$a_{ons} = 0.019$ in.	$a_{ons} = 0.046$ in.
70/20/10 [4]	101	-17.5	$a_{ons} = 0.026$ in.	$a_{ons} = 0.07$ in.
30/60/10 [5]	104	-10.5	$a_{ons} = 0.025$ in.	$a_{ons} = 0.055$ in.

[1] Percentages of $0°$, ±45 and $90°$ plies, respectively

[2] $a_{OBRG} = 0.025$ in. and $a_{OSO} = 0.08$ in. for every case

[3] X_t, X_c and S = 125, 150 and 45 ksi, respectively

[4] X_t, X_c and S = 165, 175 and 30 ksi, respectively

[5] X_t, X_c and S = 95, 108 and 60 ksi, respectively

Figure 5-4.   Failure Parameters for the Laminate Level Prediction of Static
Compressive Strengths of Laminates with Unloaded (Open) 5/16
Inch Diameter Holes.

93

LAYUP (% OF 0°, ±45° and 90° PLIES)	TEST CASE (REF. 5-1)	AVERAGE FAILURE LOAD (KIPS) (REF. 5-1)	CORRELATION PARAMETERS (INCH)			
			HILL[1]	MAXIMUM FIBER STRAIN[2]	POINT STRESS CRITERION[3]	AVERAGE STRESS CRITERION[3]
50/40/10	86	12.9	$a_0 = 0.02$	$a_0 = 0.021$	$a_{ons} = 0.015$	$a_{ons} = 0.035$
70/20/10	90	20.8	$a_0 = 0.045$	$a_0 = 0.045$	$a_{ons} = 0.035$	$a_{ons} = 0.11$
30/60/10	94	10.3	$a_0 = 0.025$	$a_0 = 0.025$	$a_{ons} = 0.015$	$a_{ons} = 0.035$

[1] Only fiber directional and shear failures are permitted

X, Y and S = 230, 10^4 and 17.3 ksi, respectively

[2] $X_{\epsilon t} = 0.012$ (ONLY FIBER FAILURE CONSIDERED)

[3] $a_{OBRG} = 0.025$, $a_{OSO} = 0.08$ in.

X_t, X_c and S (0° ply) = 230, 267 and 17.3 ksi, respectively

X_t, X_c and S (±45° ply) = 100, 100 and 190 ksi, respectively (modified)

X_t, X_c and S (90° ply) = 95, 38.9 and 17.3 ksi, respectively (modified)

Figure 5-5. Failure Parameters for the Ply Level Prediction of Static Tensile Strengths of Laminates with Unloaded (Open), 5/16 Inch Diameter Holes.

LAYUP (% OF 0°, ±45° and 90° PLIES)	TEST CASE (REF. 5-1)	AVERAGE FAILURE LOAD (KIPS) (REF. 5-1)	CORRELATION PARAMETERS (INCH)			
			HILL[1]	MAXIMUM FIBER STRAIN[2]	POINT STRESS CRITERION[3]	AVERAGE STRESS CRITERION[3]
50/40/10	98	-13.4	$a_0 \sim 0.013$	$a_0 = 0.005$	$a_{ons} \sim 0.013$	$a_{ons} = 0.030$
70/20/10	101	-17.5	$a_0 = 0.022$	$u_0 = 0.010$	$a_{ons} = 0.016$	$a_{ons} = 0.041$
30/60/10	104	-10.5	$a_0 = 0.016$	$a_0 = 0.004$	$a_{ons} = 0.014$	$a_{ons} = 0.029$

[1] Only fiber directional and shear failures are permitted

X, Y and S = 267, 10^4 and 17.3 ksi, respectively

[2] $X_{et} = 0.017$ (ONLY FIBER FAILURE CONSIDERED)

[3] $a_{OBRG} = 0.025$, $a_{OSO} = 0.08$ in.

X_t, X_c and S (0° ply) = 230, 267 and 17.3 ksi, respectively

X_t, X_c and S (±45° ply) = 100, 100 and 190 ksi, respectively (modified)

X_t, X_c and S (90° ply) = 95, 38.9 and 17.3 ksi, respectively (modified)

Figure 5-6. Failure Parameters for the Ply Level Prediction of Static Compressive Strengths of Laminates with Unloaded (Open), 5/16 Inch Diameter Holes.

5.3 Determination of Failure Parameters

Consider a laminate that transfers an applied tensile or compressive load in double shear via a fastener (see Figure 5-7). The strength of this laminate is predicted using the progressive ply failure procedure in SASCJ, assuming bilinear ply behavior (Figure 3-8) and average stress failure criteria. The strengths of the $\pm 45^{\circ}$ plies are computed using lamination theory. For each ply failure mode (net section, shear-out and bearing), a characteristic distance (a_{ons}, a_{oso} or a_{obrg}), a k_2/k_1 value and a $p^{ultimate}/p^{initial}$ value have to be determined. Figure 5-7 presents the nine parameters that yielded SASCJ predictions that agreed with the experimental observations and measurements in Reference 5-1, including laminate strength and failure modes. Note that only one failure parameter (a_{ons}) had to be changed to make predictions correlate accurately with measurements corresponding to the 30/60/10 laminate. If the a_{ons} value for the tensile-loaded 30/60/10 laminate is not changed from the 0.10 inch value, only a 17% error will result in the predicted strength (see Section 5.4).

Failure parameters based on a linear ply behavior ($k_2/k_1 = 0$, $p^{ultimate}/p^{initial} = 1$) and the Tsai-Hill criterion or the maximum strain criterion are also presented in Figure 5-7. These values, corresponding to the fully-loaded hole situation, are seen to be different from those corresponding to the unloaded hole situation in Figure 5-5. They are also very dependent on the laminate layup.

Based on the above results, it is concluded that the progressive failure procedure using the average stress failure criterion and bilinear ply behavior is the best choice among the studied methods. Therefore, subsequent correlation studies are performed using this procedure with invariant failure parameters and ply degradation rates. The invariant properties are obtained based on imposed correlation between SASCJ predictions and test measurements corresponding to a double shear (full-bearing) load transfer configuration.

5.4 SASCJ Strength Predictions for Laminates with Fully-Loaded Holes in a Single Shear Load Transfer Configuration

For AS1/3501-6 graphite/epoxy laminates, tested in Reference 5-1, the various failure parameters obtained through a trial and error procedure are

LAYUP (% OF 0°, ±45° AND 90° PLIES)	TEST CASE (REF. 5-1)	AVERAGE FAILURE LOAD (KIPS) (REF. 5-1)	CORRELATION PARAMETERS		
			HILL[1]	MAXIMUM FIBER STRAIN[2]	AVERAGE STRESS[3]
50/40/10	82	4.748	$a_o = 0.095$	$a_o = 0.085$	$a_{ons} = 0.10$
70/20/10	83	3.978	$a_o = 0.12$	$a_o = 0.03$	$a_{ons} = 0.10$
30/60/10	84	5.967	$a_o = 0.155$	$a_o = 0.13$	$a_{ons} = 0.16$
50/40/10	85	-6.494	$a_o = 0.185$	$a_o = 0.075$	$a_{ons} = 0.10$

[1] Only fiber failures and shear failures were permitted.

X_t, X_c, Y_t, Y_c and S = 230, 267, 10^4, 10^4 and 17.3 ksi, respectively

[2] $\epsilon_{11}^{tu} = 0.012$ and $\epsilon_{11}^{cu} = 0.017$ (only fiber failure considered)

[3] $a_{obrg} = 0.025$; $a_{oso} = 0.08$; k_2/k_1 for net section, bearing and shear-out = 0.1 for all ply types;

$P^{ult}/P^{initial}$ = 1.02 and 1.50 for net section and bearing, respectively

$P^{ult}/P^{initial}$ = 1.12 and 1.80 for shear-out under tension and compression, respectively

X_t, X_c and S (0° ply) = 230, 267 and 17.3 ksi, respectively

X_t, X_c and S (±45° ply) = 40, 47 and 95 ksi, respectively

X_t, X_c and S (90° ply) = 9.5, 38.9 and 17.3 ksi, respectively

Figure 5-7. Characteristic Distances and Ply Degradation Parameters for Laminates with Fully-Loaded 5/16 Inch Diameter Holes, Subjected to Static Tensile and Compressive Loading in Double Shear.

listed in Figure 5-7. These include the characteristic distances (a_{ons} = 0.10 inch, a_{obrg} = 0.025 inch, and a_{oso} = 0.08 inch), the ply modulus change corresponding to every failure mode (k_2/k_1 = 0.1 for net section, bearing and shear out), and the ultimate-to-initial ply failure load ratio for each failure mode (1.02 and 1.50 for net section and bearing, and 1.12 and 1.80 for shear-out under tension and compression, respectively). The $P^{ultimate}/P^{initial}$ ratio, corresponding to the shear-out mode of ply failure, increases when the applied load is changed from tension to compression, due to the larger shear-out (or shear-in) area under this loading condition. But, for subsequent correlation studies, $P^{ultimate}/P^{initial}$ is assumed to be 1.12 for the shear-out mode of ply failure, irrespective of the loading mode. This results in the use of constant failure parameters when strength predictions are made for bolted AS1/3501-6 graphite/epoxy laminates using the SASCJ code.

The SASCJ code and the above failure parameters (obtained through a forced correlation corresponding to a double shear load transfer situation) were subsequently used to predict the strength of laminates with fully-loaded holes in a single shear load transfer configuration. Figures 5-8 and 5-9 present a comparison between SASCJ predictions and test results from Reference 5-1. With the exception of two test cases, an excellent agreement between SASCJ predictions and test results is noticed. Under tensile loading, a 17% error between test and analysis is seen for 30/60/10 (percentages of 0°, $\pm45^\circ$ and 90° plies, respectively) laminates in a double shear configuration. Under compressive loading, a 27% difference between the SASCJ prediction and the test result in Reference 5-1, for 70/20/10 laminates in single shear, is noticed. Also, a 23% difference between test and analysis is seen for 50/40/10 laminates in a double shear load transfer configuration. These differences, under compressive loading, will be reduced if $P^{ultimate}/P^{initial}$ for the shear-out ply failure mode is assumed to vary with the shear-out area (E/D). This will be attempted later when the SASCJ code is used in the development of a design guide.

5.5   Sample SASCJ Input/Output

The details of the input data for SASCJ and its prediction of progressive ply failures are presented by considering test case 2 in Figure 5-8.

LAYUP (% 0°, ±45° AND 90° PLIES)	DOUBLE SHEAR			SINGLE SHEAR		
	TEST CASE (REF. 6-1)	FAILURE LOAD (KIPS)		TEST CASE (REF. 6-1)	FAILURE LOAD (KIPS)	
		EXPT. (REF. 6-1)	ANAL.*		EXPT. (REF. 6-1)	ANAL.*
50/40/10	82	4.75	4.67	2	4.91	4.55
70/20/10	83	3.95	3.94	21	4.05	4.04
30/60/10	84	5.97	4.97	22	5.15	5.05

* a_{one}, a_{obrg}, a_{oso} = 0.10, 0.025, 0.05 for all the layups

k_2 / k_1 = 0.1 for all failure modes

$P^{ult} / P^{initial}$ = 1.02, 1.50 and 1.12 for ns, brg and so, respectively

Figure 5-8. SASCJ Predictions for Sample Laminates with Fully-Loaded 5/16 Inch Diameter Holes, Subjected to Static Tensile Loading.
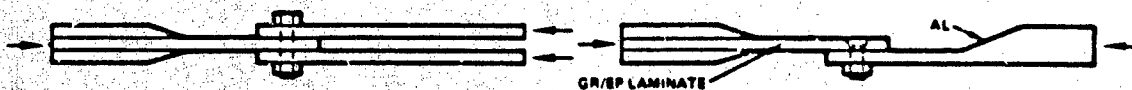
LAYUP (% 0°, ±45° AND 90° PLIES)	DOUBLE SHEAR			SINGLE SHEAR		
	TEST CASE (REF. 5-1)	FAILURE LOAD (KIPS)		TEST CASE (REF. 5-1)	FAILURE LOAD (KIPS)	
		EXPT. (REF. 5-1)	ANAL.[*]		EXPT. (REF. 5-1)	ANAL.[*]
50/40/10	85	-6.49	-5.02	8	-5.48	-4.97
70/20/10	- -	- -	-4.23	23	-5.88	-4.30
30/60/10	- -	- -	-4.91	24	-5.13	-4.07

[*] S_{ens}, S_{obrg}, S_{eso} = 0.10, 0.025, 0.08 for all layups

K_2/K_1 = 0.1, 0.1 and 0.1 for net section, bearing and shear-out failure modes, respectively, for all ply types

$P^{ult}/P^{initial}$ = 1.02, 1.50 and 1.12 for ns, brg and so, respectively

Figure 5-9. SASCJ Predictions for Sample Laminates with Fully-Loaded 5/16 Inch Diameter Holes, Subjected to Static Compressive Loading.

In this sample situation, a static tensile load is transferred from a laminate to aluminum in single shear, via a 5/16 inch diameter steel fastener. The laminate is made up of AS1/3501-6 graphite/epoxy, and has a 50/40/10 layup defined by $[(45/0/-45/0)_2 /0/90]_s$. Its E/D and W/D values are 3 and 6, respectively. Table 5-2 presents the SASCJ input data for this test case. The tensile and compressive strengths, and the inplane shear strengths, for the four ply types (with fiber orientations of 0°, 45°, -45° and 90°) were obtained using available AS1/3501-6 graphite/epoxy properties and laminate theory. Referring to Figure 3-8, the bilinear load versus deflection behavior was defined by assuming $k_2/k_1 = 0.1$ for all the failure modes, and $p^{ultimate}/p^{initial}$ was assumed to be 1.02, 1.50 and 1.12 for the net section, bearing and shear-out modes of ply failure, respectively. The rotational constraints at the fastener head and nut locations were represented by assuming R_1 and R_2 values to be 10^{12} (see Equation 3-16).

Table 5-3 presents the results predicted by the SASCJ code for the problem defined above. Nodes 1 to 30 are within the aluminum plate, and nodes 31 to 70 are within the laminate. SASCJ predicts a net section failure in the 90° plies to be the first failure. This is followed by shear-out failures in -45° plies, net section failures in the $+45^o$ plies, total failures of the 90° plies, shear-out failures in the 0° plies, etc. At 4.744 kips, total failure of the laminate is predicted. The predicted failure load is within 5% of the average measured value of 4.914 kips in Reference 5-1. Also, Table 5-3 indicates that laminate failure is predominately precipitated by shear-out failure in the 0° and -45° plies, and is accompanied by net section failures in the 90° and $+45^o$ plies. The primary mode of failure observed in Reference 5-1 is the predicted "partial shear-out" of the laminate.

5.6   SASCJ Strength Predictions for Sample Laminates with Partially-Loaded Holes -- The General Single Fastener Situation

Laminates with partially-loaded holes are analyzed by superimposing solutions for the corresponding unloaded (open) and fully-loaded hole problems (see Section 4.3). Section 5.3 discusses how the various failure parameters are obtained. Using these parameters, SASCJ is used to predict the strength of three laminates subjected to partial fastener loads. Figure 5-10

101

TABLE 5-2. INPUT DATA FOR A 50/40/10 LAMINATE-TO-ALUMINUM
SINGLE SHEAR TENSILE LOAD TRANSFER PROBLEM
(TEST CASE 2 IN REFERENCE 5-1).

```
DSNAME='TF42463.SASCJ.SL.AUSS41.DATA'        4        0.1,0.1,0.1
INVALID LINE NUMBER, NONUM ASSUMED           4        1.01,1.01,1.01
 0.0                                         4        0.1,0.1,0.1
 1                                           4        0.1,0.1,0.1
 1                                           1        0.1,0.1,0.1
 Y                                           1        0.1,0.1,0.1
 N                                           1        1.02,1.50,1.12
 ALUMINUM                                    1        0.5
 C                                           3        0.012
 ASI/3501-6 ((45/0/-45/0)2/0/90)S            3        STEEL
 40                                          1        30.0D6 0.3
 0.31                                        1        0.3125
 0.003                                       2        1.0D12
 4                                           1        1.0D12
 0.0                                         1        0.15625,0.15625
 45.0                                        3         1.8 -0.9375
 -45.0                                       3         1.8 0.9375
 90.0                                        1        -1.8 0.9375
 2                                           2        -1.8 -0.9375
 2                                           2         3.5 -0.9375
 1                                                     3.5 0.9375
 1                                                    -0.9375 0.9375
 3                                                    -0.9375 -0.9375
 3                                           10.D6    END OF DATA
 3                                           0.3      READY
 1                                           18.5D6 1.9D6
 1                                           0.85D6 0.3
 2                                           4
 2                                           0.3,0.6,0.7
 1                                           0.10,0.025,0.08
 1                                           150.D3,200.D3,200.D3,100.D3
 3                                           230.D3,320.D3,320.D3,17.3D3
 3                                           40.D3,56.D3,56.D3,95.D3
 1                                           40.D3,56.D3,56.D3,95.D3
 1                                           9.5D3,38.9D3,38.9D3,17.3D3
 1
 1
```

102

TABLE 5-3.   SEQUENTIAL FAILURE PREDICTION CORRESPONDING
TO THE DATA IN TABLE 5-2.

FAILURE MODE ABBREVIATIONS:

ND = NO ADDITIONAL DAMAGE AT CURRENT JOINT LOAD
DL = DELAMINATION
SO = SHEAR-OUT
BR = BEARING
NS = NET SECTION
SUD= ULTIMATE FAILURE AFTER SO AND DL
SU = ULTIMATE FAILURE IN SO
BU = ULTIMATE FAILURE IN BR
NSU= ULTIMATE FAILURE IN NS
ULT= ULTIMATE FAILURE

INCREMENT NO	JOINT LOAD	NODE	PLY TYPE	MODE
1	0.364D+04	49	90.000 DEGREE	NS
2	0.364D+04			ND
3	0.367D+04	50	90.000 DEGREE	NS
4	0.367D+04			ND
5	0.371D+04	51	90.000 DEGREE	NS
6	0.371D+04			ND
7	0.374D+04	52	90.000 DEGREE	NS
8	0.374D+04			ND
9	0.387D+04	35	-45.000 DEGREE	SO
10	0.387D+04			ND
11	0.392D+04	36	-45.000 DEGREE	SO
12	0.392D+04			ND
13	0.420D+04	31	45.000 DEGREE	NS
14	0.420D+04			ND
15	0.422D+04	33	0.0 DEGREE	SO
16	0.422D+04			ND
17	0.425D+04	32	45.000 DEGREE	NS
18	0.425D+04			ND
19	0.427D+04	43	-45.000 DEGREE	SO
20	0.427D+04			ND
21	0.428D+04	34	0.0 DEGREE	SO
22	0.428D+04			ND
23	0.431D+04	44	-45.000 DEGREE	SO
24	0.431D+04			ND
25	0.432D+04	49	90.000 DEGREE	NSU
26	0.432D+04			ND
27	0.433D+04	50	90.000 DEGREE	NSU
28	0.433D+04			ND
29	0.435D+04	51	90.300 DEGREE	NSU
30	0.435D+04			ND
31	0.436D+04	52	90.000 DEGREE	NSU
32	0.436D+04	37	0.0 DEGREE	SO
33	0.436D+04			ND
34	0.440D+04	38	0.0 DEGREE	SO
35	0.440D+04			ND
36	0.452D+04	39	45.000 DEGREE	NS
37	0.452D+04			ND
38	0.453D+04	41	0.0 DEGREE	SO
39	0.453D+04			ND
40	0.456D+04	40	45.000 DEGREE	NS
41	0.456D+04			ND
42	0.456D+04	42	0.0 DEGREE	SO
43	0.456D+04			ND
44	0.462D+04	57	-45.000 DEGREE	SO
45	0.462D+04			ND
46	0.464D+04	58	-45.000 DEGREE	SO
47	0.464D+04			ND
48	0.466D+04	45	0.0 DEGREE	SO
49	0.466D+04			ND
50	0.469D+04	46	0.0 DEGREE	SO
51	0.469D+04			ND
52	0.472D+04	47	0.0 DEGREE	SO
53	0.472D+04			ND
54	0.472D+04	65	-45.000 DEGREE	SO
55	0.472D+04			ND

103

TABLE 5-3. SEQUENTIAL FAILURE PREDICTION CORRESPONDING
TO THE DATA IN TABLE 5-2. (CONCLUDED)

56	0.473D+04	66	-45.000 DEGREE	SO
57	0.473D+04			ND
58	0.474D+04	46	0.0 DEGREE	SO
59	0.474D+04			ND
60	0.474D+04	31	45.000 DEGREE	NSU
61	0.474D+04	32	45.000 DEGREE	NSU
62	0.474D+04	53	0.0 DEGREE	SO
63	0.474D+04	54	0.0 DEGREE	SO
64	0.474D+04	55	0.0 DEGREE	SO
65	0.474D+04	56	0.0 DEGREE	SO
66	0.474D+04	59	0.0 DEGREE	SO
67	0.474D+04	60	0.0 DEGREE	SO
68	0.474D+04	39	45.000 DEGREE	NSU
69	0.474D+04	40	45.000 DEGREE	NSU
70	0.47.D+04	61	45.000 DEGREE	NS
71	0.474D+04	62	45.000 DEGREE	NS
72	0.474D+04	63	0.0 DEGREE	SO
73	0.474D+04	64	0.0 DEGREE	SO
74	0.474D+04	67	0.0 DEGREE	SO
75	0.474D+04	68	0.0 DEGREE	SO
76	0.474D+04	69	45.000 DEGREE	NS
77	0.474D+04	35	-45.000 DEGREE	SU
78	0.474D+04	33	0.0 DEGREE	SU
79	0.474D+04	34	0.0 DEGREE	SU
80	0.474D+04	36	-45.000 DEGREE	SU
81	0.474D+04	37	0.0 DEGREE	SU
82	0.474D+04	38	0.0 DEGREE	SU
83	0.474D+04	41	0.0 DEGREE	SU
84	0.474D+04	42	0.0 DEGREE	SU
85	0.474D+04	43	-45.000 DEGREE	SU
86	0.474D+04	44	-45.000 DEGREE	SU
87	0.474D+04	45	0.0 DEGREE	SU
88	0.474D+04	46	0.0 DEGREE	SU
89	0.474D+04	47	0.0 DEGREE	JU
90	0.474D+04	48	0.0 DEGREE	SU
91	0.474D+04	53	0.0 DEGREE	SU
92	0.474D+04	54	0.0 DEGREE	SU
93	0.474D+04	55	0.0 DEGREE	SU
94	0.474D+04	56	0.0 DEGREE	SU
95	0.474D+04	57	-45.000 DEGREE	SU
96	0.474D+04	58	-45.000 DEGREE	SU
97	0.4_.D+04	59	0.0 DEGREE	SU
98	0.474D+04	60	0.0 DEGREE	SU
99	0.474D+04	61	45.000 DEGREE	NSU
100	0.474D+04	62	45.000 DEGREE	NSU
101	0.474D+04	63	0.0 DEGREE	SU
102	0.474D+04	64	0.0 DEGREE	SU
103	0.474D+04	65	-45.000 DEGREE	SU
104	0.474D+04	66	-45.000 DEGREE	SU
105	0.474D+04	67	0.0 DEGREE	SU
106	0.474D+04	68	0.0 DEGREE	SU
107	0.474D+04	69	45.000 DEGREE	NSU
108	0.474D+04	70	45.000 DEGREE	NS
109	0.474D+04	70	45.000 DEGREE	NSU

THE JOINT FAILED DURING INCREMENT NUMBER 109

THE FAILURE LOAD = 0.4743590D+04 LBS

104
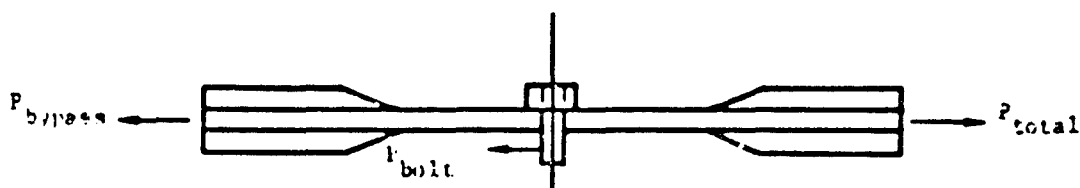
LAYUP	TEST CASE (REF. 5-1)	BEARING/ TOTAL LOAD	FINAL FAILURE LOAD (KIPS)	
			EXPT. (REF. 5-1)	ANAL. *
50/40/10	86	0	12.9	13.1
	87	0.167	10.7	10.9
	88	0.285	10.1	8.32
	89	0.375	9.44	7.92
	2	1.0	4.91	4.74

* For the full-bearing and the open hole cases,

a_{ens} , a_{obrg}, a_{eos} = 0.10, 0.025, 0.08 inch, respectively

k_2/k_1 = 0.1 for ns, brg and so failure modes for all ply types

$p^{ult}/p^{initial}$ = 1.02, 1.50 and 1.12 for ns, brg and so, respectively

Ply properties are presented in Figure 5-6

Figure 5-10. Comparison of SASCJ Predictions with Experimental Measurements for 50/40/10 AS1/3501-6 Laminates with Partially-Loaded 5/16 Inch Diameter Holes, Under Tensile Loading.

compares SASCJ predictions with experimental measurements (Reference 5-1) when a tensile load is applied on 50/40/10, AS1/3501-6, graphite/epoxy laminates with partially-loaded 5/16 inch diameter holes. SASCJ predictions agree very well with experimental measurements for the listed fastener bearing-to-total load ratios.

Similar results for tension-loaded 70/20/10 laminates, with partially-loaded 5/16 inch diameter holes, are presented in Figure 5-11. The maximum difference between SASCJ predictions and test results for this case is seen to be approximately 30%. A better correlation between test and analysis is demonstrated by tension-loaded 30/60/10 laminates with partially-loaded holes (see Figure 5-12).

Figures 5-13 to 5-15 compare SASCJ predictions with test results from Reference 5-1, corresponding to a compressive applied load on 50/40/10, 70/20/10 and 30/60/10 laminates with partially loaded, 5/16 inch diameter holes. Again, SASCJ predictions agree very well with test results on 50/40/10 and 30/60/10 laminates, and agree reasonably well with test results on 70/20/10 laminates, for the listed bearing/total load ratios.

Figures 5-10 to 5-15 demonstrate an acceptable correlation between analytical predictions and test results for a general single fastener location in a bolted laminate. This, in conjunction with the demonstrated correlation in Section 5.4, validates the use of SASCJ for predicting the strength of bolted laminates.
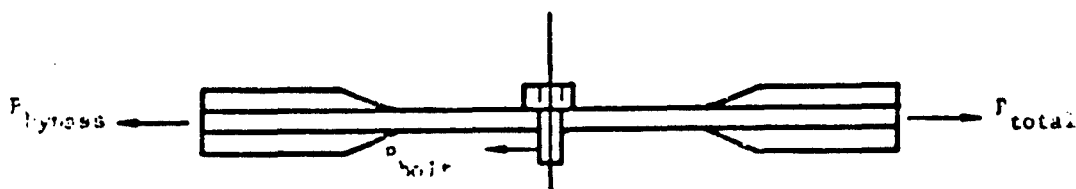
LAYUP	TEST CASE (REF. 5-1)	BEARING/ TOTAL LOAD	FINAL FAILURE LOAD (KIPS)	
			EXPT. (REF. 5-1)	ANAL. [*]
70/20/10	90	0	20.8	18.3
	91 [+]	0.167	15.9	10.8
	92 [+]	0.285	12.8	8.37
	93 [+]	0.375	11.6	7.79
	21 [++]	1.0	4.08	4.04

[*] For the full-bearing and open hole cases,

a_{ons} , a_{obrg}, a_{oso} = 0.10, 0.025, 0.05 inch, respectively

k_2/k_1 = 0.1 for ns, brg and so failure modes for all ply types

$p^{ult}/p^{initial}$ = 1.02, 1.50 and 1.12 for ns, brg and so, respectively

[+] Tests were conducted with countersunk steel fasteners (tension head, countersunk depth = 0.1 inch)

[++] Tests were conducted with protruding head, steel fasteners

Figure 5-11. Comparison of SASCJ Predictions with Experimental
Measurements for 70/20/10 AS1/3501-6 Laminates
with Partially-Loaded 5/16 Inch Diameter Holes,
Under Tensile Loading.

P_{bypass} ← F_{brg} → P_{total}

LAYUP	TEST CASE (REF. 5-1)	BEARING/ TOTAL LOAD	FINAL FAILURE LOAD (KIPS)	
			EXPT. (REF. 5-1)	ANAL.[*]
30/60/10	94	0	10.3	8.40
	95[+]	0.167	9.08	7.51
	96[+]	0.285	9.11	7.16
	97[+]	0.375	8.63	6.59
	22[++]	1.0	5	4.55

[*] For the full-bearing and open hole cases,
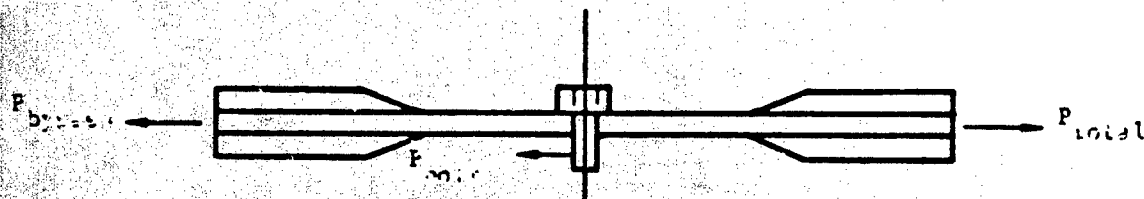
a_{ons}, a_{obrg}, a_{oso} = 0.10, 0.025, 0.08 inch, respectively

k_2/k_1 = 0.1 for ns, brg and so failure modes for all ply types

$p^{ult}/p^{initial}$ = 1.02, 1.50 and 1.12 for ns, brg and so, respectively

[+] Tests were conducted with countersunk, titanium fasteners (shear head, countersunk depth = 0.07 inch)

[++] Tests were conducted with protruding head, steel fasteners

Figure 5-12. Comparison of SASCJ Predictions with Experimental Measurements for 30/60/10 AS1/3501-6 Laminates with Partially-Loaded 5/16 Inch Diameter Holes, Under Tensile Loading.
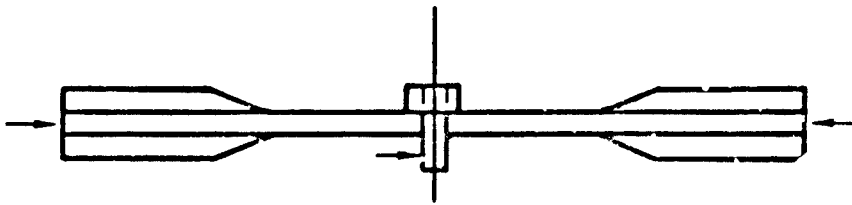
<table>
<tr><th rowspan="2">LAYUP</th><th rowspan="2">TEST CASE
(REF. 5-1)</th><th rowspan="2">BEARING/
TOTAL LOAD</th><th colspan="2">FINAL FAILURE LOAD
(KIPS)</th></tr>
<tr><th>EXPT.
(REF. 5-1)</th><th>ANAL.*</th></tr>
<tr><td rowspan="4">50/40/10</td><td>98</td><td>0</td><td>-13.4</td><td>-14.2</td></tr>
<tr><td>99</td><td>0.2</td><td>-14.1</td><td>-11.8</td></tr>
<tr><td>100</td><td>0.33</td><td>-11.5</td><td>-11.0</td></tr>
<tr><td>6</td><td>1.0</td><td>-5.48</td><td>-4.97</td></tr>
</table>

* For the full-bearing case,

a_{ons}, a_{obrg}, a_{oso} = 0.10, 0.025, 0.03 inch, respectively

a_2, a_1 = 0.1, 0.1 and 0.1 for ns, brg and so failure modes, respectively,

for all ply types

$P^{ult}/P^{initial}$ = 1.02, 1.50 and 1.12 for ns, brg and so, respectively

Figure 5-13. Comparison of SASCJ Predictions with Experimental
Measurements for 50/40/10 AS1/3501-6 Laminates with
Partially-Loaded 5/16 Inch Diameter Holes, Under
Compressive Loading.
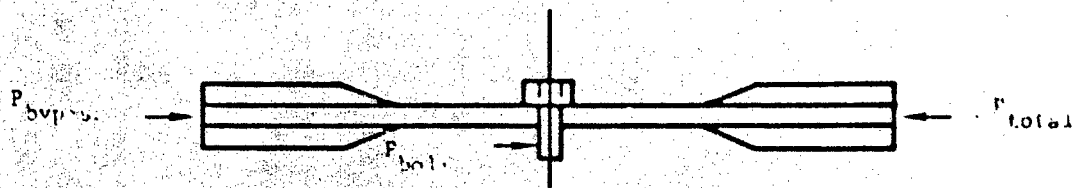
LAYUP	TEST CASE (REF. 5-1)	BEARING/ TOTAL LOAD	FINAL FAILURE LOAD (KIPS)	
			EXPT. (REF. 5-1)	ANAL.*
70/20/10	101	0	-17.5	-19.3
	102 ⁺	0.2	-15.7	-12.2
	103 ⁺	0.33	-12.4	-8.69
	23 ⁺⁺	1.0	-5.88	-4.90

* For the full-bearing case,

$a_{ one}$, $a_{ obrg}$, $a_{ ese}$ = 0.10, 0.025, 0.08 inch, respectively

k_2/k_1 = 0.1, 0.1 and 0.1 for ns, brg and se failure modes, respectively,

for all ply types

$p^{ult}/p^{initial}$ = 1.02, 1.50 and 1.12 for ns, brg and se, respectively

⁺ Tests were conducted with countersunk steel fasteners (tension head, countersunk depth = 0.1 inch)

⁺⁺ Tests were conducted with protruding head, steel fasteners

Figure 5-14.   Comparison of SASCJ Predictions with Experimental
Measurements for 70/20/10 AS1/3501-6 Laminates with
Partially-Loaded 5/16 Inch Diameter Holes, Under
Compressive Loading.

110

LAYUP	TEST CASE (REF. 5-1)	BEARING/ TOTAL LOAD	FINAL FAILURE LOAD (KIPS)	
			EXPT. (REF. 5-1)	ANAL.[*]
30/60/10	104	0	-10.5	-9.46
	105[+]	0.2	-10.8	-10.3
	106[+]	0.33	- 8.64	-9.73
	24[++]	1.0	- 5.13	-4.97

[*] For the full- bearing case,

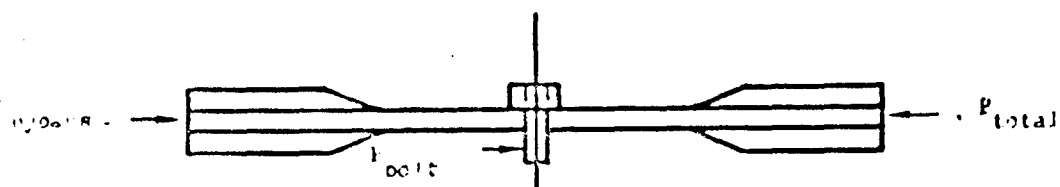$s_{one} \cdot s_{ebrg} \cdot s_{see}$ = 0.10, 0.025, 0.05 inch, respectively

k_2/k_1 = 0.1, 0.1 and 0.1 for ns, brg and se failure modes, respectively, for all ply types

$p^{ult}/p^{initial}$ = 1.02, 1.50 and 1.12 for ns, brg and se, respectively

[+] Tests were conducted with countersunk, titanium fasteners (shear head, countersunk depth = 0.07 inch)

[++] Tests were conducted with protruding head, steel fasteners

Figure 5-15. Comparison of SASCJ Predictionswith Experimental
Measurements for 30/60/10 AS1/3501-6 Laminates
with Partially-Loaded 5/16 Inch Diameter Holes,
under Compressive Loading.

111

SECTION 6

CONCLUSIONS

A strength analysis (SASCJ) was developed for laminated and/or metallic plates bolted together by a single fastener. This analysis includes a two-dimensional analysis of a finite anisotropic plate with a loaded or unloaded hole (FIGEOM), a fastener analysis that enables an approximate prediction of the local three dimensional stress state, accounting for fastener flexibility, load eccentricity, fastener torque, etc. (FDFA), and a progressive failure procedure based on bilinear ply behavior. FIGEOM and FDFA predictions were validated using available numerical and analytical solutions. SASCJ strength predictions were shown to correlate very well with test results from Reference 5-1.

The major accomplishments of the reported program task are summarized below:

(1) The developed SASCJ code accounts for finite (actual) planform dimensions of bolted plates. It is, therefore, capable of predicting the effect of small E/D and W/D values ($\leq$ 3 and 6, respectively) on the strength of bolted laminates.

(2) The combination of the two-dimensional anisotropic plate analysis (FIGEOM) and the fastener analysis (FDFA) approximately accounts for the complex three-dimensional stress/strain state at the fastener location. This also enables an analytical assessment of the effect of important joint parameters that include fastener flexibility, load eccentricity (single versus double shear load transfer), fastener torque, laminate stacking sequence, etc.

(3) The progressive failure procedure in the SASCJ code, incorporating a bilinear ply behavior into average stress failure criteria, provides significant improvements in the strength predictive capability. It enables the use of unmodified ply properties and invariant failure parameters to predict the sequence of ply failures until one of the bolted

112

plates suffers total failure (joint failure). It predicts the failure
modes at the ply level, accounting for a realistic combination of many
failure modes in the bolted laminate.

(4) The invariant failure parameters, required as input by the SASCJ code,
are obtainable from a limited number of tests on bolted laminates in a
double shear load transfer configuration. These include the character-
istic distances for the average stress criteria and the k_2/k_1 and
$p^{ultimate}/p^{initial}$ ratios for net section, bearing and shear-out
failure modes. This report includes failure parameter values for the
AS1/3501-6 graphite/epoxy material system. For a different material
system, only a few double shear, full-bearing tests have to be con-
ducted to determine the applicable failure parameters.

(5) The SASCJ code can predict the strength of an isolated single fastener
region in a laminate bolted to another plate using many fasteners, pro-
vided the fastener load is known. The SASCJ code can, therefore, be
directly combined with a two-dimensional load distribution analysis
to predict the strength of laminates bolted to other structural elements
using many fasteners. This strength analysis of multifastener joints in
composite structures is currently under development in the ongoing
Northrop/AFWAL program.

(6) The SASCJ code is currently being used to develop a design guide for
bolted joints. Expressions are being developed to quantify the effect
of fastener torque on the joint strength. The effects of the geometry
and the properties of the bolted plates and the fastener are being
systematically studied. Obtained results are being analyzed and trans-
lated into applicable design guidelines.

The above accomplishments of the SASCJ code represent a significant
improvement over the currently available strength analysis code (BJSFM).
Nevertheless, SASCJ does contain a restriction and a limitation that should
be addressed in future developmental efforts. The code is currently re-
stricted to a protruding head fastener geometry, and cannot predict the
effect of a flush-head (countersunk) fastener geometry. Also, the fastener
bearing load is always assumed to be cosinusoidal in form, and is assumed

to act over half the hole boundary. This results in a state of stress that is not very accurate near the hole boundary. The computed ply stresses are, therefore, accurate only at planform locations that are at least a laminate thickness away from the hole boundary. But, failure predictions are based on stresses computed over characteristic distances that are smaller or nearly equal in magnitude compared to the laminate thickness. This leads to an inaccuracy in the predicted joint strength, and the degree of inaccuracy is unknown. A modification of the FIGEOM and FDFA analyses in the SASCJ code is strongly recommended as a future analytical effort to eliminate the mentioned restriction and limitation.

REFERENCES

1-1. Ramkumar, R. L., et al., "Bolted Joints in Composite Structures: Design, Analysis and Verification," ongoing Northrop/AFWAL Contract No. F33615-82-C-3217, Northrop Corporation, Aircraft Division, Hawthorne, CA.

1-2. Garbc, S. P. and Ogonowski, J. M., "Effect of Variances and Manufacturing Tolerances on the Design Strength and Life of Mechanically Fastened Composite Joints," Volume 1, AFWAL-TR-81-3041, April 1981.

2-1. Kudva, N. J. and Madenci, E., "Stress Analysis of Finite Geometry Composite Bolted Joints Using Modified Boundary Collocation Techniques," Northrop Corporation Report, NOR 83-198, October 1983.

2-2. Jones, R. M., Mechanics of Composite Materials, Scripta Book Company/McGraw Hill, 1975.

2-3. Lekhnitskii, S. G., Anisotropic Plates, Gordon and Breach, 1968.

2-4. Oplinger, D. W., and Gandhi, K. R., "Stresses in Mechanically Fastened Orthotropic Laminates," AFFDL-TR-74-103, September 1974.

2-5. Hyer, M. W. and Klang, E. C., "Stresses Around Holes in Pin-Loaded Orthotropic Plates," Proceedings of the 25th Structures, Structural Dynamics and Materials Conference, Sponsored by AIAA/ASME/ASCE/AHS, Palm Springs, California, May 1984.

2-6. Mangalgiri, P. D., "Pin-Loaded Holes in Large Orthotropic Plates," AIAA Journal, Vol. 22, No. 10, pp. 1478-1484, October 1984.

2-7. Ogonowski, J. M., "Analytical Study of Finite Geometry Plates with Stress Concentrations," Proceeding of the 21st Structures, Structural Dynamics and Materials Conference, sponsored by AIAA/ASME/ASCE/AHS, Seattle, May 1980.

2-8. Bowie, O. L., "Solutions of Plane Crack Problems by Mapping Techniques," Mechanics of Fracture 1, edited by G. C. Sih, Noordhof International Publishing Company, 1973.

2-9. Garbo, S. P., and Ogonowski, J. M., "Effect of Variances and Manufacturing Tolerances on the Design Strength and Life of Mechanicall, Fastened Composite Joints," AFVAL-TR-81-3041, Volume 1, April 1981.

REFERENCES (Continued)

2-10. Ramkumar, R. L. and Tossavainen, E. W., "Bolted Joints in Composite Structures: Design, Analysis and Verification; Task I Test Results -- Single Fastener Joints," AFWAL-TR-84-3047, August 1984.

3-1. Harris, H. G. and Ojalvo, I. U., "Simplified Three-Dimensional Analysis of Mechanically Fastened Joints," Proceedings of the Army Symposium on Solid Mechanics: The Role of Mechanics in Design--Structural Joints, September 1974.

3-2. Harris, H. G., Ojalvo, I. U. and Hooson, R. E., "Stress and Deflection Analysis of Mechanically Fastened Joints, "Air Force Flight Dynamics Laboratory Technical Report, AFFDL-TR-70-49, May 1970.

3-3. Barrois, W., "Stresses and Displacements due to Load Transfer by Fasteners in Structural Assemblies, "Engineering Fracture Mechanics, Vol. 10, pp. 115-176, 1978.

3-4. Hetenyi, M., Beams on Elastic Foundation, University of Michigan Press, Ann Arbor, Michigan, 1946.

3-5. Kirkner, D. J., "Vibration of a Rigid Disc on a Transversely Isotropic Elastic Half Space," International Journal of Numerical and Analytical Methods in Geomechanics, Vol. 6, pp. 293-306, 1982.

3-6. Ramkumar, R. L. and Tossavainen, E. W., "Bolted Joints in Composite Structures: Design, Analysis and Verification; Task I Test Results -- Single Fastener Joints," AFWAL-TR-84-3047, August 1984.

4-1. Whitney, J. M. and Nuismer, R. J., "Stress Fracture Criteria for Laminated Composites Containing Stress Concentration," Journal of Composite Materials, Vol. 8, pp 253-265, July 1974.

4-2. Agarwal, B. L., "Static Strength Prediction of Bolted Joints in Composite Material," AIAA Journal, Vol. 18, pp 1371-1375, 1980.

4-3. Ramkumar, R. L., "Bolted Joint Design," Test Methods and Design Allowables for Fibrous Composites, ASTM STP 734, C. C. Chanis, Ed., American Society for Testing and Materials, pp 376-395, 1981.

4-4. Garbo, S. P. and Ogonowski, J. M., "Effect of Variances and Manu-facturing Tolerances on the Design Strength and Life of Mechanically Fastened Composite Joints," Volume 1, AFWAL-TR-81-3041, April 1981.

REFERENCES (Concluded)

5-1.   Ramkumar, R. L. and Tossavainen, E. W., "Bolted Joints in Composite
        Structures: Design, Analysis and Verification: Task I Test Results --
        Single Fastener Joints," AFWAL-TR-84-3047, August 1984.

5-2.   Whitney, J. M. and Nuismer, R. J., "Stress Fracture Criteria for
        Laminated Composites Containing Stress Concentration," Journal of
        Composite Materials, Vol. 8, pp 253-265, July 1974.

5-3.   Agarwal, B. L., "Static Strength Prediction of Bolted Joints in
        Composite Material," AIAA Journal, Vol. 18, pp 1371-1375, 1980.

5-4.   Ramkumar, R. L., "Bolted Joint Design," Test Methods and Design
        Allowables for Fibrous Composites, ASTM STP 734, C. Chamis,
        Ed., American Society for Testing and Materials, pp 376-395, 1981.

5-5.   Garbo, S. P. and Ogonowski, J. M., "Effect of Variances and Manu-
        facturing Tolerances on the Design Strength and Life of Mechanically
        Fastened Composite Joints," Volume 1, AFWAL-TR-81-3041, April 1981.